

**ANALYSIS OF EVACUATED ANNULUS TUBE COLLECTOR  
ASSISTED SOLAR DESALTIFICATION SYSTEM**

**THESIS**

Submitted in fulfillment of the requirements

For the degree of

**DOCTOR OF PHILOSOPHY**

By

**ASHOK KUMAR SINGH**  
(2K18/PHDME/533)

Under the supervision of

**Prof. SAMSER**

Department of Mechanical Engineering  
Delhi Technological University, Delhi



**DEPARTMENT OF MECHANICAL ENGINEERING  
DELHI TECHNOLOGICAL UNIVERSITY  
DELHI - 110042 (INDIA)**

**SEPTEMBER 2022**



All rights reserved.

**Copyright © 2022 Delhi Technological University, Delhi**

(Formerly Delhi College of Engineering)

Shahabad Daulatpur, Main Bawana Road, Delhi-110042 (India)



*Dedicated to*

*My parents (Maate & Babu ji)*

*My family (Mrs. Aaradhana Singh, Ritu & Suraj)*



DELHI TECHNOLOGICAL UNIVERSITY  
Shahabad Daultpur, Main Bawana Road  
Delhi-110042 (India)

## DECLARATION

I hereby declare that the *Thesis* entitled “**Analysis of Evacuated Annulus Tube Collector Assisted Solar Desaltification System**” submitted by me in fulfillment of the requirements for the degree of *Doctor of Philosophy* to **Delhi Technological University** (Formerly Delhi College of Engineering) is a record of *bona fide work* carried out by me under the guidance of **Prof. SAMSHER**, Department of Mechanical Engineering, DTU, Delhi.

I further declare that the work reported in this *Thesis* has not been submitted and will not be submitted, either in part or in full, for the award of any other degree or diploma in any other Institute or University.

A handwritten signature in blue ink, appearing to read 'Ashok'.

**ASHOK KUMAR SINGH**

Roll No: 2K18/PHDME/533

Department of Mechanical Engineering  
Delhi Technological University, Delhi



DELHI TECHNOLOGICAL UNIVERSITY  
Shahabad Daulatpur, Main Bawana Road  
Delhi-110042 (India)

## CERTIFICATE

This is to certify that the *Thesis* entitled “**Analysis of Evacuated Annulus Tube Collector Assisted Solar Desaltification System**” submitted by **Mr. Ashok Kumar Singh** to **Delhi Technological University** (Formerly Delhi College of Engineering), in fulfillment of the requirements for the degree of *Doctor of Philosophy* is a record of *bona fide work* carried out by him. Ashok Kumar Singh has worked under my guidance and supervision and has fulfilled the requirements for the submission of this *Thesis*, which to my knowledge has reached requisite standards.

The results contained in this *Thesis* are original and have not been submitted to any other university or institute for an award of any degree or diploma.

A handwritten signature in blue ink, appearing to read 'Samsheer', is positioned above the printed name of the professor.

**Prof. SAMSHER**

Professor

Department of Mechanical Engineering

Delhi Technological University (DTU)

Bawana, Delhi-110042

## ACKNOWLEDGEMENTS

I would like to express my heartiest gratitude to my research supervisor, mentor, and guide *Prof. SAMSHER* for his supervision, advice and continuous guidance from the conception of this research as well as imparting extraordinary experiences throughout the work. His advice on both research as well as on my career have been priceless. He has been tremendous mentor for me. If I would stand proud of my achievements, he is the main creditors. It is my privilege to be under his tutelage. Perseverance, exuberance, positive approaches are just some of the traits he has imprinted on my personality. I thankfully acknowledge him for his vital contribution, which made him a backbone of this research and hence to this *Thesis*. These lines are dedicated to my Guide:

“गुरुर्ब्रह्मागुरुर्विष्णुर्गुरुर्देवोमहेश्वरः  
गुरुः साक्षात्परब्रह्मात्स्मैश्रीगुरवे नमः”

I would like to express my gratitude to *Prof. Jai Prakash Saini*, Vice chancellor, Delhi Technological University, Delhi for providing this opportunity to carry out this work in this prestigious institute.

I would like to express my gratitude to *Prof Yogesh Singh*, Ex-Vice Chancellor, DTU, Delhi, *Prof. S.K. Garg*, DRC Chairman, and Head of the Department of Mechanical Engineering. I am thankful to *Prof. A. Trivedi*, Dean IRD, *Prof. Vipin*, *Prof. Ranganath. M. Singari*, and *Dr. Anil Kumar*, Department of Mechanical Engineering for their kind support to accomplish this work.

I express my special thanks to *Mr. Anand Kushwaha*, *Mr. Dharamveer*, *Mr. Phool Singh*, *Mr. Neeraj Kant*, *Mr. Md. Gulam Mustafa*, *Mr. Md. Hussam*, research scholar, Delhi Technological University, Delhi for helping me in difficult time and providing unflinching moral support. I would like to acknowledge the help and cooperation of *Dr. V.K. Dwivedi*, *Dr. Rajesh Tripathi*, *Dr. M.K. Lohumi*, and *Mr. Manohar Singh* of Galgotias College of Engineering and Technology, Greater Noida for carrying out my research. My sincere thanks to anonymous reviewers, whose insightful and constructive comments and suggested revisions improved the organization and clarity of the research.

I am greatly indebted to my parents for their love and blessings to see me scaling greater heights of life. Words fail me to express my appreciation to my respected parents *Sri Ram Nayan Singh* and *Smt. Kamala Singh* whose blessings have helped me to achieve my goal. My younger brothers *Mr. Umesh Singh* and *Mr. Arvind Singh* deserve special mention for their inseparable support and patience. I truly appreciate the support which I got from my parents in law *Sri. Arvind Kumar Singh, Smt. Shanti Devi*, and my wife *Mrs. Aaradhana Singh*, my daughter *Ritu*, and son *Suraj* throughout my research work for giving me the mental and moral support with continuous motivation and encouragement in my highs and lows during the PhD journey. Also, I express my special thanks to my brothers in law *Mr. Vishwajeet Pratap Singh* and *Mr. Amarjeet Pratap Singh* for their continuous moral support during the hard times and the entire perusal of this course.

I would like to extend my thanks to everybody who was essential to the successful realization of this *Thesis*, as well as expressing my regret that I could not mention personally one by one. Finally, I would like to express my gratitude to *Almighty 'ॐ'* for giving me patience and strength to achieve such a blissful moment of life.

**ASHOK KUMAR SINGH**

## ABSTRACT

Pure water is one of the basic elements required for continuing healthy life on the Earth, whereas the adverse situations due to water stress faced by human beings more or less all over the globe. As the large scale industrialization, rapid escalation in agriculture and population all over the world create more difficult situations for freshwater demand and supply chain and hence many of the people are forced to use contaminated, brackish, or salty water that cause various health related problems. To tackle and overcome the challenges related to water stress, the use of renewable energy (solar energy) in solar desalination systems (eco friendly, economical and self sustainable technology of water purification) may one of the best solutions to treat the brackish/saline water into potable one. Solar desalination is the process of receiving potable water against the brackish water by harnessing solar energy through solar desalination systems which replicates the natural hydrological succession with a difference of closed cyclic operation in a confined chamber.

In the present study, a novel design of solar desalination systems (SDS) with evacuated annulus tube collector (EATC) augmented unique combination of modified compound parabolic concentrators (MCPC) has been analyzed for Techno-Environ-Economic-Energy-Exergy-Matrices observations under the specific meteorological conditions of New Delhi, India. Two different models (a) Evacuated annulus tube collector assisted single slope solar desalination system, (b) Evacuated annulus tube collector assisted double slope solar desalination system, have been analyzed in the proposed work of research. The current approach emphasizes the utility of EATC-MCPC that effectively improves the solar absorbing performance of the irradiated solar energy uniformly through its periphery, as well as enhancing the thermo siphons working loom appreciably than the conventional applications of EATCs. The proposed system is being optimized to get the maximum possible basin water temperature as  $\sim 99.5^{\circ}\text{C}$  for the larger water depth (0.16m) at the same orientation of both, SDS top cover and EATC ( $30^{\circ}$ ).

The developed thermal model and respective characteristic equations have been utilized to analyze the proposed systems. The analysis is primed on the basis of



performance evaluation of the system directly or indirectly that depends on the productivity of potable water, energy, exergy efficiencies, energy-exergy metrics, various economic analyses of the system, and also techno-eco impact to the environment. The performances of the proposed systems are being compared with the former researches in the influence of different governing parameters. The system's energy-exergy (kWh), efficiency (%), mass flow rate (kg/hr), yield cost (\$/kg), pollutants mitigate (ton), production cost (\$) with respect to the energy input (kWh), exergo-economic factor, environmental cost (\$), payout time, total annual cost of the establishments (\$), and life cycle conversion efficiencies are computed under the different variable parameters such as solar intensity, ambient temperature, water depth, and number of EATCs to depict the worthy performances for the optimized integral combination of the proposed systems.

It has been observed that the double slope solar desalination system produces greater yield at moderate circulation rate (thermo siphon) of water. And, this system is much better in overall terms of performance except energy-exergy efficiency than the single slope solar desalination system under the same design parameters and climatic conditions. The establishment cost of the system is quite low for both the systems. Also, the productivity for both the system's are found more than 100% that depict the systems as appreciably feasible. The noticeable yield output at low production cost, environmental revenue credits, high mitigation, and low pay-off time makes the system compatibly sustainable and feasible with smaller and effective collector areas for the respective solar irradiations.

The overall work has been intensively analyzed to get the responsible, and system effective results which are nourished with detailed result discussion and conclusions with future recommendations that may enlighten the researchers to motivate for the additional possible developments in this field for the betterment to the society, environment, and the sustainable growth of human beings ecologically.

**Keywords:** Solar desalination system; Modified parabolic concentrator; Evacuated annulus tube collector; Yield; Energy; Exergy; Efficiency; Economic; Environmental cost; Exergo-economy; Productivity; Energy-exergy matrices

# INDEX

Content	Page No.
Declaration	i
Certificate	ii
Acknowledgements	iii
Abstract	v
Index	vii
List of Figures	x
List of Tables	xiv
Nomenclature	xv
<b>CHAPTER 1: Introduction</b>	<b>1 – 13</b>
1.1 Introduction	2
1.1.1 Necessity of Potable Water: A Motivation	2
1.1.2 Solutions for Potable Water	3
1.2 Solar Dsaltification System (SDS)	4
1.3 Solar Thermal Collectors	6
1.4 Organization of Thesis	11
<b>CHAPTER 2: Literature Survey</b>	<b>14 – 29</b>
2.1 Introduction	15
2.1.1 Solar Still Viabilities	15
2.1.2 Techno-Eco Design Viability	18
2.1.3 Thermo Siphon Considerations	18
2.2 Research Gap	26
2.3 Problem Statement with Research Objectives	27
2.4 Research Scope	27
2.5 Research Contribution	28
<b>CHAPTER 3: Methodology</b>	<b>30 – 67</b>
3.0 Introduction	31
3.0.1 Analytical Methodology	31
3.1 Evacuated Annulus Tube Collector Assisted Single Slope Solar Desaltification	34

System	
3.1.1 Proposed Novel Design (SS-SDS-EATC-MCPC): System Description and Specifications	35
3.1.2 Techno-Eco-Design: Solar Insolation Perspective	39
3.1.3 Geometric Considerations of MCPC	40
3.1.4 Solar Insolation Response Over the Inclined Surface	40
3.1.5 Thermal Model	42
3.1.5.1 Parallel array of N-EATC-MCPC	42
3.1.5.2 Single Slope Solar Desalting System	45
3.1.5.3 Mass Flow Observation of N-EATC-MCPC Parallel Array	48
3.1.6 System Performance Parameters	49
3.1.6.1 Yield Production	49
3.1.6.2 Energetic Observations	49
3.1.6.3 Exergetic Observations	50
3.1.7 Energy-Exergy Matrices Observations	51
3.1.7.1 Pay off Time	51
3.1.7.2 Pay off Factor	52
3.1.7.3 Efficiency for Life Cycle Conversion	52
3.1.8 Economic Observations	53
3.1.8.1 System Economics	53
3.1.8.2 Exergo-Economics	54
3.1.8.3 Environ-Energy-Exergy-Economics	55
3.2 Evacuated Annulus Tube Collector Assisted Double Slope Solar Desalting System	56
3.2.1 System Depiction and Requisites (DS-SDS-EATC-MCPC)	57
3.2.2 Solar Irradiance: East-West Inclined Surface	59
3.2.3 Thermal Model: DS-SDS Unit	60
3.2.4 Eco-Design Requisites and Performance Observations	64
3.2.5 Energy-Exergy Matrices Observations	66
3.2.6 Different Economic Observations	66
<b>CHAPTER 4: Results and Discussion</b>	<b>68 – 91</b>
4.0 Introduction	69
4.1 Evacuated Annulus Tube Collector Assisted Single Slope Solar Desalting System	70

4.1.1 Thermal Model Validation With Comparative Improvement Observation	71
4.1.2 Optimization of the Proposed Model	71
4.1.3 Performance Analysis: Energy-Exergy Considerations	72
4.1.4 Energy Matrices Viabilities	75
4.1.5 Techno-Eco-Design Requisites: An Optimum-Environ-Economic Viability	76
4.2 Evacuated Annulus Tube Collector Assisted Double Slope Solar Desalting System	78
4.2.1 Optimization of the Proposed Model	78
4.2.2 Performance Analysis: Energy-Exergy Considerations	79
4.2.3 Energy Matrices Viabilities	82
4.2.4 Techno-Eco-Design Requisites: An Optimum-Environ-Economic Capability	83
4.3 Comparative Result Analysis	84
4.3.1 Energetic-exergetic Approach of Performance	87
4.3.2 Energy Matrices Comparison	89
4.3.3 System Economic Comparison	90
4.3.4 Environ-economic Comparison	90
<b>CHAPTER 5: Conclusions and Recommendations for Future Work</b>	<b>92 – 95</b>
5.0 Introduction	93
5.1 Conclusions	93
5.2 Recommendations for Future Work	95
<b>Appendix-A</b>	<b>96</b>
<b>Appendix-B</b>	<b>97</b>
<b>Appendix-C</b>	<b>100</b>
<b>References</b>	<b>103</b>
<b>List of Publications</b>	<b>113</b>
<b>Curriculum Vitae</b>	<b>115</b>

## LIST OF FIGURES

Fig. No.	Figure Caption	Page No.
1.1	Variety of SDS and different combinations that show a research gap that is being undertaken by introducing the proposed novel techno-eco-design of SDS-EATC-OCPC-CCPC system	4
1.2	Schematic plan view of conventional SDS system representing solar energy distribution, utilization, and losses accordingly	5
1.3	Schematic plan view of conventional double slope SDS system representing solar energy distribution, utilization, and losses accordingly	6
1.4	Different solar thermal collectors with its possible hindrances while adaptation of these in comparison to the thermo siphon EATC that are integrated with SDS systems	7
1.5	Schematic representation of various types of evacuated tube collectors, (a) <i>Charter and Window (1978)</i> ; (b) <i>Beekley and Mather (1978)</i> ; (c – h) <i>Williams (1983)</i> ; (i – j) <i>Norton (1992)</i>	9
1.6	Classification of ETC introduced with novel techno-eco-design combination of EATC that have possible integrations to SDS and also not been introduced in earlier researches	9
1.7	Schematic representation of evacuated annulus double glaze tube collector (EATC)	10

---

1.8	Fractional representation of reflectivity and transmittance during the propagation of solar irradiation through glazing for ETC	11
2.1	Schematic representation of the proposed systems for the current research work	28
3.1	Computational algorithm and flowchart for the methodological steps	33
3.2	Proposed system i.e. single slope solar desalination unit assisted evacuated annulustube collector and modified compound parabolic concentrator (SS-SDU-EATC-MCPC)	35
3.3	Schematic plan view of EATC-CCPC covering underneath half part of the EATC under the corresponding solar insolation	38
3.3a	Schematic elevation view of N-EATC-MCPC covering either side and underneath half simultaneously of the EATC under the corresponding solar insolation	39
3.4	Double slope solar desalination unit with evacuated annulus tube collector and modified compound parabolic concentrator (DS-SDU-EATC-MCPC)	57
4.1	Representation of hourly variations of different solar irradiative radiations on the horizontal surface round the sun shine hours	70
4.2	Validation and comparative observation for the thermal models of the proposed system under the hourly variations of basin water, inner glass top cover temperature, and yield output	71

---

---

4.3	Representation of basin water maximum temperatures against the variable water depth conditions and constant number of EATCs of the proposed system	72
4.4	Temperature variations at different sections in the system for an archetypal clear day in the month of June	73
4.5	Heat transfer coefficient variations at different segments in the system for an archetypal clear day in the month of June (N=4)	73
4.6	Hourly variations of mass flow rate, yield output, and $(T_w - T_{g,i})$ in the month of June of an archetypal clear day	74
4.7	Energy-Exergy gain of the system under the respective clear day conditions in the month of June	75
4.8	Energy-Exergy efficiency variations of the system under the respective clear day conditions in the month of June (N= 4)	75
4.9	Energy matrices distribution of the proposed model (n= 30yrs.)	76
4.10	Variations of life cycle conversion efficiency over a period of the system's life	76
4.11 (A, B, C)	Variation of annual productivity and exergo-economic factor under the influence of different interest rates of the proposed system	77
4.12	Representation of basin water maximum temperatures against the variable water depth conditions and constant number of EATCs of the proposed system	79

---

---

4.13	Temperature variations at different sections in the system	79
4.14	Heat transfer coefficient variations at different segments in the system	80
4.15	Yield representation at different basin temperatures and corresponding mass flow rate	81
4.16	Energy-Exergy gain of the system under the respective clear day conditions	82
4.17	Energy-Exergy efficiency variations of the system under the respective clear day conditions in the month of June (N= 4)	82
4.18	Energy matrices distribution of the proposed model (n= 30yrs.)	83
4.19	Variations of life cycle conversion efficiency over a period of the system's life	83
4.20	Variation of annual productivity and exergo-economic factor under the influence of different interest rates of the proposed system	84
4.21	Comparative observations of environ-economic perspectives under the influence of different solar desalination systems with respect to the proposed systems	91

---



## LIST OF TABLES

---

Table No.	Table Caption	Page No.
2.1	Overview of performance observations and applications of EATC assisted SDU for the related research gap identification	22
3.1	Specifications and computational design parameters of SS-SDS	36
3.2	Specifications and computational design parameters of EATC	37
3.3	Specifications and computational design parameters of MCPC	37
3.4	Specifications and computational design parameters of the proposed novel system (DS-SDS)	58
3.5	Specifications and computational design parameters of EATC-MCPC	58
4.1	Overall glimpse of the results in a comparative manner and related observations with possible behavioral reasons	84
4.2	Comparative performance in terms of distillate output for various solar desalination systems in combination with solar thermal collectors	88

---

## NOMENCLATURE

$A_a$	accumulated aperture area of MCPC
$A_g$	area of exposed top glazing ( $m^2$ )
$A_b$	area of exposed basin liner ( $m^2$ )
$A_{rc}$	area of receiver collector of EATC
$C_w, C_f$	specific heat capacity of water mass (J/kg K)
$d$	inner diameter of inner concentric tube of EATC (m)
$E_e$	energy gain (kWh)
$E_x$	exergy gain (kWh)
$F'$	collector (EATC) efficiency factor
$h_{ba}$	overall heat transfer coefficient from basin liner to atmosphere ( $W/m^2 K$ )
$h_{bw}$	convective heat transfer coefficient from basin liner to basin water mass ( $W/m^2 K$ )
$h_{t-g}, h_o$	thermal loss coefficient of convection from outer glaze to atmosphere ( $W/m^2 K$ )
$h_{t-wg}$	total heat transfer coefficient from water surface to top glaze cover ( $W/m^2 K$ )
$h_{c-w}$	convective heat transfer coefficient of water surface to cover surface ( $W/m^2 K$ )
$h_{e-wg}$	evaporative heat transfer coefficient of water surface to cover surface ( $W/m^2 K$ )
$h_{r-wg}$	radiative heat transfer coefficient from water surface to cover surface ( $W/m^2 K$ )
$h_{r-ev}$	radiative thermal loss coefficient of EATC through vacuum zone ( $W/m^2 K$ )
$h_{saf}$	total heat transfer coefficient from absorber to water of EATC tube ( $W/m^2 K$ )
$I_d(t)$	diffused (reflected from ground) solar radiation ( $W/m^2$ )
$I_s(a)$	absorbed intensive heat of solar energy into selective absorber ( $W/m^2$ )

- $I_s(t)$  instantaneous irradiative solar energy over exposed surface area of SDS ( $\text{W/m}^2$ )
- $I_b(t)$  irradiated solar beam radiation over EATC collectors ( $\text{W/m}^2$ )
- $K_g$  thermal conductivity of glaze ( $\text{W/m K}$ )
- $K_b$  thermal conductivity of basin liner material ( $\text{W/m K}$ )
- $K_w$  thermal conductivity of water ( $\text{W/m K}$ )
- $L$  water mass latent heat of vaporization ( $\text{J/kg}$ )
- $L_{EATC}$  length of EATC tube (m)
- $\dot{m}_{ewg}$  hourly distillate production ( $\text{kg/h}$ )
- $\dot{m}_f$  mass flow rate of water in EATC ( $\text{kg/s}$ )
- $m_w$  basin water mass quantity (kg)
- $m_f$  EATC water mass quantity (kg)
- $p_w$  partial vapor pressure over the basin water surface ( $\text{Pa, N/m}^2$ )
- $p_{gi}$  partial vapor pressure over the inner surface of top glaze ( $\text{Pa, N/m}^2$ )
- $\dot{Q}_{N-EAT}$  additional rate of heat gain to SDS from parallel N-EATC-MCPC ( $\text{kJ/s}$ )
- $\dot{q}_{ewg}$  rate of change of useful heat transfer of evaporation (basin water to cover) ( $\text{kJ/s}$ )
- $R_{i1}$  inner radius of inner tube (m)
- $R_{i2}$  outer radius of inner tube (m)
- $R_{o2}$  outer radius of outer tube (m)
- $R_{sc}$  reflectivity of selective absorber
- $T_a$  ambient temperature ( $^{\circ}\text{C}$ )
- $T_b$  basin composite liner temperature ( $^{\circ}\text{C}$ )

$t_b$	thickness of composite basin liner (m)
$t$	time (s)
$t_g$	thickness of heat transfer path through top cover glaze (m)
$T_{sa}$	temperature of selective absorber ( $^{\circ}\text{C}$ )
$T_f$	temperature of working fluid (water) into the EATC ( $^{\circ}\text{C}$ )
$T_{fo1}$	identical EATC outlet temperature of water mass ( $^{\circ}\text{C}$ )
$T_{N-fo}$	outlet temperature of accumulative water mass coming out from N-EATC ( $^{\circ}\text{C}$ )
$T_w$	SDS basin water mass temperature ( $^{\circ}\text{C}$ )
$T_{go}$	SDS top cover glaze outer surface temperature ( $^{\circ}\text{C}$ )
$T_{gi}$	SDS top cover glaze inner surface temperature ( $^{\circ}\text{C}$ )
$U_{saa}$	overall heat transfer (loss) coefficient from outer glaze tube of EATC
$V$	average wind velocity (m/s)

### ABBREVIATION

ALN	aluminum nitride
SS	single slope
DS	double slope
SDS	solar desalination system
EATC	evacuated annulus tube collector
FPC	flat plate collector
CPC	compound parabolic concentrator
OCPC	oriented compound parabolic concentrator

MCPC modified compound parabolic concentrator

CCPC cusp compound parabolic concentrator

### GREEK LETTERS

$\nu$  kinematic viscosity water ( $\text{m}^2/\text{s}$ )

$\beta'$  factor of volumetric thermal expansion of water ( $\text{K}^{-1}$ )

$\alpha$  absorptivity of selective absorber

$\mu$  dynamic viscosity of water ( $\text{N}\cdot\text{s}/\text{m}^2$ )

$\alpha_g$  absorptivity of glass

$\alpha_w$  absorptivity of water

$\alpha_b$  absorptivity of composite basin liner

$\eta_i$  instantaneous efficiency (%)

$\eta_e$  energy efficiency (%)

$\eta_x$  exergy efficiency (%)

$\tau$  transmissivity

$\sigma$  Stefan-Boltzmann constant ( $\text{W}/\text{m}^2 \text{K}^4$ )

$\rho$  density ( $\text{kg}/\text{m}^3$ )

$\varepsilon_{eff}$  effective emissivity

$\varepsilon_g$  emissivity of glaze

$\varepsilon_w$  emissivity of water mass

## SUBSCRIPTS

E east

e energy

f fluid

g glass

hr hourly

rc receiver

sa selective absorber

W west

w water

x exergy



**CHAPTER: 1**

***INTRODUCTION***

## CHAPTER: 1

### INTRODUCTION

---

#### 1.1 INTRODUCTION

##### 1.1.1 Necessity of Potable Water: A Motivation

Pure water is one of the basic elements required for continuing healthy life (as majorly human body contains the most significant amount of water i.e., >70%) on the Earth. And, the adverse situations are continuously increasing due to water stress faced by human beings more or less all over the globe day by day also, because of the incremental growth of population. Pure water is basically consumed by living beings, industries, agriculture, etc. which are continuously increasing day by day. More than 70% of earth's surface is enclosed with water. Out of the existing water on earth surface, only less than 3% is pure water. Further, more than 2% water is locked up in the ice caps and glaciers and less than 1% is available for the use of human being. As the natural water mass sources are shrinking day by day and safe consumable water remains unreachable for majority of human beings about 1.1 billion people over the globe (*Gadgil, 1998*). The salinity of most available water on the earth is up to 10,000ppm out of sea water as its salinity ranges more than 30,000ppm up to 45,000ppm. As the population keeps increasing, this creates more difficult situations for freshwater demand and supply chain and hence many of the people are forced to use contaminated, brackish, or salty water. Contaminated water cannot be directly used because it can cause various health related problems such as skin cancer (*Tseng, 1977*). A report has also been evolved and confirmed water born diseases like skin cancer (*EPA, 1988, 2007*). Moreover, black foot disease, diarrhea, etc. was reported by *Lu (1990)*. So, to assure the purity of consuming water before its use is quite necessary. *Pugsley et al. (2016)* established a ranking system to point out the potable water scarce or water stressed continents around the world in terms of water stress index that reflect most of the middle eastern continents along with major part of India under gone in the highly potable water stress zone (>0.422). As for as the Indian continent is concerned, it is a tropical country having more than 16% of the total population on the earth along with the 4% of potable water accessibility only and that may exceed further by the increase in population as expected based on the past experiences to be 1.6



billion up to the year 2050. Several places in India mainly rural and coastal zones are facing severe scarcity of potable water. The main reason behind water related diseases is consumption of contaminated water and moreover, kids are desperately at high risk to water-borne diseases.

### 1.1.2 Solutions for Potable Water

Water harvesting refers to a better way for improving the approachable water sources but the direct consumption of such type of water may cause serious health issues as discussed above. Such brackish or saline water has excessive particulate deposits of primary metals (i.e., Na, Mg, Ca, K, B, etc.) and can be reduced up to 10 to 500 ppm by using various membrane based water treatment conventional plants (*IRENA, 2015*), whereas, up to 1-50 ppm can be achieved easily by the application solar desalination technology (*Zhou et al. 2016*). Other than brackish, saline, or contaminated water, SDS is very much able to efficiently treat industrial and domestic liquid wastes (*Zarasvand et al., 2013*). The potable water from the solar desalination system (SDS) is one of the purest forms of water that is better than rainy water (*Imad and Badran, 2004*). By using renewable energy source, especially solar energy, one can produce pure water by using solar desalination system which is one of the most feasible, innovative and economic technique for saline and dirty water purification. The purified water by this system have pH in the range of 7 – 8 with ~200ppm total dissolved solids which refers a good water quality agreement as recommended by World Health Organization and Bureau of Indian Standards. However, the human beings can consume water having salinity up to 1,000 ppm as per World Health Organization and Bureau of Indian Standards (*HanSon et al., 2004*). Also, the distilled water can be further converted into health rich water by modifying the required amount of minerals, for example, 1, 0.3, 0.05, 5, and 0.2 of mg/l for Cu, Fe, Mn, Zn, and Al, respectively based on the EPA and WHO (*EPA, 2007; WHO, 2011*). Further, the amount of potable water depends on various constraints as the type of still design, weather conditions, and sound association with different types of solar collectors, etc. So, researchers/scientific bodies are searching to stand this system/technology as a frontier one against the other water treatment technologies on the world platform (*Goswami, 2015; Hussain and Lee, 2015*). And, such kind of appreciation for SDS technology appeared due to its marvelous capabilities other than the desalination of water, for producing affordable potable water, hot water, steam or air for space conditioning, etc., that may be utilized in domestic or commercial applications as shown in [Fig. 1.1](#).

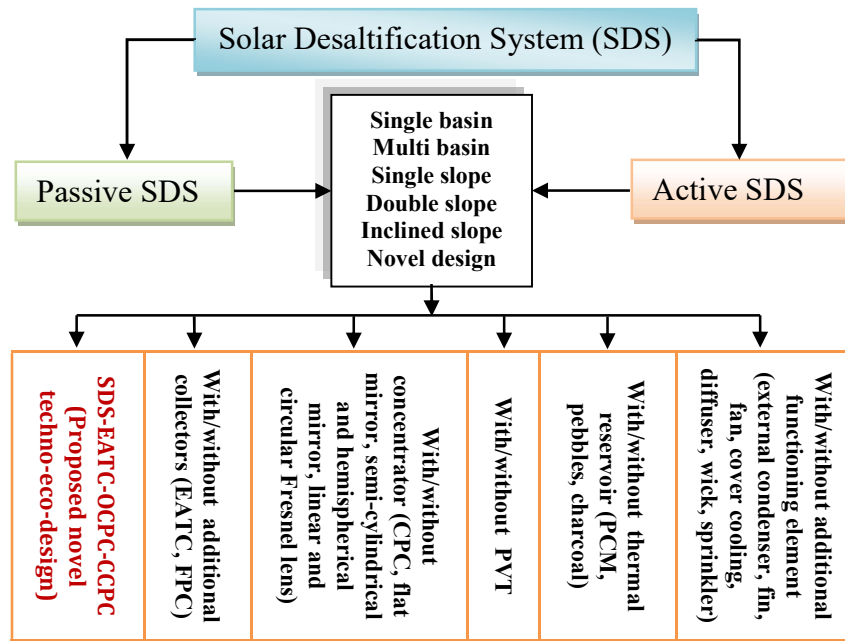


Fig. 1.1 Variety of SDS and different combinations that show a research gap that is being undertaken by introducing the proposed novel techno-eco-design of SDS-EATC-OCPC-CCPC system

## 1.2 Solar Desalination System (SDS)

Solar desalination systems (SDS) use richly available solar irradiative energy but to improve its performance and usability some other embryonic medium requires to be used. It imitates the natural hydrological succession with the difference of closed cyclic operation of working. Solar stills are broadly classified as passive solar distillation system (refers still without any kind of external power production or consumption with the help of any external or internal source) and active solar distillation system (refers still with some external or internal power producing or consuming devices). The solar distiller unit is further configured as single and double slope type SDS as well as with various combinations as shown in Figs. 1.2 – 1.3. Fiber reinforced plastic and transparent glass cover is used to prepare distillation system. Still basin liner is kept dark black for absorbing maximum solar radiation. It is generally used South facing for single slope solar desalination systems and East-West facing for double slope solar desalination systems for getting maximum solar radiation in northern hemisphere (Dev et al., 2009 and 2011). The

solar radiation incidents on the inclined glass cover of still, then it comes to water surface after that it comes to still basin liner. All components reflect some solar radiation and rest is absorbed by these and the maximum solar radiation is absorbed by water surface and still basin liner. The dilution of solar radiation through the water mass is based on water quantity, liner area and its absorptive capabilities. Maximum energy is absorbed by basin liner which is convected to water and as a result, rise of water temperature. After that evaporation happens from the evaporative surface of water and it reaches to the inner surface of glass cover and by releasing its latent heat to the glass cover, it condenses there and condensed water trickles go to the lower end of the glass cover in still basin through a particular passage under gravity. In active solar desalination unit, one can apply forced mode of water flow that increases the water temperature and consequently evaporation of water increases. As a result, temperature difference between the evaporative face of water and the inside face of glass cover rises, this causes a faster distillation process.

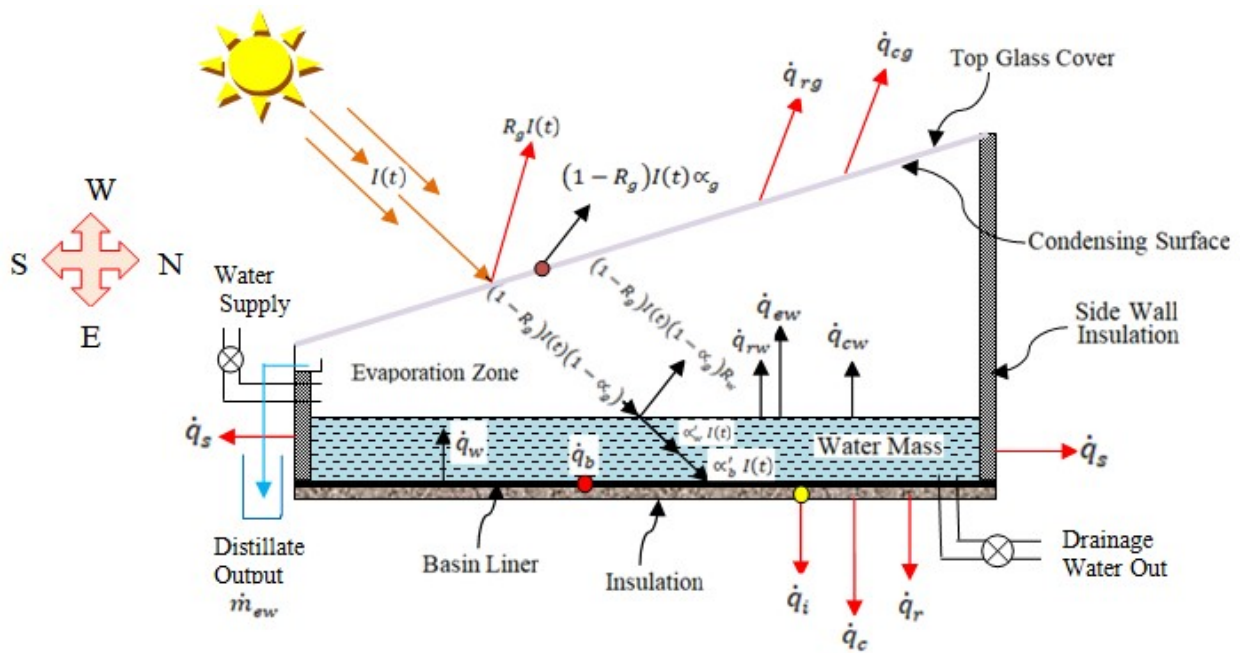


Fig. 1.2 Schematic plan view of conventional SDS system representing solar energy distribution, utilization, and losses accordingly

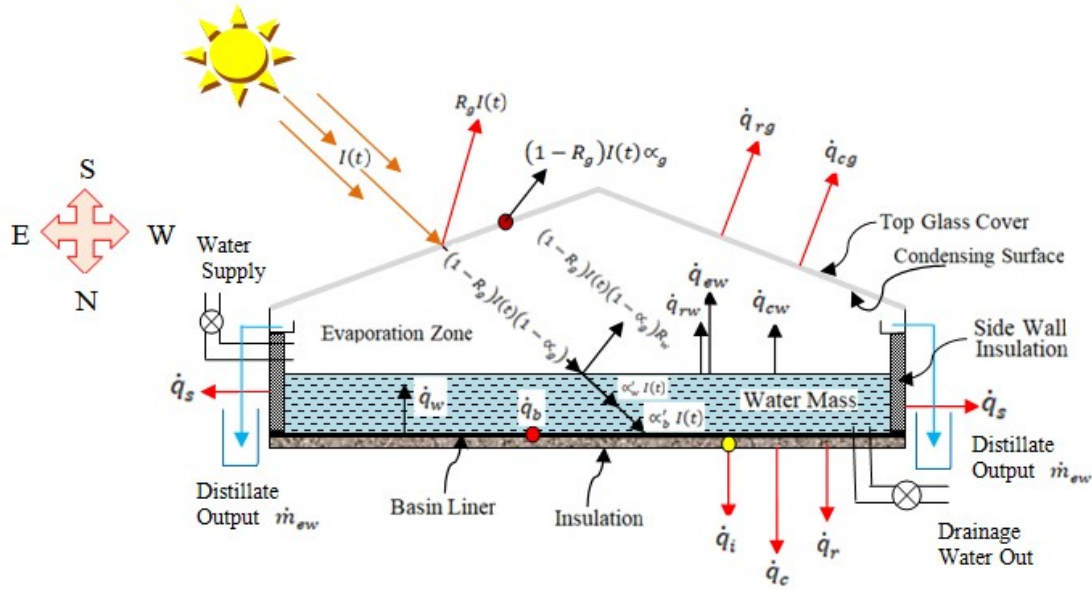


Fig. 1.3 Schematic plan view of conventional double slope SDS system representing solar energy distribution, utilization, and losses accordingly

### 1.3 Solar Thermal Collectors

It can be used external sources for raising the water temperature like PVT, CPC, heat exchangers, fins, FPC and nano-particles, EATC, etc. as shown in Fig. 1.4.

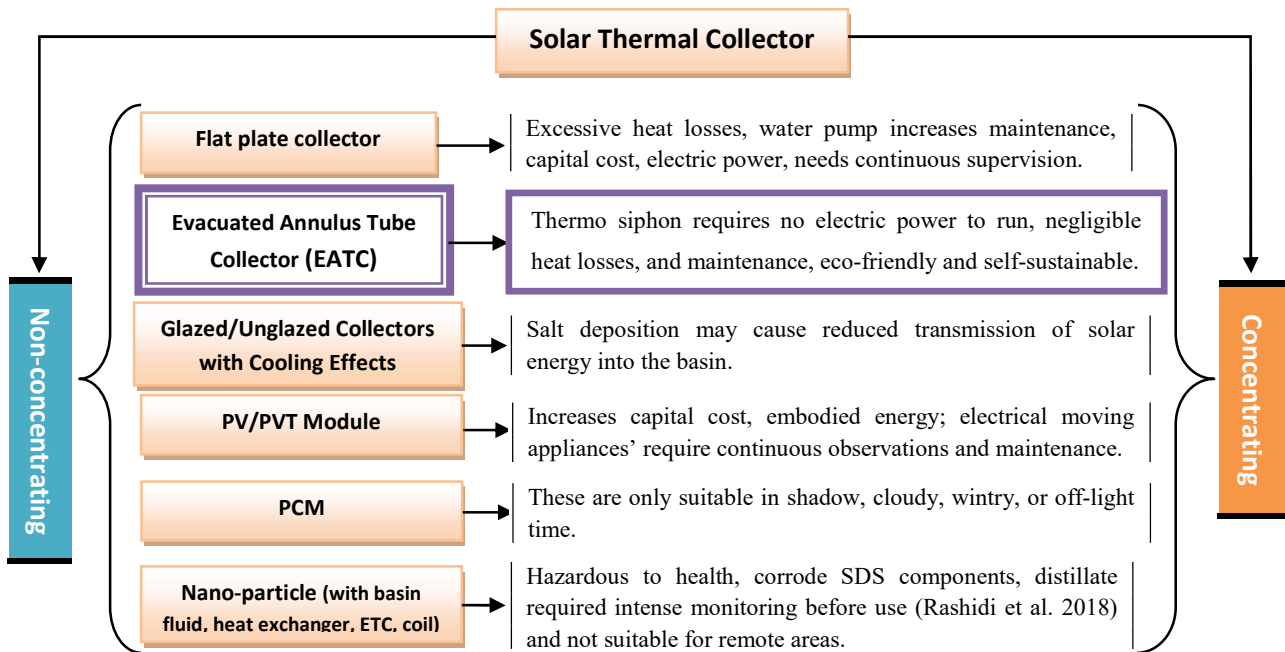
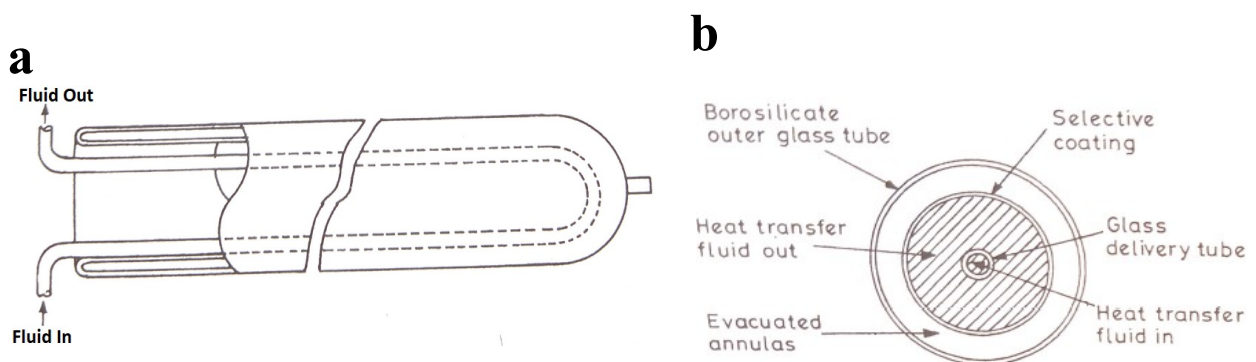


Fig. 1.4 Different solar thermal collectors with its possible hindrances while adaptation of these in comparison to the thermo siphon EATC that are integrated with SDS systems

Generally, pump is used to develop a force circulation of water which is further operated by either direct electricity or by PVT module and other collectors phase change material (PCM) have its individual goodness utilized in shadow, cloudy, wintry, or off-light time. However, collectors with cooling effect produce salt deposition that may cause reduced transmission of solar energy into the basin, hence reduces performance of the system. And, as for as the nanoparticles are concerned, it is hazardous to health, corrode SDS components, distillate required intense monitoring before use and not suitable for remote areas also (Rashidi et al. 2018). Out of these, evacuated annulus collectors are one of the best solar collectors that are utilized in the proposed research work because it has least solar and thermal losses, also doesn't require any solar tracking. Evacuated annulus tube collectors are of various types as depicted in Figs. 1.5 – 1.6. Out of which, evacuated annulus tube collector (EATC) traps the majority of solar irradiative energy into it. Further, the schematic diagrams (Fig. 1.5) are representing various types of evacuated tube collectors as, a. U-tube covered by evacuated glazed surface (*Charter and Window, 1978*), b. Tubular collector with concentric delivery tube (*Beekley and Mather, 1978*), c. Series of single glazed evacuated tube top cover collector, d. Single glazed evacuated glazing with metal tube and absorber plate, e. U-tube with absorber plate inside the single glazed evacuated tube, f. Concentric Cu-tube, steel absorber plate, and Al-reflector, g. Single glazed ETC filled with insulator and peripheral U-tube, h. ETC integrated circular metal fin and U-tube with cusp reflector (*Williams, 1983*), i. Single glazed evacuated tube collector with eccentric heat pipe and cusp reflector, j. Coaxial evacuated tube and heat pipe with metal fin (*Norton, 1992*).



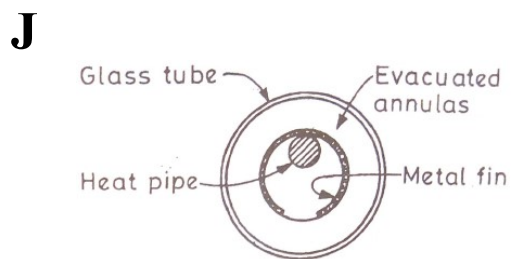
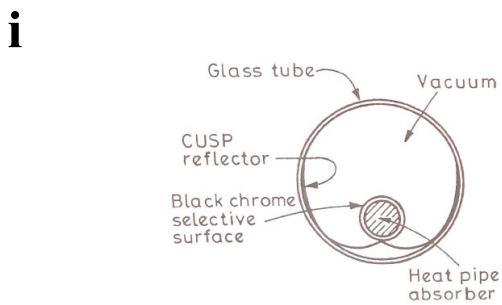
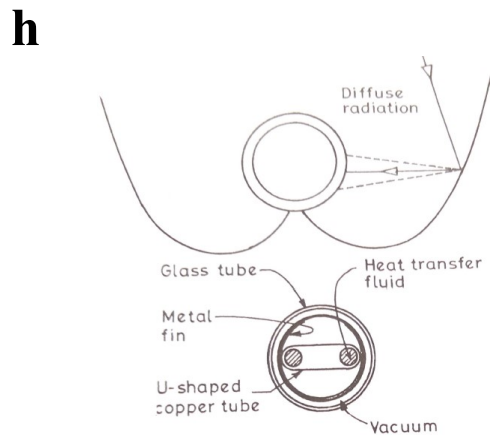
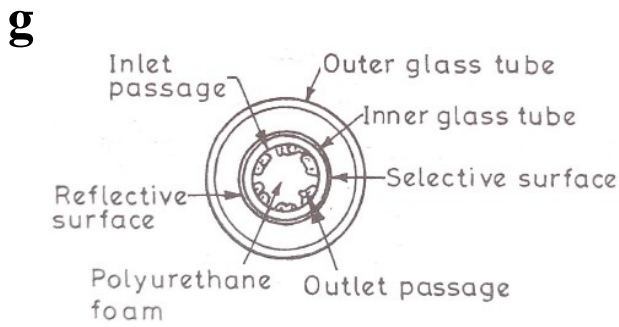
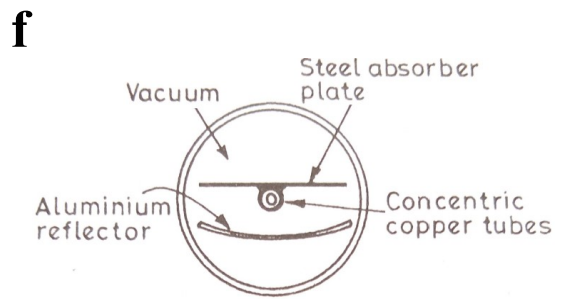
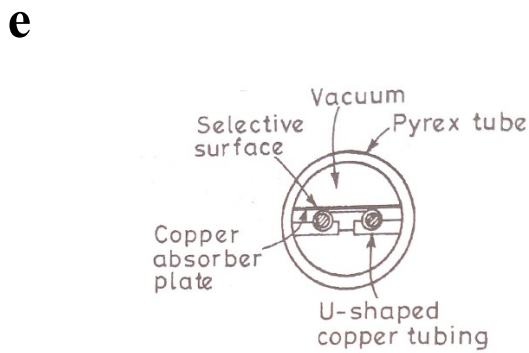
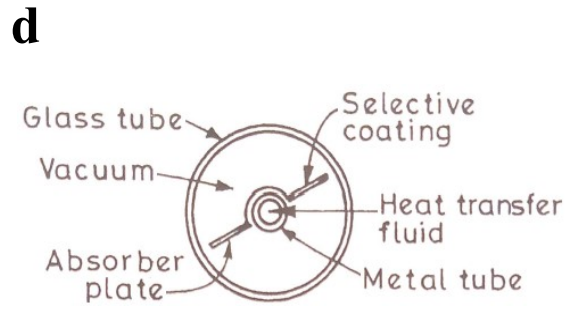
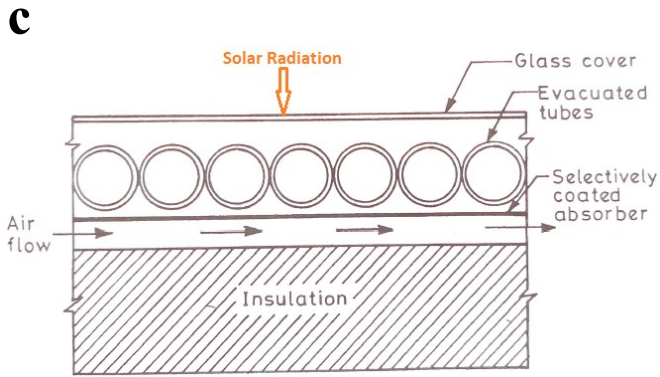


Fig. 1.5. Schematic representation of various types of evacuated tube collectors, (a) *Charter and Window (1978)*; (b) *Beekley and Mather (1978)*; (c – h) *Williams (1983)*; (i – j) *Norton (1992)*

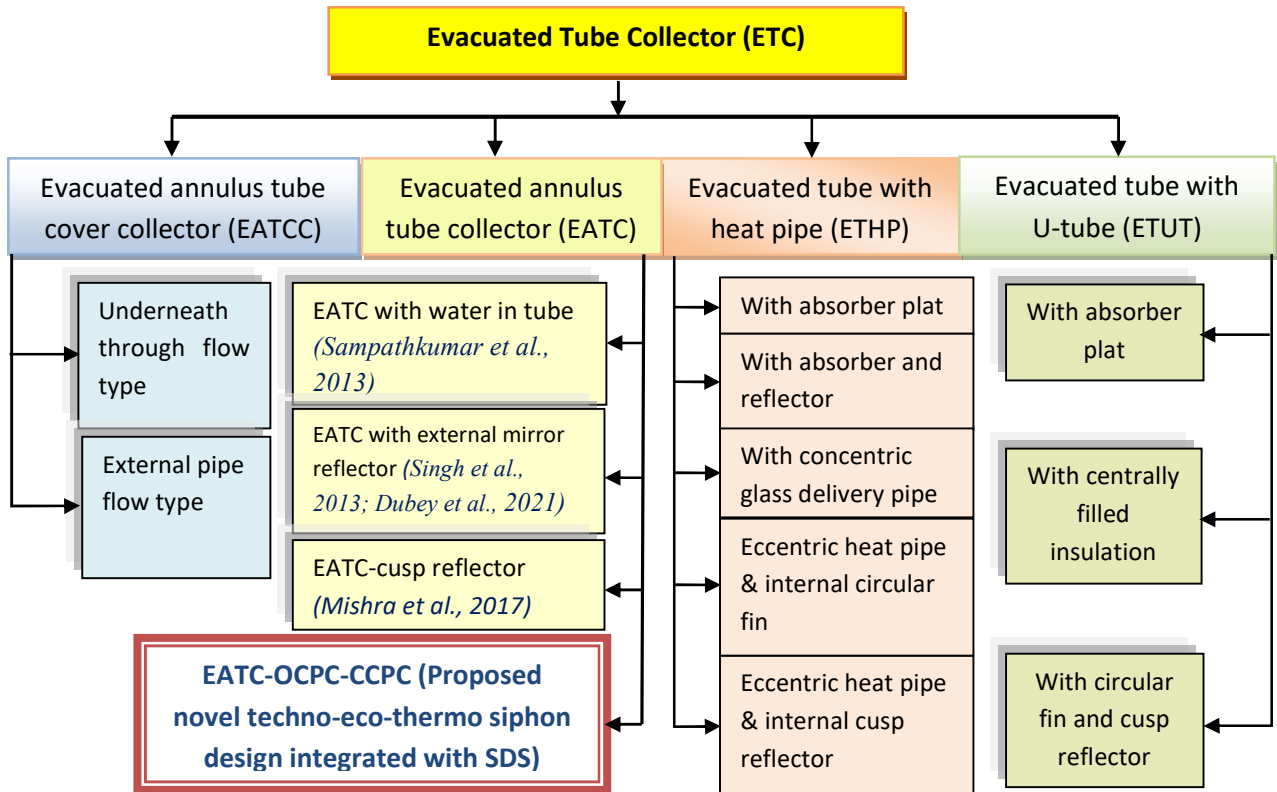


Fig. 1.6. Classification of ETC introduced with novel techno-eco-design combination of EATC that have possible integrations to SDS and also not been introduced in earlier researches

As it is well known that the performance of SDS is directly based on the solar radiation in addition with the proper utilization of it by the system. But, it has been reported that the maximum heat loss (up to 26% of incident solar energy) happens within the range in between basin water mass surface to top glass condensing surface with other simultaneous losses of 11% due to reflection from outer surface of top glass cover, 5% due to absorbed solar radiation into glass cover, about 10% due to condensed vapor inside the solar still itself gets re-evaporated again and again, 7% due to unaccounted heat losses, and 2% from still side walls, edges, and bottom sides, etc. (*Malik et al., 1982*). So it is very much obvious to improve the heat gain with corresponding performance of SDUs, three methodologies can be applied as either do suitable modifications in the system design or associate the system with some efficient supplementary components or both by which the overall heat gain can be improved effectively.

So, to improve the overall performance of the system, a significant solar thermal collector component aligned in the parallel fashion of identical nature, i.e., evacuated annulus tube collectors (EATC) are integrated with the SS-SDS system as represented in Fig. 1.7. The EATC is a proficient association of concentrically integrated with double cylindrical glaze tubing (high borosilicate 3.3 glasses with one end open and another adiabatically closed) having selective absorber coating of three layers (Cu + Stainless Steel-ALN + ALN) over the outer surface of inner glaze under vacuum atmosphere. This unique combination of EATC makes it greatly efficient in receiving more than 95% of the irradiated solar energy incident over the EATC selective absorber coating. The EATC dimensions that have been selected for the current proposed work have OD, ID, tube thickness, and tube gap as 0.058m, 0.047m, 0.002m, and 0.007m, respectively.

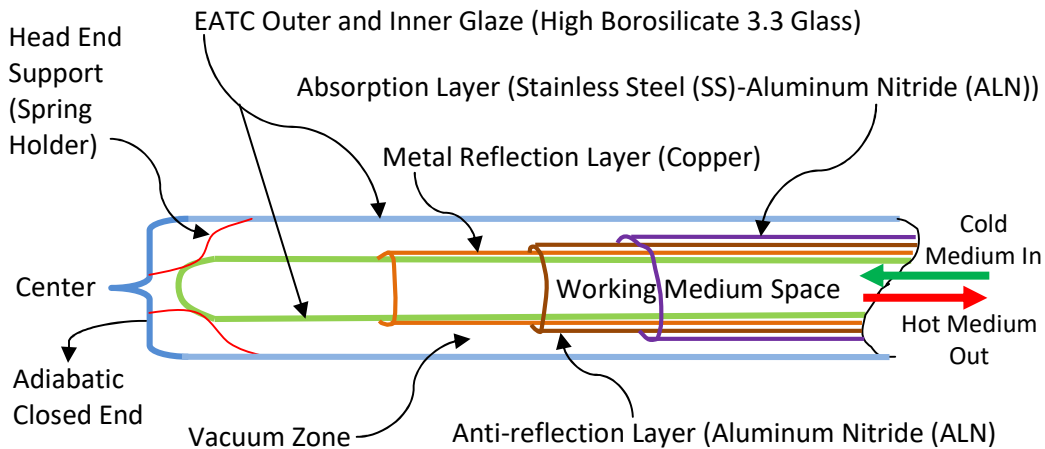


Fig. 1.7. Schematic representation of evacuated annulus double glaze tube collector (EATC)

The concentric double glazed cylindrical tubing with vacuum and selective absorber provides not only support to absorb and trap major short wave high energy solar spectrum but also minimizes the heat loss by allowing minimal high wavelength (very low energy) radiations transmitted out to the EATC tubing. And, it is due to the infinite reflections inside the parallel double glazing absorbs most of the solar spectrum energy within it and possible to leave marginal low energy waves outside it, as represented in Fig. 1.8. In the proposed set ups of techno-eco-design analysis of SS/DS-SDS-EATC-MCPC, the EATC has been utilized with its ultimate potential ability due to the participation of the all-round periphery of EATC to absorb the maximum possible solar energy incident (direct or indirect) over it. And, thermo siphon



working principle makes it further economical and efficiently self-sustainable for the continuous heating of water loop during the sufficient daylight time. A manual operated valve mechanism is provided at the opening of EATC to check the reverse flow of water mass while having insufficient temperature difference for the operation of automated thermo-siphon working conditions, and at that time, the composite basin liner will supply heat to its ultimate capacity to the basin water mass throughout the off light time for the continuous production of potable water.

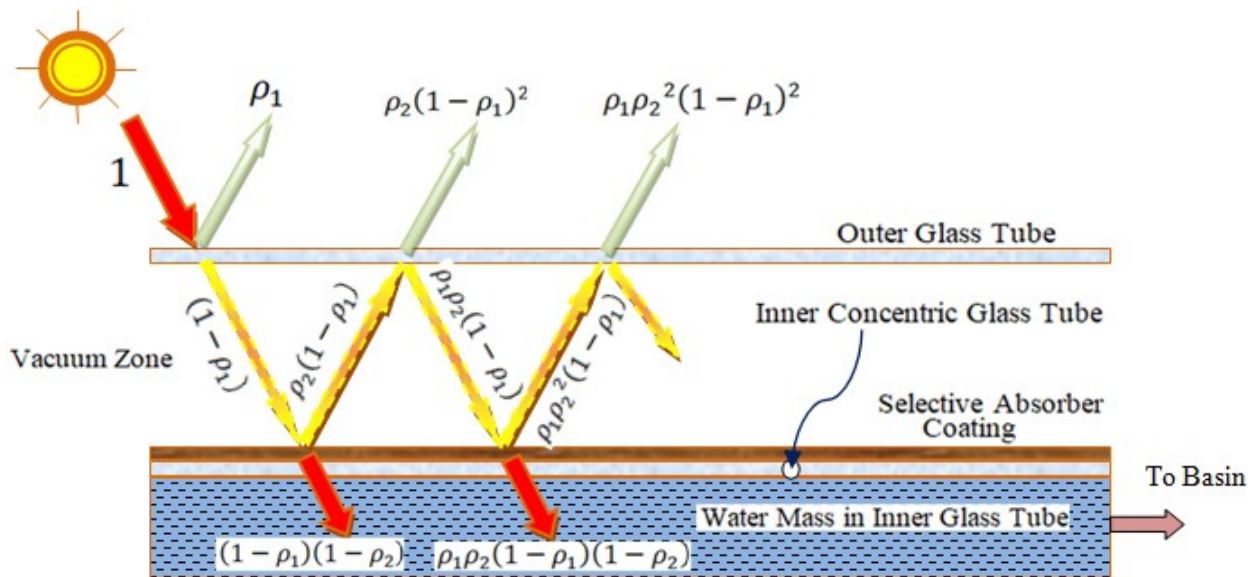


Fig. 1.8. Fractional representation of reflectivity and transmittance during the propagation of solar irradiation through glazing for ETC

#### 1.4 Organization of Thesis

The overall *Thesis* is prepared in five chapters comprises, introduction, literature survey, methodology (i.e., a sequential follow up and thermal modeling for the evacuated annulus tube collector assisted solar desalination systems), results and discussion, conclusions and recommendations for future work followed by the appendixes, references, list of publications, and curriculum vitae. Further, the schemes of the entire chapters are represented as follows:

**Chapter one** reflects the realistic background of consumable water among human beings and related issues of its consumption. It defined the generalized introduction towards solar desalination technology with a motivation related to necessity of potable water for the

sustainable growth of inhabitants. This chapter offers a better solution for the production of potable water, i.e., solar desalination technology. Further, the types of SDS systems, working principle, heat distribution scheme with losses over the different segments of the components have been discussed. Finally, the organization of the thesis has been presented here for the better understanding of the systematic flow of the research work done.

**Chapter two** establishes a vital stage of solar desalination technology (historical background to latest developments) along with a brief glimpse of different systems for the treatment of brackish/saline water in comparison to the other water treatment devices and technologies through the literature survey. In this chapter, the problem statement has been identified with the proposed research gap and targeted objectives for the present research work that has been carried out at the *Delhi Technological University (DTU), Delhi*. Also, the research scope and research contribution to the society have been presented in this chapter to justify the goodness of this technology towards the society and thus the nation.

**Chapter third** sets the analytical methodology with sequential steps to achieve the research objectives as mentioned in chapter two. The exploration of evacuated annulus tube collector assisted single and double slope solar desalination systems with its detailed assumptions, analytical parameters, system description, and specifications have been done that are utilized while developing thermal model of the proposed systems. Then the detailed thermal model and characteristic equations along with the respective performance parametric observations are given in terms of mathematical expressions under the meteorological conditions of *New Delhi* for a clear archetypal day in the summer season of the month June.

**Chapter four** contains the results and discussion for both the proposed systems (SS/DS-EATC-MCPC) that comprise the evaluation of glass cover temperatures, water (basin and EATC) temperature, effect of solar insolation for thermo siphon mass flow rate in EATC due to MCPC, yields, hourly energy-exergy and corresponding efficiencies of the system, energy-exergy matrices, various economic analyses (economic, exergo-economic, and environ-economic), and the evaluation of pollutants emission-mitigations, and environmental cost (i.e., carbon credit values in the international market) of the proposed systems. Further, a comparative study is being presented for both the proposed systems with each other as well as with the

previous researches based on the similar parameters of different systems and selected accordingly the best performing solar desalting system under the respective parameters.

The **chapter five** represents the conclusion of the entire observations made for both the proposed systems in this *Thesis*. Further, the entire observations are concluded with recommendations for future work that may enlighten the researchers to move ahead for further possible developments in this field for the betterment to the environment, and the society.

*The next chapter establishes a vital stage of solar desalting technology (historical background to latest developments) along with a brief glimpse of different systems for the treatment of brackish/saline water in comparison to the other water treatment devices and technologies through the literature survey. In this chapter, the problem statement has been identified with the proposed research gap and targeted objectives for the present research work that has been carried out at the Delhi Technological University (DTU), Delhi. Also, the research scope and research contribution to the society have been presented in this chapter to justify the goodness of this technology towards the society and thus the nation.*

**CHAPTER: 2**

*LITERATURE SURVEY*

## CHAPTER: 2

### LITERATURE SURVEY

---

#### 2.1 INTRODUCTION

As the population keeps increasing, this creates more difficult situations for freshwater demand and supply chain and hence many of the people are forced to use contaminated, brackish, or salty water. Contaminated water cannot be directly used because it can cause various health related problems such as skin cancer (*Tseng, 1977*). A report has also been evolved and confirmed water born diseases like skin cancer (*EPA, 1988, 2007*). Moreover, black foot disease, diarrhea, etc. was reported by *Lu (1990)*. So, to assure the purity of consuming water before its use is quite necessary. *Pugsley et al. (2016)* established a ranking system to point out the potable water scarce or water stressed continents around the world in terms of water stress index that reflect most of the middle eastern continents along with major part of India under gone in the highly potable water stress zone ( $>0.422$ ). As for as the Indian continent is concerned, it is a tropical country having more than 16% of the total population on the earth along with the 4% of potable water accessibility only and that may exceed further by the increase in population as expected based on the past experiences to be 1.6 billion up to the year 2050. Several places in India mainly rural and coastal zones are facing severe scarcity of potable water and to meet the expectations of the demand of potable water, solar desalination systems may play very important role in this field, as depicted in the following literature survey.

##### 2.1.1 Solar Still Viabilities

The existing conventional water treatment technologies, such as reverse osmosis technology (*Malaeb and Ayoub, 2011*) and membrane desalination technology with advancements (*Camacho et al., 2013; Goh et al., 2016*) were studied and reviewed. As these systems are using conventional power sources to run the system having higher installation, running, and maintenance costs that restrict its applications in remote areas, especially where such resources are not available. In contrast, the solar desalination system utilizes lavishly and freely available renewable energy sources like sun light energy and wind energy to actuate the overall system for the water treatment process. The historical background of solar desalination was mentioned by

*Nebbia and Menozzi (1966)*. After that various effects of design, working conditions and climatic parameters were revealed on the basis of daily, monthly and annual performance of passive type single, double slope solar distillation system specifically for Indian climatic conditions (*Garg and Mann, 1976*). *Soliman (1976)* presented his first ever study on the working and performance of solar distillation associated with flat plate collector (FPC). *Sodha et al. (1981)* analyzed the performance with new design of multiple wick solar distillation system and the minimum thermal capacity was attained at high temperature through wet jute clothe at the basin liner, and achieved the higher absorptivity for the same solar radiation. Later on by *Malik et al. (1982)* in their book presented the past background of solar desalination systems. After that the working and performance of solar distillation associated with flat plate collector (FPC) was revealed by *Rai and Tiwari (1983)* in which they found better yield of the system. *Tiwari et al. (1984)* shows the additional performance improvement by incorporating double condensing cover. The various designs of solar distillation system were studied by *Tiwari and Garg (1985)*. The performance of different designs with higher life of solar distiller units (SDU) was studied by *Tiwari and Yadav (1987)*. They concluded that passive single slope performs better in cold than passive double slope and vice versa in summer. The recital of single slope solar still with collectors and heat exchanger (natural circulation mode) was theoretically analyzed by *Lawrence and Tiwari (1990)*. They showed many advantages of natural circulation mode in passive solar stills over the force circulation mode in active solar stills. Later on, the study of 4 dissimilar designs of SDU (same basin area) was analyzed by *Tayeb (1992)*. He showed that a higher ratio of condensation area to evaporative area leads to a higher productivity. The further improvement of solar stills has been examined by improving heat and mass transfer (HMT) mode, temperature variation between basin water and inner glass cover (*Tiwari et al., 1992 and 2003; Tripathi et al., 2005; Tiwari et al., 2007*). The heat and mass transfer mechanism of SDU by its modeling, theoretical and practical analyses were further examined by *Tsilingiris (2010)*. The experimental study for heat transfer coefficients on single and double SDU at dissimilar basin water depths was investigated (*Dwivedi et al., 2009*). Further, review on various designs of SDUs, performance analysis based on energy matrices, review on special design stills and performance enhancement analysis was done for the given set of conditions of the systems by many researchers (*El-Sebaili et al., 2015; Singh et al., 2018, 2019*).

The improvements in the field of solar desalination technology were continuously improving by the efforts of numerous researchers and presented the advancements in this field by *Singh (2020) and Singh et al. (2020)* that shows the improved results in yield with the proficient combinations of supporting components integrated to solar desalination system and one of that the evacuated annulus tube collectors (EATC). In the positive favor of EATC, *Morrison et al. (2005)* and *Sato et al. (2012)* found EATC as a better solution in its thermo siphon mode due to its natural circulation of hot and cold water mass and uniform inter mixing and exchange of thermal energy to these streams. *Kumar et al. (2014)* observed SDS-EATC and found better performance pertains with the system in terms of energy efficiency (33.8%) and exergy efficiencies, i.e., 2.6% under the influenced mass circulation rate. *Ranjan et al. (2016)* studied SDS system, having exergy efficiency (4.93%) and energy efficiency (30.42%) under the influence of optimum parameters of individual components of the system. Further, different important considerations and implementations of economic, environ-economic, and energy matrices for solar desalination systems have been studied for its feasible viabilities by many researchers in the past couple of years. *Mittal et al. (2014)* found 1.58 kg, 0.0114 kg, and 0.0046 kg emissions of CO<sub>2</sub>, SO<sub>2</sub>, and NO, respectively, while producing one kilowatt of electrical energy through the premium quality Indian coal. In this progression, *Dwivedi and Tiwari (2010)* analyzed SDS system for carbon mitigates and credit values at the rate of \$20.0/ton of CO<sub>2</sub> in the international market and found ₹15,333 carbon monetary value for the thirty years of the system's working life. *Tiwari et al. (2015)* investigated for exergy-enviro-economic of the solar still system and reported better exergy cost like \$6.29/year at the rate of \$14.5/ton of CO<sub>2</sub>. Later on, *Reddy and Sharon (2017)* analyzed evacuated type series flow SDS for environ-economic observations and found an economic establishment with 221.8 tons (CO<sub>2</sub>), 1.6 tons (SO<sub>2</sub>), and 0.7 tons (NO) of emissions. And, SDS with different absorbers was analyzed with better results of the economy and lower yielding cost, i.e., \$0.34/liter (*Yousef et al., 2019*). Further, a study for the tubular SDS gives a much lower yield cost, i.e., \$0.04/liter at the interest rate of 5%, for the 30 yrs. of the system working life, and \$4.42/year exergo-enviro-economic cost (*Bait, 2019*). *Singh and Samsher (2021a)* analyzed the passive solar still having evacuated annulus tube collectors for environ-economical, and energy matrices observations.

### 2.1.2 Techno-Eco Design Viability

The need for techno-eco-design is pretty obvious that may be achieved by the emphasized utilization of the available solar energy (direct, diffuse, or reflected) over the integrated solar desalting system with the help of additional functioning elements and different solar thermal collectors as shown in Figs. 1.1, 1.4, and 1.6. Subsequently, the progressive development of different techno-designs of EATC assisted SDS systems are presented in this segment, which indicates the research gap undertaken in this regard for the proposed work of research.

*Dev and Tiwari (2012)* utilize a thermo siphoned SDS-EATC (24 nos.) with an additional heat chamber that has unmanaged use of EATC because the more numbers of EATC has more underneath areas of the tube's periphery left without its significant use. *SamPATHKumar et al. (2013)* experimentally investigated with a large number of EATC (15 nos.) integrated with SDS system. Also, *Singh et al. (2013)* undertook a theoretical study for a passive type SDS-EATC system having EATC (10 nos.) and found 3.8 l/m<sup>2</sup> in a day yield with the respective energy (54.4%) and exergy (8.25%) efficiencies. In the same consequence, *Yari et al. (2016)* studied SDS-EATC with 30 nos. of EATC in forced mode of water mass circulation and observed very disappointing results (58% decrement in yield) again as expected and experienced by the previous work done by *Kumar et al. (2014)*. Then, *Issa and Chang (2017)* experimentally analyzed the SS-SDS (30°) with EATC (5 nos.) lay parallel to horizontal and found 3.6 l/day/m<sup>2</sup> yield, 19% thermal efficiency. It was due to the unused half EATC and its horizontal orientation. Whereas, *Patel et al. (2019)* tested experimentally on a series of SDS-EATC systems to desalinate high saline water and have EATCs at 30° inclined orientation and reported 4.05 liters yield/m<sup>2</sup>/day with 28.23% still efficiency with the unused bottom half of EATC. Later on, *Singh (2020)* revealed many other possibilities of novel designs and proficient combination with different elements utilized in solar desalting technology as a next step to enhance the overall performance of the solar desalting systems. It is pretty clear from the above study that the SDS-EATC with thermo siphon working principle is one of the best practices.

### 2.1.3 Thermo Siphon Considerations

This context reveals the usability of thermo siphon characteristics in EATC and assisted systems with the possible research gap identification in terms of the existing thermo siphon



model and techno-design considerations. *Morrison et al. (2005)* analyzed a set of 21 numbers of EATC for solar heating and evaluated respective characteristics of performances that influence the circulation rate of mass flow in EATC having enough velocity to transport the absorbed solar heat and also creates turbulent effect into the SDS-EATC that disturbs the scaling, stratification, and other deposition into it. *Budihardjo et al. (2007)* worked on EATC to analyze the effective water heating under responsible parameters under the rectangular loop of thermo siphon model for one Sun solar radiation. Further, *Budihardjo and Morrison (2009)* extended the above research in the same mode with more numbers of EATC (30) and compared the results with FPC performances. The results showed the performance of EATC better than the FPC. *Koffi et al. (2008)* analyzed thermo siphon approach in a solar water heating system theoretically and experimentally with a very good agreement of results.

As far as the EATC applications in all over the globe, it has a remarkable scenario all over the world and plays important role in coping up the demand and supply of energy to the society for various purposes such as solar water heating, space heating, desalination plants, etc. *Mamouri et al. (2014)* experimented on inclined SDS integrated ETC heat pipe under 0.02 m water depth and due to EATC, basin temperature reaches up to 83.93°C and produces 6.35 l/m<sup>2</sup>/day maximum yield because of the copper heat pipe concentrically involved in ETC tube that is responsible for heat absorption and release to water mass in a thermo siphon way from heat pipe. *Mosleh et al. (2015)* revealed a new design in which a solar tracked ETC-CPC assisted heat pipe with an external tube condenser. The effective heat utilized by brackish water inside basin is directly affected by heat pipe and depends on partial filling of basin i.e. decrease in water column increases water vapor with corresponding higher yield. It was due to lesser water column provides larger space for vaporization. The overall system performs better for oil filled heat pipe (HP) and produces 0.93 l/m<sup>2</sup>/h with 65.2% efficiency. *Behnam and Shafii (2016)* experimented for desalination with humidification-dehumidification of water in a closed loop cycle after heating through ETC-HP. System performs well with 6.3 l/m<sup>2</sup>/day and 65% efficiency because of the vapor chamber charged with closely reversed moist air cycle through air pump but may cause a problem to pump in terms of rusting, performance and ultimately maintenance of the system due to moist air circulation through it. Also, *Singh et al. (2017)* analyzed theoretically SDS-EATC and found 8 l/m<sup>2</sup>/day yield for 12 optimum numbers of EATCs. This was further improved by utilizing compound parabolic collectors (CPC) underneath the EATCs and having

all other parameters same as before but the results appeared not considerably high as expected by the use of CPC in the existing system due to the limitations in the analysis. Further, *Abdaspour et al. (2019)* revealed a new approach for vacuum pump that is utilized to transfer water vapor of cylindrical basin connected thermo siphon operated EATC-U-tube (oil filled) to separately established condensing chamber and reported  $8.07 \text{ l/m}^2/\text{day}$  maximum yield with 50% efficiency at 0.094 \$/l potable water cost. The result appeared much better due to better insulation (glass wool) and possibility of ~100% condensation of vapor with the help of vacuum pump and water pump feeding vapor and water to condensing chamber. *Xu et al. (2019)* revealed a system producing super heated steam that is further processed for distillate production through EATC-HP, steam chamber, and water cooled condenser and found  $1.3 \text{ l/m}^2/\text{day}$  at  $130^\circ\text{C}$  temperature.

Further, evacuated solar collectors have many types but few of them are popular in which EATC is the simplest form of ESC and these can easily follow passive (thermo siphon) as shown in [Fig. 2.1](#). To improve the system performance, EATCs are the best choice due to its outstanding thermal performances with no convective and conduction heat losses with nominal radiation losses only and also doesn't require any solar tracking that makes the element much efficient to improve overall heat gain drastically. EATC is much cheaper and have economic establishment and long life utility with easy transportability and convenient installation that well handles adverse climatic conditions also (*Morrison et al., 1984; Kalogirou, 2003*).

*Dev and Tiwari (2012)* experimented on single slope ( $30^\circ$ ) solar still with inclined ( $40^\circ$ ) EATC and heat chamber in the composite climate of New Delhi, India under  $1 \text{ m}^2$  basin area. System contains 220 kg water mass in basin with additional water in 24 EATCs. Under such conditions, the performance of the system reported as  $630 \text{ l/m}^2/\text{year}$ , with  $1.9 \text{ l/m}^2/\text{day}$  and 30.1% thermal efficiency.

*Sampathkumar et al. (2013)* experimented on single slope still ( $30^\circ$ ) with thermo siphon EATC placed horizontally in the climatic regime of Tamilnadu, India. The results were observed for 235 days. System had yield up to  $3.9 \text{ l/m}^2/\text{day}$  with 43% thermal efficiency. *Singh et al. (2013)* investigated theoretically for single slope still with EATC in the composite climate of New Delhi, India for  $1 \text{ m}^2$  basin area assisted EATC that increases the overall solar receiver area by 1.65 times the basin area. System performs better under 0.03 m water depth and shows yield  $3.8 \text{ l/m}^2/\text{day}$  with 54.4% and 8.25% energy and exergy efficiencies respectively.

*Kumar et al. (2014)* had improved their previous work by utilizing pump in the existing system for providing forced circulation (0.006 l/s) of water mass maintaining water depth (0.03 m) under the same parameters as taken before. But the result was not satisfactory because of only 2.6% improvement in yield output under utmost optimum conditions and moreover 8.7% loss appeared in yield output while system running in normal conditions days. Efficiencies are also decreased in this observation and found as 33.8% and 2.6% energy and exergy efficiencies respectively which are 37.9% and 68.5% lower than the previous results correspondingly.

*Shafii et al. (2016)* analyzed EATC (30°) with steel tube condenser to treat water in the climatic conditions of Tehran, Iran. And found 52.6% efficiency for 80% filled water in EATC without steel maze and produces 0.83 l/m<sup>2</sup>/h on the other hand 65.6% efficiency for the same EATC with steel maze produces 1.01 l/m<sup>2</sup>/h yield at the cheaper cost for 0.0134 \$/l. *Yari et al. (2016)* analytically studied about the power production along with solar distillation through thermo siphon EATC (30 nos.) based on same parameters as of earlier study done by *Singh et al. (2013)* and reported 58% decrease than the earlier study due to the overall increase in temperature difference at condensing top cover that can be further supported by PV module mounted over the top of still's basin. As the temperature gain by PV module was high as 88.82°C and basin temperature up to 90.42°C that is quite enough to decrease in distillate performance, that is as fast as the vapor produces as slow as the condensation follows.

*Issa and Chang (2017)* experimented on single inclined solar still with EATC (5 nos., horizontal orientation) in the climatic conditions of West Texas where higher wind speed recorded as 6.4 m/s with ambient temperature as 30.95°C. The result was observed as 3.6 l/m<sup>2</sup>/day maximum daily yield with 6 years payback time of the system. The improved yield was appeared due to open atmospheric conditions having airy surrounding which maintains higher temperature difference in condensing area that is helpful to produce greater yield.

*Patel et al. (2019)* establishes a series of systems and experimented for treating sea water in the meteorological conditions of Gujarat, India. The experiment was conducted for 0.04 m basin water depth under the effective basin area of 2.12 m<sup>2</sup> and results better yield output up to 4.05 l/m<sup>2</sup>/day and 28.23% system efficiency. System easily overflows the salt but also there is a big challenge for salt deposition of salt over still, heat chamber and EATC.

Table 2.1: Overview of performance observations and applications of EATC assisted SDU for the related research gap identification

System design	Working and tool used	Solar receiver area	Performance	Improvements	Research Gap
SDS- EATC- HC ( <i>Dev et al., 2012</i> )	Passive for EATC chamber and active for heat chamber to SDS. Analytical work and MATLAB	792% due to ETC (24) only for 840 W/m <sup>2</sup> solar intensity	Thermal efficiency 30.1% with 0.275, 0.41 l/m <sup>2</sup> /h maximum yields in winter and summer respectively and 1.9 l/m <sup>2</sup> /day maximum daily yield with 56.8°C, 94 °C maximum water temperatures attained by ETCs respectively.	It improves thermal gain by ~3.96 times of solar heat gain absorbed by the overall solar distiller system. Direct contact of both the working mediums tends instant mixing and uniform heat gain.	Lengthier water loop, No. of EATC with unused bottom half and additional embodied energy
SDS - EATC ( <i>Sampath kumar et al., 2013</i> )	Passive working. Experimental work validated with theoretical work and MATLAB	495% due to ETC (15) only for 980 W/m <sup>2</sup> solar intensity	System thermal efficiency 43% with 7.03 l/m <sup>2</sup> /day maximum daily yield with 86°C maximum water temperature attained by ETC and basin.	It improves thermal gain by ~2.48 times of solar heat gain absorbed by the overall solar distiller system. Direct contact of working mediums tends instant mixing and uniform heat gain.	Number of EATC and unused bottom half of ETC with additional embodied energy
SDS - EATC ( <i>Singh et</i>	Passive working to heat saline	330 % due to ETC (10)	System thermal efficiency 54.5% with 3.8 l/m <sup>2</sup> /day	It improves thermal gain by ~1.65 times of solar heat gain	Number of ETC and

<i>al., 2013)</i>	water of SDS. Analytical work and MATLAB	only for 610 W/m <sup>2</sup> solar intensity	maximum daily yield with 94°C maximum water temperature attained by ETC and basin.	absorbed by the overall solar distiller system. Direct contact of working mediums tends instant mixing and uniform heat gain.	unused bottom half of ETC with additional embodied energy
SDS - EATC ( <i>Kumar et al., 2014)</i>	Active working for EATC to heat saline water of SDS. Analytical work and MATLAB	330% due to ETC (10) only for 610 W/m <sup>2</sup> solar intensity	Thermal efficiency 33.8% with 3.47 l/m <sup>2</sup> /day optimum yield and 3.9 l/m <sup>2</sup> /day maximum possible yield with 92.6°C maximum water temperature attained by ETC and basin.	It improves thermal gain by ~1.65 times of solar heat gain absorbed by the overall solar distiller system but mass circulation decreases optimum temperature increment.	Number of EATC and unused bottom half of EATC with additional embodied energy
EATC-HP-CPC and tube condenser ( <i>Mosleh et al., 2015)</i>	EATC-heat pipe to basin water and condensation in a separate chamber. Experimental work	0.27 m <sup>2</sup> area for ETC (1), 1.8 m <sup>2</sup> for tracked intensity of 790 W/m <sup>2</sup>	Maximum thermal efficiency up to 65.2% with 0.93 l/m <sup>2</sup> /h maximum yield with 80°C maximum water temperature in basin.	CPC improves thermal gain of the system due to higher concentration ratio (6.77). Larger basin column improves better vaporization.	Condenser increases embodied energy and lower ΔT reduces performance
Steel tube condenser-EATC ( <i>Shafii et al., 2016)</i>	EATC heats saline water and produces excessive steam.	100% due to ETC (2) only	Thermal efficiency 65.6% with 0.83 l/m <sup>2</sup> /day yield (without maze) and 1.01 l/m <sup>2</sup> /day	Steel maze improves thermal efficiency by 2.4% than without steel maze.	Unused bottom half of EATC with

	Experimental work		maximum yield (with steel maze) and 97°C for ETC.		additional embodied energy
EATC with single inclined solar still ( <i>Issa et al., 2017</i> )	Active working for ETC to heat saline water of single inclined solar still. Experimental work	165% due to ETC (5) only for 870 W/m <sup>2</sup> solar intensity	System thermal efficiency 19% with 3.6 l/m <sup>2</sup> /day optimum yield in a day with 80°C maximum water temperature attained by ETC and basin.	It improves thermal gain by ~1.65 times of solar heat gain absorbed by the overall solar distiller.	Unused bottom half of EATC with additional embodied energy
SDS - EATC ( <i>Yari et al., 2016</i> )	Passive working for ETC to heat saline water of SDS. Theoretical with MATLAB	990% due to ETC (30) only for 610 W/m <sup>2</sup> solar intensity	System thermal efficiency 54.5% with 4.77 l/m <sup>2</sup> /day maximum daily yield with 92.42°C maximum water temperature attained by ETC and basin.	It improves thermal gain by ~4.8 times of solar heat gain absorbed by the overall solar distiller system. Direct contact of both the working mediums tends instant mixing and uniform heat.	Number of EATC and unused bottom half of EATC
SDS - EATC-U tubes ( <i>Singh et al., 2017</i> )	Active working of system and major solar heat collection by U-tube and basin. Theoretical	24% due to ETC (12) only for 950 W/m <sup>2</sup> solar intensity	Optimum performance with ~ 8 l/m <sup>2</sup> /day maximum yield.	Exposed u-tube section improves thermal gain. Cleaner use of ETC and water regulating (0.016 l/s) pump improves performance.	Number of ETC, unused bottom half of ETC with additional embodied energy

	with MATLAB				
Stepped solar still-EATC (Patel et al., 2019)	Passive working for ETC to heat saline water of heat chamber and still. Theoretical with MATLAB	14.2% due to ETC (5) only for 716 W/m <sup>2</sup> solar intensity	System thermal efficiency 28.23% with 4.05 l/m <sup>2</sup> /day maximum daily yield with 70.5°C maximum water temperature in basin and 72.2°C attained by ETC.	It improves thermal gain of basin water. Stepped basin improves better vaporization and condensation, also self cleanable of deposited salt over water surface.	Number of EATC and unused bottom half of EATC
EATC-oil filled U-tube with vacuum pump (Abbaspo ur et al., 2019)	Active heat and vapor transfer of U-tube and basin to condenser accordingly. Experimental work	0.53 m <sup>2</sup> area for ETC (2)	Maximum thermal efficiency up to 50% with 8.07 l/m <sup>2</sup> /day maximum yield.	Exposed u-tube section improves thermal gain. Vapor chamber and water pump improves condensation.	Unused bottom half EATC with additional embodied energy
EATC-HP with evaporator external condenser (Xu et al., 2019)	Passive heat and vapor transfer to condenser. Experimental work	5.7 m <sup>2</sup> area for ETC (24)	Steam yield increased up to 25% for 20% liquid filling ratio in Cu tube heat pipe.	Exposed HP section improves thermal gain. Condenser chamber charged with steam and cold water.	Unused bottom half of EATC with additional embodied energy
EATC with	Thermo siphon	396% due to	System thermal efficiency 49.9%	It improves thermal gain by ~1.98 times	Unused bottom

semi-cylindrical still with 'V' top cover (Feilizadeh et al., 2019)	working for ETC to heat water of modified solar still. Experimental work	ETC only for 990 W/m <sup>2</sup> solar intensity	with 16.96 l/m <sup>2</sup> /day optimum yield in a day with 76°C maximum water temperature attained by basin.	of solar heat gain absorbed by the overall solar distiller.	half of EATC with additional embodied energy
Forced flow based DS-SDS-EATC (Dubey et al., 2021)	330% increase due to EATC (10 nos.) under 610 W/m <sup>2</sup> solar radiation	330% increase, EATC (10 nos.) under 610 W/m <sup>2</sup> solar radiation	33.8%, 4.9% energy, and exergy efficiencies, respectively, with ~5.5 l/m <sup>2</sup> daily yields reaching 98.9°C max water temperature.	The improvement in thermal gain up to ~1.65 times as compared to the SDS. Performance decreases with the increase in water temperature.	No of EATC and non-uniform used bottom half EATC, extra embodied energy

## 2.2 RESEARCH GAP

The mentioned literature survey shows extensive work on passive and active solar desalination systems (Table 2.1). However, less literatures available on the analysis of evacuated annulus tube collectors assisted solar desalination systems (SDS-EATC) with variety of modifications in it and indeed a wide range of applicability of EATCs is possible in potable water production systems. The usability of EATC (45°) in SDS (30°) systems based on thermo siphon working principle is represented by some of the researchers as Singh et al. (2013) investigated theoretically. Sampathkumar et al. (2013) experimented on single slope still (30°) with thermo siphon EATC (0°). Further, basin type solar desalination systems incorporating compound parabolic concentrator collectors and evacuated annulus tube collectors have not been analyzed by any researchers. Also, response of solar insolation on collectors due to concentrators



for thermo siphon approach, in EATC assisted CPC and cusp CPC have not been analyzed by any other researcher. Hence, basin type solar desalination systems integrated with compound parabolic concentrator collector and evacuated annulus tube collectors will be analyzed in the proposed research. The analysis will be done on the basis of energy metrics, various economic analysis of the system, various efficiencies and productivity. The performance of the proposed system will be compared with results of earlier researches also.

### 2.3 PROBLEM STATEMENT WITH RESEARCH OBJECTIVES

The research gap motivates to contribute ahead in this area up to certain extent that can establish a mile stone in the field of solar powered potable water production technology. Based on the research gap, certain problem statements have been established as,

- i. Treatment of brackish water with the help of solar desalination technology.
- ii. Suitability to cope up the supply and demand chain of potable water in remote and coastal areas of airy and sunny regions.
- iii. Better utilization of associative components in solar desalination systems up to its optimum performance capabilities.
- iv. Establishment of environment friendly and economic renewable energy system in terms of yield production, and operational aspects throughout the service life.

To solve the above identified problem statements, the following research objectives have been framed that can be achieved by the analytical studies of the proposed systems that have been taken in the current research work as shown in [Fig. 2.1](#).

- i. To develop a new system for potable water production
- ii. To do modeling of the proposed system
- iii. To analyze system performance based on energy, exergy, and productivity
- iv. To carry out energy matrices and different economic analysis of the system

### 2.4 RESEARCH SCOPE

The analysis of evacuated annulus tube collectors assisted solar desalination systems based on thermo siphon working principle is quite required to reveal the next level of development in the field of solar desalination technology. Further, many more researchers have also been worked

in this area with certain research gaps and have been encountered in the form of a glimpse, as represented in Table 2.1. So by fulfilling the research gap (improper utilization of entire huge number of EATC, rectangular thermo siphon loop, unused or imbalanced use of EATC's underneath segment) one can improve the production of potable water and also, holds better services by the application of modified compound parabolic concentrators (MCPC, a set of novel arrangement of parabolic diffusers, i.e., oriented CPC (OCPC) in association with cusp CPC (CCPC) for parallel arrayed EATCs). These are observed in all respect that the proposed systems with novel techno-eco-thermo-siphon-design of EATC-OCPC-CCPC integrated with SDS (Fig. 2.1) is much capable to hold better position than the existing researches in this field. Based on the above study, it is being confirmed that such combinations and response of solar insolation on collectors due to concentrators for thermo siphon approach in EATC assisted CCPC-OCPC have not been analyzed by any researcher so far. So, these novel techno-eco combinations of the proposed systems have better research scope for the betterment to the society.

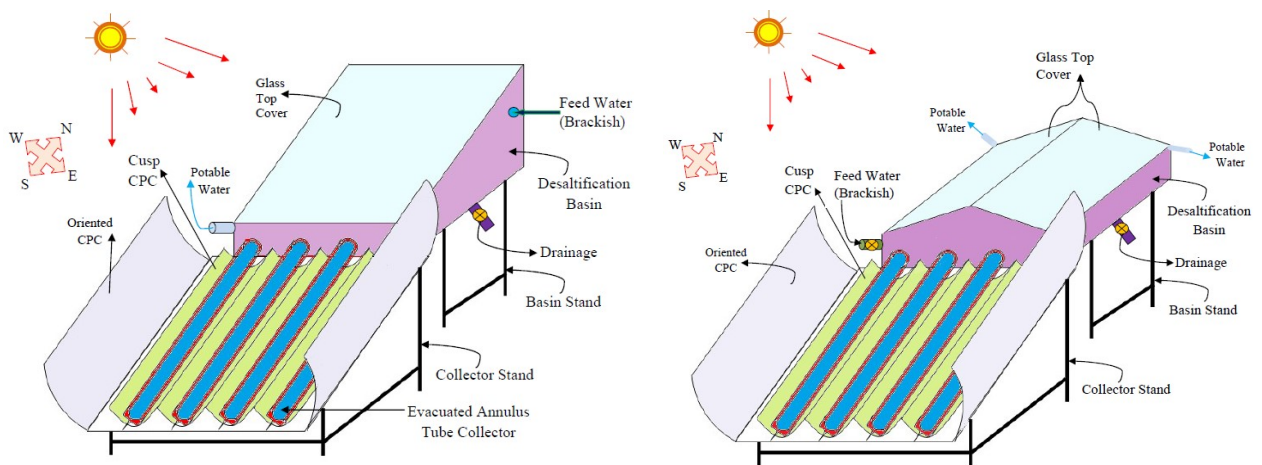


Fig. 2.1. Schematic representation of the proposed systems for the current research work

## 2.5 RESEARCH CONTRIBUTION

The research contribution towards the researchers and the society in terms to potable water production through a proficient, self-sustainable, and economical establishment serving to the society in an eco-friendly manner. The complete set-up has been modeled accordingly to ensure its full-fledged and accurate working throughout the day and thus life. The proposed models show the furthestmost advantage of the modified compound parabolic concentrator for the overall

solar heat transfer mechanism and corresponding mass flow through the EATC to the SDS basin which contributed a lot in the related researches as follows:

- i. Oriented compound parabolic concentrator (OCPC) assisted cusp compound parabolic concentrator (CCPC), i.e., accumulatively MCPC approximates the uniform heat gain through all around the periphery of the EATC.
- ii. Greater mass flow rate due to the downward shifting of conical heat transfer interface of hot and cold water due to heavier and denser fluid property of colder water and this makes additional push to the hot water which facilitates the higher flow velocity of hot water circulation towards the still basin. And, this results in a fast and uniform heat gain with de-stratification and de-scaling effects into the SDS-EATC association.
- iii. Circumferential heat addition into EATC has a longitudinally conical loop and cross-sectionally circular loop for the intermixing of hot and cold water streams. The underneath circumferential area of EATC illuminated uniformly by CCPC and shadow effect of EATC over CCPC and corresponding diffused beam attenuation is neglected.
- iv. The proposed system doesn't need any hydraulic pump, hence saves electrical energy without the constant supervision of the system that directly benefits in terms of the monetary value and additional manpower.
- v. The overall combination produces a comparatively greater yield at a competitive price with lower embodied energy, establishment, running, and maintenance cost. Also, provides the revenue through earned carbon credits from international market, which benefits environmental health and indirect economic returns to the nation of mother land.

*The coming chapter sets the analytical methodology with sequential steps to achieve the research objectives as mentioned in chapter two. The exploration of evacuated annulus tube collector assisted single and double slope solar desalting systems with its detailed assumptions, analytical parameters, system description, and specifications have been done that are utilized while developing thermal model of the proposed systems. Then the detailed thermal model and characteristic equations along with the respective performance parametric observations are given in terms of mathematical expressions under the meteorological conditions of New Delhi for a clear archetypal day in the summer season of the month June.*

**CHAPTER: 3**

***METHODOLOGY***

## CHAPTER: 3

### METHODOLOGY

---

#### 3.0 INTRODUCTION

The exploration of evacuated annulus tube collector and modified parabolic concentrator assisted single and double slope solar desalination systems (i.e., proposed models for the present research work) with its analytical parameters, and specifications have been done. Then the detailed thermal model and characteristic equations along with the respective performance parametric observations (yield, energy-exergy gain, efficiency, matrices, and environ-economics, etc.) are given in terms of mathematical expressions under the meteorological conditions of New Delhi for a clear archetypal day in the summer season of the month June. The current approach emphasizes the utility of EATC-MCPC that effectively improves the solar absorbing performance of the irradiated solar energy uniformly through its periphery, as well as enhancing the thermo siphons working loom appreciably than the conventional applications of EATCs. The proposed systems (SS-SDS and DS-SDS) are being optimized to get the maximum possible basin water temperature (<boiling point) and larger water depth (0.16m) for the maximum yield output at the same orientation of SDS top cover and EATC (30°) for given solar insolation.

#### 3.01ANALYTICAL METHODOLOGY

The working approach requires various parameters (solar radiation intensity, ambient temperature, wind velocity, various heat transfer coefficients, thermal conductivity, emissivity, heat absorption capacity, reflectivity, thermo siphon mass flow rate, etc.) that are utilized in the different governing equation, empirical relationships, energy balance equations, etc., to analyze the performance of the proposed system. The brief of process followed is given below.

**First step:** In the very first step, the development of the system has been done for potable water production based on the previous studies and research gap identified through the literature survey. The initial consideration for the development of the system is being taken as a response to solar insolation over the inclined surface of solar collectors, which are obtained from the Meteorological Department of India (IMD, Pune) for the horizontal surface. This readily

available data is further converted correspondingly by following *Liu and Jordan (1960)* for computing the solar incidence response over the inclined surface.

**Second step:** Thermal modeling of the proposed systems (SS/DS-SDS-EATC-MCPC) has been done that is basically governed by the energy balance equations applied at different segments, i.e., inner-outer surface of the top glass cover (East, West, and South sides accordingly), basin water, basin liner, EATC selective absorber, and EATC carried water of the projected model. Further, the resulting expressions of energy balanced governing equations are fed into MATLAB computational tool to obtain different unknowns like, inner-outer top glass temperatures, selective absorber temperature, EATC and basin water temperature with the help of empirical relations for thermo-physical properties of water (Appendix A), different heat transfer coefficients (evaporative, convective, and radiative), vapor pressure into basin chamber, etc., in terms of predefined known quantities.

**Third step:** Following the above step for evaluating the condensing cover temperature and basin water temperature under the influence of additional heat gain received by EATC-MCPC parallel array, the yields have been obtained for the proposed solar still systems. Also, hourly energy-exergy gain and corresponding efficiencies for both the proposed systems are evaluated. Then additions of hourly, daily, and monthly energy-exergy will provide the respective outputs of the proposed systems. Moreover, the effect of solar insolation for thermo siphon mass flow rate in EATC due to MCPC is computed.

**Fourth step:** Further, energy, exergy matrices for the proposed solar still have been carried out using the above findings. Also, various economic analyses (economic, exergo-economic, and environ-economic) of the proposed system have been carried out. The environ-economic analysis consists of the evaluation of pollutants emission-mitigations, net carbon credit, and environmental cost. Further, the comparative observations are being done based on the yield production, energetic-exergetic gain and efficiencies, energy matrices, system economic analysis, and environ-economic analysis for both the studied systems. Finally, a comparative study is being presented for the both the proposed combinations of SDS systems with the previous researches based on the similar parameters. The above mentioned methodological steps are represented in the flowchart (Fig. 3.1).

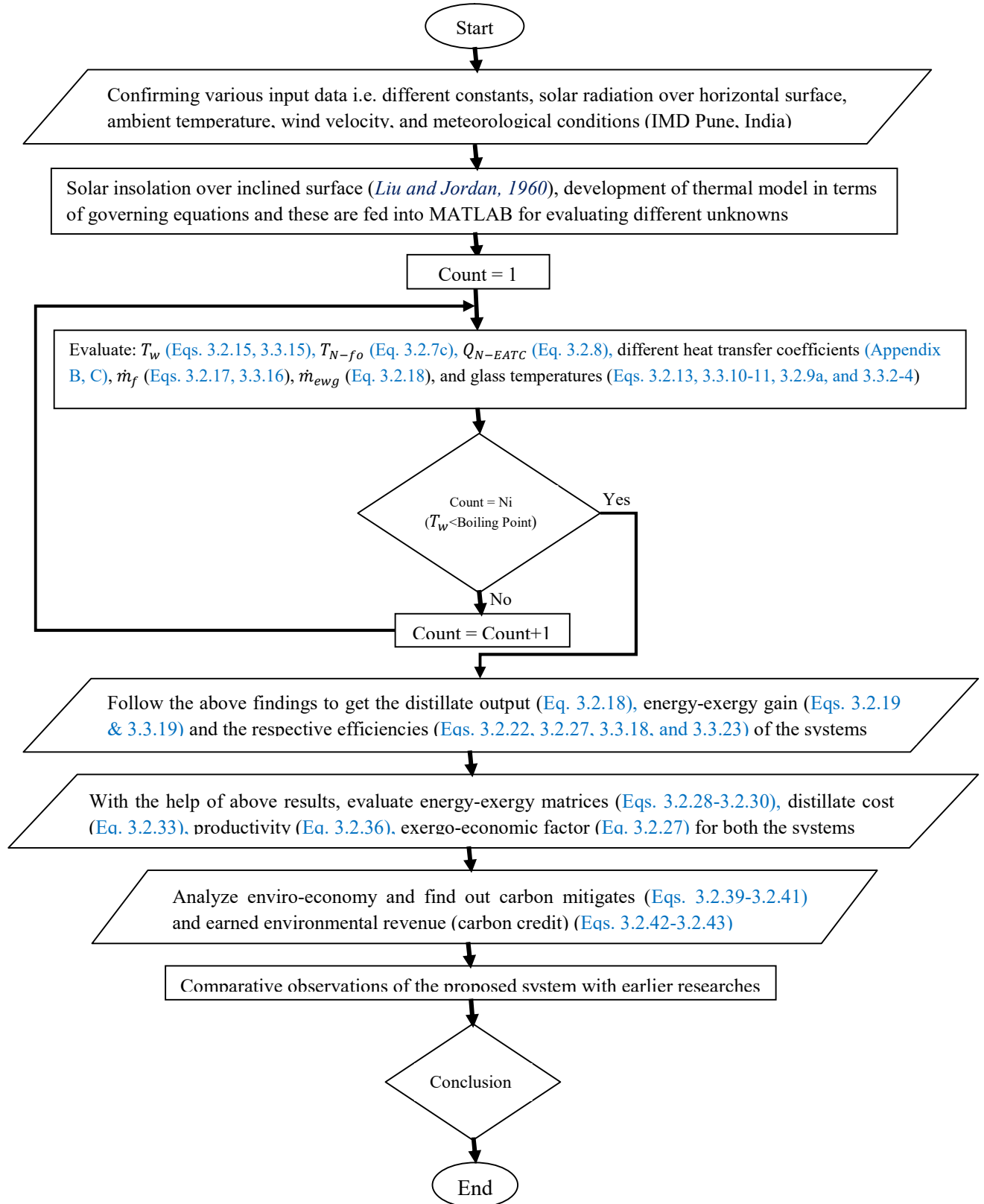


Fig. 3.1. Computational algorithm and flowchart for the methodological steps

### 3.1 EVACUATED ANNULUS TUBE COLLECTOR ASSISTED SINGLE SLOPE SOLAR DESALTIFICATION SYSTEM

As per the previous literature available, thermo siphon working approach for SDS-EATC always presents the most favorable scenario for the protracted working of the system. However, the available literature is missing with the optimum utilization of EATC with its circumferential area utilizations for receiving uniform solar radiation. And, the previous study of EATC merely presents a rectangular thermo siphon model rather than the uniform encyclical thermo siphon loop model that is possible with the help of a novel techno-eco combination of SDS-EATC-MCPC that performs effortlessly up to its optimum level in terms of efficiency, economy, life cycle conversion, and potable water productivity to serve the human being society ecologically. The generalized research gap that has been identified as improper utilization of entire huge number of EATC, rectangular thermo siphon loop, unused or imbalanced use of EATC's underneath segment, which can be rectified by the application of modified compound parabolic concentrators (MCPC, a set of novel arrangement of parabolic diffusers, i.e., oriented CPC (OCPC) in association with cusp CPC (CCPC) for parallel arrayed EATCs). These are observed in all respect of the proposed system with novel techno-eco-thermo-siphon-design of EATC-OCPC-CCPC integrated with SS-SDS (Fig. 3.2). Based on the above study, it is being confirmed that the evacuated annulus tube collector assisted single slope solar desalination system with modified compound parabolic concentrator has not been analyzed by any researcher so far. Also, the response of solar insolation on collectors due to concentrators for thermo siphon approach in EATC assisted CPC and cusp CPC have also not been analyzed by any researcher along with the effects of governing parameters for this novel techno-eco combination of the proposed system. The following objectives have been targeted to be discussed in the present communication of work which is achieved by the analytical study of the proposed system as shown in Fig. 3.2.

- i. To develop a novel system for potable water production
- ii. Thermal modeling of the proposed system
- iii. To analyze the system performance based on the energy, exergy, and productivity
- iv. To carry out energy matrices and different economic analyses of the system



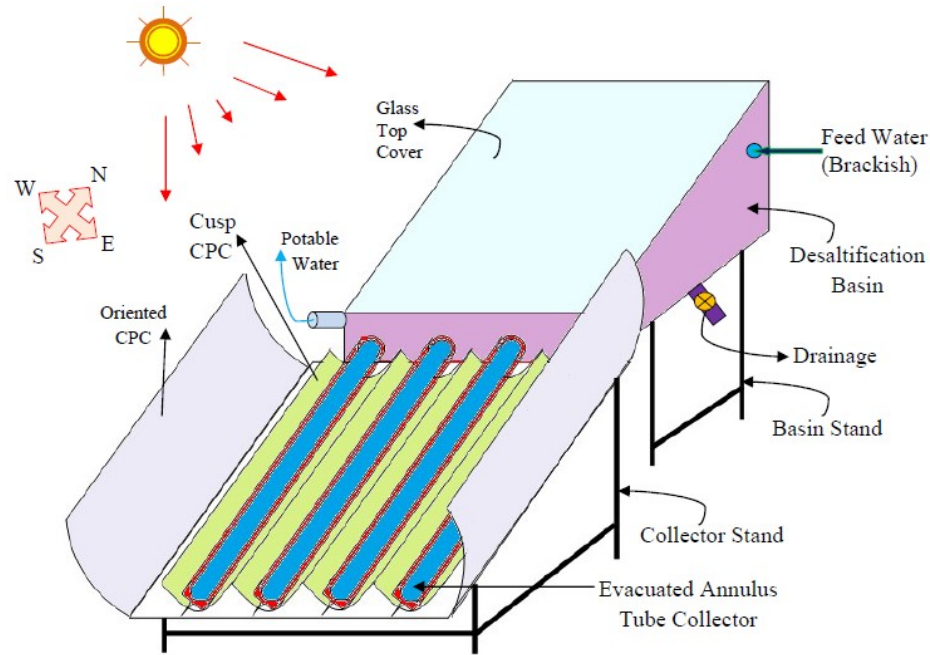


Fig. 3.2 Proposed system i.e. single slope solar desalination unit assisted evacuated annulus tube collector and modified compound parabolic concentrator (SS-SDU-EATC-MCPC)

### 3.1.1 Proposed Novel Design (SS-SDS-EATC-MCPC): System Description and Specifications

In the present study, the proposed model shows the furthestmost advantage of the modified compound parabolic concentrator for the overall solar heat transfer mechanism and corresponding mass flow through the EATC into the SDS basin in the following manner:

- i. Oriented compound parabolic concentrator (OCPC) assisted cusp compound parabolic concentrator (CCPC), i.e., accumulatively MCPC approximates the uniform heat gain through all around the periphery of the EATC.
- ii. Greater mass flow rate due to the downward shifting of conical heat transfer interface of hot and cold water due to heavier and denser fluid property of colder water and this makes additional push to the hot water which facilitates the higher flow velocity of hot water circulation towards the still basin. And, this results in a fast and uniform heat gain with de-stratification and de-scaling effects into the SDS basin chamber.
- iii. Circumferential heat addition into EATC has a longitudinally conical loop and cross-sectionally circular loop for the intermixing of hot and cold water streams.

- iv. The proposed system doesn't need any hydraulic pump, hence saves electrical energy without the constant supervision of the system that directly benefits in terms of the monetary value and additional manpower.
- v. The overall combination produces a comparatively greater yield at a competitive price with lower embodied energy, establishment, running, and maintenance cost also provides the revenue benefits through earned carbon credits in the international market, which benefits the environmental health and indirect economic returns to the nation of the mother land.

The schematic representation of the proposed system is given in Fig. 3.2. The location coordinates of this place on the globe based on latitude, longitude, and mean sea level are  $28^{\circ} 35'$ ,  $77^{\circ} 12'$ , and 216m, respectively. The specifications and parameters related to the components (SDS, EATC, MCPC, etc.) of the proposed system (South face oriented) are given in Tables 3.1 – 3.3. The SDS system is made up of fiber reinforced plastic (FRP) and attached with EATC-MCPC under passive working conditions. The SS-SDS basin chamber is covered with window glass at its top having 0.78 W/m K thermal conductivity and oriented at  $30^{\circ}$  (Tiwari and Tiwari, 2007; Tiwari, 2014), which is the best suited angle for such systems in Northern hemisphere to receive maximum radiation round the year.

Table 3.1 Specifications and computational design parameters of SS-SDS

<b>Single Slope Solar Desalination System (SS-SDS)</b>			
<b>System Parameter</b>	<b>Specification</b>	<b>System Parameter</b>	<b>Specification</b>
Basin base length	1m	Material of framework	Mild Steel
Basin base width	1m	Basin orientation	South
South face wall height	0.260m	Depth of water	0.16m
North face wall height	0.837m	Thickness of basin liner	0.05m
Top cover glaze area	1.155m <sup>2</sup>	Thickness of insulation	0.05m
Inclination of top glaze cover and EATC	$30^{\circ}$	$m_w$	160kg
Material of basin body	FRP	$\alpha_g$	0.05
Material of insulation	Glass wool	$\alpha_b$	0.97

Basin cover material	Glass	$\alpha_w$	0.34
Cover glaze thickness	0.004m	$n_o$	1
$\sigma$	$5.6697 \times 10^{-8}$ W/m <sup>2</sup> K <sup>4</sup>	$n_g$	1.5
$\varepsilon_g$	0.9	$n_w$	1.3
$\varepsilon_w$	0.9	$K_g$	0.78 W/m K
C	0.54	$n$	0.25
$K_b$	0.33 W/m K	$K_{i(glass\ wool)}$	0.03 W/m K

Table 3.2 Specifications and computational design parameters of EATC

Table 3.3 Specifications and computational design parameters of MCPC

Evacuated Annulus Tube Collector (EATC)		Modified Compound Parabolic Concentrator	
System Parameter	Specification	System Parameter	Specification
Tube length	1.8m	OCPC length	1.8m
CPC (Al-foil) density	2710 kg/m <sup>3</sup>	OCPC effective aperture opening (left-right)	0.935m
Inner tube ID	0.047m	OCPC overall aperture opening	2.87m
Inner tube OD	0.049m	OCPC-EATC effective concentration ratio	2.5
Outer tube ID	0.056m	CCPC length	1.8m
Outer tube OD	0.058m	CCPC aperture opening	0.314m
Concentric tube spacing (vacuum zone)	0.007m	CCPC-EATC effective concentration ratio	2
Thickness of glaze	0.002m	OCPC orientation to EATC plane	39.89°~ 40°
Selective absorber area	0.0034 m <sup>2</sup>	OCPC orientation to horizontal	30°
EATC material	High borosilicate 3.3 glass	CCPC orientation	30°

Center distance	0.314m	CPC (Al-foil) thickness	0.3mm
$F'$	0.968	Reflectivity	0.86
$R_{sc}$	0.05	CPC material	1060 aluminum alloy
$\alpha$	0.95	CPC color	Silver
$\tau$	0.95	CCPC-EATC gap	0.079m
$h_{saf}$	100 W/m <sup>2</sup> K	MCPC-EATC effective concentration ratio	2

Further, the modified compound parabolic concentrator (MCPC) defines combined effect of cusp compound parabolic concentrator (CCPC) and oriented compound parabolic concentrator (OCPC) integrated with EATC to improve its overall performance as shown in Figs. 3.3 – 3.3a.

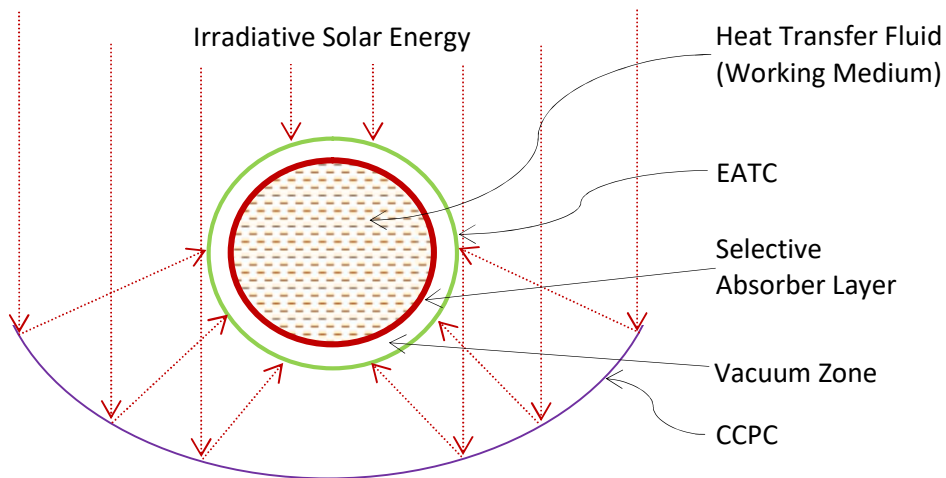


Fig. 3.3. Schematic plan view of EATC-CCPC covering underneath half part of the EATC under the corresponding solar insolation

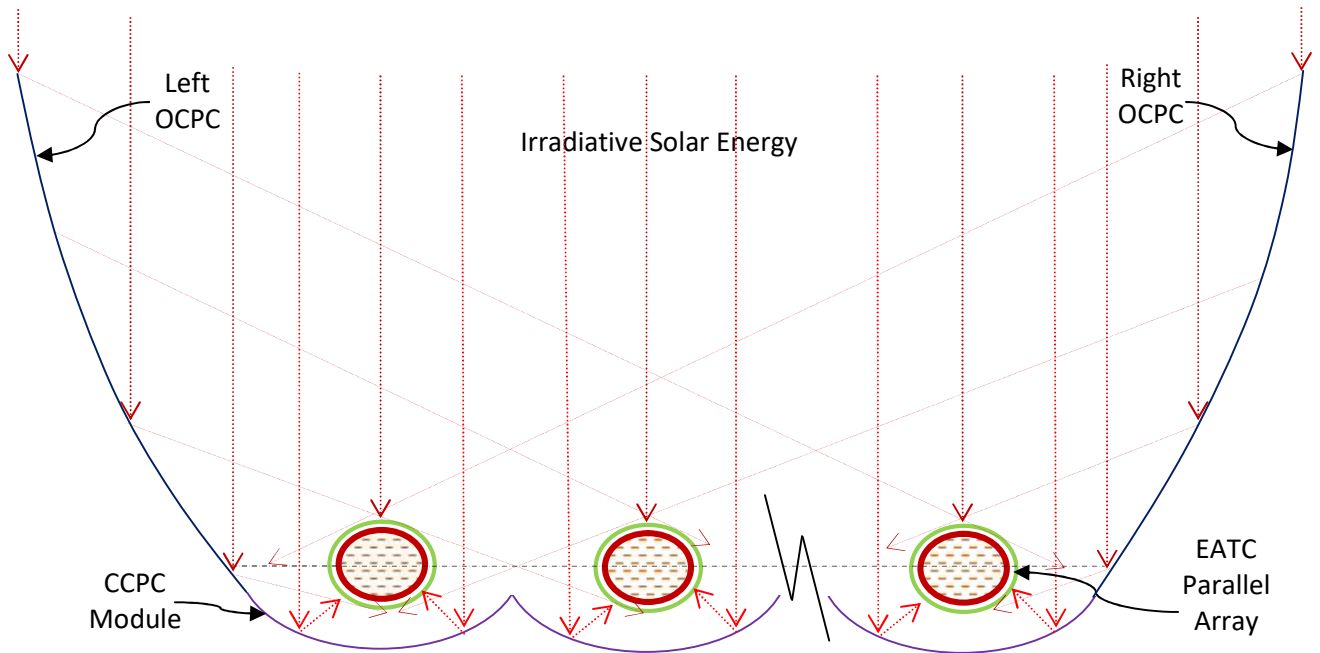


Fig. 3.3a. Schematic elevation view of N-EATC-MCPC covering either side and underneath half simultaneously of the EATC under the corresponding solar insolation.

### 3.1.2 Techno-Eco-Design: Solar Insolation Perspective

The geometrical consideration has the key basis for redirecting the incident solar insolation towards the selective absorber of EATC. In this perspective, certain considerations have been undertaken while developing the techno-eco-design for better influence of irradiative solar insolation towards the absorber as follows,

- i. A directed beam from oriented CPC hits EATC between extreme pointed tangents.
- ii. The underneath circumferential area of EATC illuminated uniformly due to cusp CPC.
- iii. The shadow effect of EATC over CCPC and corresponding diffused beam attenuation is neglected due to small EATC diameter in comparison to the arc length of cusp reflectors.
- iv. The entire circumferential area for the internal diameter (outer tube) of EATC has been considered as the solar radiation trapping zone because the incident solar beam flux gets trapped for the absorption at the selective absorber (inner coaxial tube outer surface), and an only negligible amount of lowest energy of longer wavelength can escape from the EATC outer glaze tubing.

### 3.1.3 Geometric Considerations of MCPC

The extensive utilization of EATC with its full potential has been maintained through the application of CCPC and OCPC. The geometrical diagram of identical EATC with CCPC in the influence of responsive solar insolation has been explored, as shown in Fig. 3.3. Further, the complete assembly of EATC-MCPC has been configured with the detailed exploration of OCPC and CCPC as demonstrated in Fig. 3.3a. The CCPC and OCPC have been efficiently parabolized to cover the entire peripheral area of EATC (approximately uniform) with respect to the incident solar radiation over it. The developed expressions for CCPC and OCPC are presented in such a way that the entire solar radiation between the aperture areas efficiently redirected towards the EATC (within the extreme tangents) without any solar beam losses and are presented as follows:

- a) Expression for CCPC:  $x = 17.7\sqrt{y}$
- b) Expression for OCPC:  $x(x - 2.8) = 4.7y + 4696.3$

### 3.1.4 Solar Insolation Response Over the Inclined Surface

The proposed system has broadly three elements where the solar irradiative energy incidents, namely SDS top glaze cover (oriented at  $30^\circ$ ), EATC (oriented at  $30^\circ$ ), and MCPC, geometrically aligned with the entire association. As the entire system is oriented in such a way that receives the maximum possible solar radiation over it and the available solar irradiated energy on the horizontal surface is readily provided by the Indian Meteorological Department, Pune, India, which should be converted accordingly to get the respective solar insolation response over the inclined surface. Following *Liu and Jordan (1960)* for computing the solar incidence response over the inclined surface, first of all, one can get the cosine component of inclination angle ( $\theta_i$ ) of irradiated solar energy over the inclined surface as represented,

$$\begin{aligned} \cos\theta_i = & (\cos\phi \cdot \cos\beta + \sin\phi \cdot \sin\beta \cdot \cos\gamma) \cdot \cos\delta \cdot \cos\omega + \cos\delta \cdot \sin\omega \cdot \sin\beta \cdot \sin\gamma + \\ & \sin\delta \cdot (\sin\phi \cdot \cos\beta - \cos\phi \cdot \sin\beta \cdot \cos\gamma) \end{aligned} \quad (3.1a)$$

As the proposed system (SS-SDS-EATC-MCPC) is oriented towards the facing due south, so the azimuth angle will be zero ( $\gamma = 0$ ). Hence, the above Eq. (3.1a) can be further rearranged as,

$$\cos\theta_i = \cos(\phi - \beta) \cdot \cos\delta \cdot \cos\omega + \sin\delta \cdot \sin(\phi - \beta) \quad (3.1b)$$

Also, the Zenith angle ( $\theta_z$ ) for that surface can be expressed as,

$$\text{Cos}\theta_z = \text{Cos}\phi \cdot \text{Cos}\delta \cdot \text{Cos}\omega + \text{Sin}\delta \cdot \text{Sin}\phi \quad (3.1c)$$

where, the angles  $\phi$ ,  $\delta$ , and  $\omega$  are termed as latitude angle of the analytical regime, declination, and hour angle, respectively. Further, following the relation (Cooper, 1969) for computing declination as expressed,

$$\delta = 23.45 \cdot \text{Sin} \left[ \left( \frac{360}{365} \right) \cdot (284 + n) \right] \quad (3.1d)$$

where the term 'n' represents the n<sup>th</sup> day of the year for which declination angle has to be depicted. And, hour angle ( $\omega$ ) can be analyzed by following the relation as given,

$$\omega = (ST - 12) \times 15^\circ \quad (3.1e)$$

where the term ST refers to the local solar time and angle  $15^\circ$  is a multiplier factor representing the rotational angle of the Earth in its axis by  $15^\circ$  hourly. Further, following the meteorological data of solar insolation irradiated over the horizontal surface, one can find the net amount of equivalent solar radiation in an inclined surface at an arbitrary angle (Liu and Jordan, 1962) as given by the expression,

$$\text{Total solar radiation on inclined surface (IS)} = \text{Diffuse radiation on IS} + \text{Beam radiation on IS} + \text{Ground reflected radiation on IS} \quad (3.1f)$$

$$I_s(t) = I_b(t) \cdot R_b + I_d(t) \cdot R_d + \rho' \cdot R_r \cdot \{I_b(t) + I_d(t)\} \quad (3.1g)$$

where the term  $R_b$  refers to the ratio of solar flux beam radiation over inclined to the horizontal surface. Similarly,  $R_d$  refers the ratio of solar flux diffused radiation for tilted to the horizontal surface, and an equivalent factor in terms of inclination angle ( $\beta$ ) is also used to compute  $R_d$  as given in Eq. (3.1i). And, the term  $R_r$  shows the reflected radiation multiplier factor from the ground and opposite in nature that of the solar diffuse radiation multiplier factor as expressed,

$$R_b = \frac{\text{Inclined surface beam radiation } (I_N \cdot \text{Cos } \theta_i)}{\text{Horizontal surface beam radiation } (I_N \cdot \text{Cos } \theta_z)} = \frac{\text{Cos } \theta_i}{\text{Cos } \theta_z} \quad (3.1h)$$

$$R_d = (1 + \text{Cos}\beta)/2 \quad (3.1i)$$

$$R_r = (1 - \text{Cos}\beta)/2 \quad (3.1j)$$

### 3.1.5 Thermal Model

This segment focuses on the development of the characteristic equations for the proposed system (SS-SDS-EATC-MCPC) that is entirely dependent on the energy balance equations. And, these equations are followed by the 1<sup>st</sup> law of thermodynamics (i.e. the conservation of energy law), and 2<sup>nd</sup> law of thermodynamics. Further, the developed thermal model and respective balanced energy equations for the different components of the system have been rearranged accordingly to get the solved expressions of the unknown parameters in the form of well known parameters for a particular instance of time. During the analytical observation, certain assumptions have been considered to simplify the complex mathematical analyses of the proposed thermal model, so the assumptions supporting the energy balance equations are mentioned as follows:

- i. The system is in a quasi-steady state, air tight, lumped, and completely leak proof (*Badran and Abu-Khader 2007*).
- ii. All the components of the SS-SDS-EATC-MCPC model are perfectly integrated without any temperature gradient transversely to the elemental thickness (*Badran and Abu-Khader 2007*).
- iii. In EATC, the interface of cold and hot water junction is ideally a conical one, but for simplicity in calculations, it is taken as the concentric loop formation of uniform circular profile throughout the EATC segment.
- iv. The EATC collector array is identical, and no interaction happens between adjacent tubing's.
- v. Heat flow in EATC is unidirectional and radial only with uniform and laminar intermixing of hot and cold water streams.
- vi. EATC is detached during the off-light time and represents a low pressure head system having two ends, i.e., closed end adiabatic and open end at constant pressure.
- vii. The heat absorbing capabilities of the glass, insulation, and walls are negligible.

#### 3.1.5.1 Parallel array of N-EATC-MCPC

The combination of MCPC to EATC helps in boosting the incident solar radiations (direct and concentrated) over the EATC. The entire solar energy (beam and directed) hits the all-around curved surface area of EATC and after reflecting a negligibly small amount of incident



solar energy, it reaches to its prior to the next destination that is at the selective absorber coating over the outer curved surface area of inner coaxial glaze tube, where more than 95% of the incident solar energy gets absorbed and only less than 0.05% of very low intensity energies are lost back to the atmosphere. And finally, the energy absorbed by the selective absorber coating is transmitted to the thermo-siphony looped flowing water mass into the coaxially inner tube of the EATC. And, the corresponding energy balance equations for the solar energy receiver (selective absorber coating) and flowing fluid medium (water mass) are written in given below:

a) Energy balance equation for EATC selective absorber

The selective absorber (sandwiched coating of micro-thin layers of Cu-ALN-SS) is the heart part of the EATC tube that absorbs the maximum of the incident solar energy, which is further transferred to the adjacent water mass flowing into the inner coaxial tube with the least losses to the atmosphere. The same can be expressed in the form of an energy balance equation with its physical significance as written here as,

*Absorbed intensive heat of solar energy at selective absorber =  
Heat transmitted from selective absorber to EATC water mass +  
Overall heat loss from EATC to ambient followed by galzing and vacuum zone*

$$I_s(a) = I_b(t) \cdot (\alpha \tau)_{eff} = F' \cdot h_{saf}(T_{sa} - T_f) + U_{saa}(T_{sa} - T_a) \quad (3.2.1)$$

where,  $U_{saa}$  refers the overall heat transfer (loss) coefficient from the outer glaze tube followed by the vacuum zone and inner glaze concentric tube of EATC. Further, Eq. (3.2.1) can be rearranged, and one can get the temperature of the selective absorber ( $T_{sa}$ ) as expressed,

$$T_{sa} = \frac{(\alpha \tau)_{eff} \cdot I_b(t) + F' h_{saf} T_f + U_{saa} T_a}{F' h_{saf} + U_{saa}} \quad (3.2.2)$$

The different terms of the above equation are given in Appendix B.

b) EATC working fluid (water mass) energy equation

The flowing fluid into the EATC is completely filled with water, so due to the direct contact of working fluid to the maximum temperature section of the EATC (i.e., adjacent to the selective

absorber), water receives respective thermal gain by the selective absorber simultaneously. And, the energy balance equation can be signified as,

*Amount of thermal energy carried by EATC water mass =  
Respective heat gain of water mass by the selective absorber*

$$\dot{m}_f C_f \frac{dT_f}{dx} dx = F' \cdot h_{saf} (T_{sa} - T_f) \cdot (2\pi R_{i1}) dx \quad (3.2.3)$$

Further, solving the equation under the respective boundary conditions as follows,

$$T_f = \begin{cases} T_{fi}, & x = 0 \\ T_{fo1}, & x = L_{EATC} \end{cases} \quad (3.2.4)$$

The working medium (water mass) temperature into the first EATC and expressed as follows,

$$T_{fo1} = \frac{(A_{rc} \cdot F_r)}{\dot{m}_f C_f} [F_1 (\alpha \tau)_{eff} I_b(t) + U_L T_a] + F_2 T_{fi} \quad (3.2.5)$$

where different terms are further expressed in Appendix B. The coating of selective absorber area ( $A_{rc}$ ) over the inner tube of EATC are calculated by  $(2\pi R_{o1} L_{EATC})$  expression. Further, following the parallel connected EATC-MCPC collectors, every EATC will respond similarly as in the above Eq. (3.2.5) due to the identical integration of EATC to the SDS basin that forms thermo siphon loop into the respective EATC tube, and a similar fashion is happening into the adjacent evacuated tubes also. So, the expression for  $T_{foN}$  for the  $N^{\text{th}}$  tube can be represented for the instantaneous solar irradiations as follows,

$$T_{foN} = \frac{(A_{rc} \cdot F_r)}{\dot{m}_f C_f} [F_1 (\alpha \tau)_{eff} I_b(t) + U_L T_a] + F_2 T_{fi} \quad (3.2.6)$$

And, the net temperature ( $T_{N-fo}$ ) achieved by the parallel array of N-EATC-MCPC channels can be calculated and represented as written,

$$\frac{1}{T_{N-fo}} \propto \frac{1}{T_{fo1}} + \frac{1}{T_{fo2}} + \dots + \frac{1}{T_{foN}} \quad (3.2.7a)$$

$$T_{N-fo} = \frac{N'(A_{rc} \cdot F_r)}{N \cdot \dot{m}_f C_f} \{F_1 (\alpha \tau)_{eff} I_b(t) + U_L T_a\} + F_2 T_{fi} \quad (3.2.7b)$$

$$T_{N-fo} = \frac{(A_{rc} \cdot F_r)}{\dot{m}_f C_f} \{F_1(\alpha \tau)_{eff} I_b(t) + U_L T_a\} + F_2 T_w \quad (3.2.7c)$$

where  $N'$  is the proportionality constant and approximately equal to  $N$ . And, the inlet temperature ( $T_{fi}$ ) of water into the EATC is equal to the SDS basin water temperature ( $T_w$ ). Further, as the parallel array of N-EATC-MCPC is connected to the SDS basin, so the additional amount of heat gain ( $\dot{Q}_{N-EAT}$ ) is received by the still basin chamber, which is quantified as given below and different other parameters of the equation can be identified by following the Appendix B,

Net amount of heat gain = Overall energy transfer to the SDS basin chamber –  
Overall heat loss to the atmosphere –  
Overall energy remain sustained into the EATC water mass

$$\dot{Q}_{N-EAT} = F_1(\alpha \tau)_{eff} I_b(t)(A_{rc} \cdot F_r) - (A_{rc} \cdot F_r)U_L(T_{fi} - T_a) - \dot{m}_f C_f \cdot T_{fi}(N - 1) \quad (3.2.8)$$

### 3.1.5.2 Single Slope Solar Desalination System

The thermal modeling of the overall solar desalination system refers to the energy balance equations generated for top cover glaze surfaces (inner and outer), composite basin liner, and basin water mass additionally supplied with energy gain from a parallel array N-EATC-MCPC.

a) Top cover glaze energy equation (ambient exposed surface)

The solar energy incident over the top cover of SDS oriented towards the South facing. After fractional absorption and reflection, it gets entered into the chamber. The hot atmosphere heats the top glaze cover. The condensing surface of the glaze conducts heat outward towards the lower heat zone, and that heat is further convected to the atmosphere. So, the energy balance equation can be expressed as,

Heat conducted from inside to outside through glaze =  
Heat convected from outer side of glaze to the atmosphere

$$\frac{K_g A_g}{t_g} (T_{gi} - T_{go}) = h_{t-g} A_g (T_{go} - T_a) \quad (3.2.9)$$

Further, the above equation can be rearranged to express  $T_{go}$  as given below.

$$T_{go} = \left( T_{gi} \frac{K_g}{t_g} + h_{t-g} \cdot T_a \right) / \left( h_{t-g} + \frac{K_g}{t_g} \right) \quad (3.2.9a)$$

The different terms of the above equation are given in Appendix B.

b) Top cover glaze energy equation (condensing surface)

The condensing zone is subjected to two ways heat input, 1<sup>st</sup> receives solar heat and 2<sup>nd</sup> heat gain (irradiative, evaporative, and convective) from basin water mass. And a thermally conductive heat loss is also being there towards the outward of the top glaze cover. All this can be expressed in the form of an energy balance equation as,

*Fractional solar flux transmitted energy from outer to inner glaze +  
Heat gain from water surface (convective, radiative, evaporative) =  
Heat lost through conductive heat transfer from inner glaze to outer glaze*

$$\alpha_g^A \cdot I_s(t) \cdot A_g + h_{t-wg} \cdot A_b \cdot (T_w - T_{gi}) = \frac{K_g \cdot A_g}{t_g} (T_{gi} - T_{go}) \quad (3.2.10)$$

where,  $\alpha_g^A$ , and  $h_{t-wg}$  refer (Appendix B) the partial solar flux absorbed by the top cover glazing and total heat transfer coefficient from water surface to top glaze cover (irradiative, evaporative, and convective) respectively (*Dunkle, 1961; Cooper, 1973; Singh and Samsher, 2020; Singh and Samsher, 2021*).

c) SDS basin water mass energy equation

The basin water mass increases its temperature in the form of sensible heating by absorbing the attenuated solar flux, convected thermal energy from basin liner, and additionally convected thermal energy through the parallel array of N-EATC-MCPC arrangement. Also, an overall heat loss occurs from the water surface to the top glaze covering. In view of this, one can establish the thermal balance equation as written,

*Fractional solar energy transmitted through cover glaze to water mass +  
Heat gain to basin water mass from composite liner +  
Additional convected thermal energy through parallel array of N – EATC – MCPC =*

Total heat transfer from basin water surface to top cover glaze +  
Amount of sensible heat stored into the basin water mass

$$\alpha_w^A \cdot I_s(t) \cdot A_b + h_{bw} \cdot A_b \cdot (T_b - T_w) + \dot{Q}_{N-EATC} = h_{t-wg} \cdot A_b \cdot (T_w - T_{gi}) + m_w C_w \cdot \frac{dT_w}{dt} \quad (3.2.11)$$

where the term  $\alpha_w^A = \{(1 - R_g)(1 - \alpha_g)(1 - R_w)\alpha_w\}$  is the partial solar flux absorbed by the SDS basin water mass. And,  $R_w = [1 - (4n_o n_w) / \{(n_o + n_w^2)(1 + n_o)\}]$  is the reflectivity of water similarly represented as the term ' $R_g$ '. Further, term  $h_{bw}$  refers convective heat transfer coefficient from basin composite liner to the basin water mass (Tiwari, 2014).

d) SDS basin composite liner energy equation

The composite basin liner is the ultimate destination where the completely attenuated partial solar fluxes are absorbed. This liner also losses its heat to the water mass and atmosphere (negligible), and these can be expressed in the form of thermal balance equation as written,

Net fractional solar flux energy received by basin liner =  
Heat gain to basin water mass from basin liner +  
Overall heat loss transfer from basin liner underneath to ambient

$$\alpha_b^A \cdot I_s(t) \cdot A_b = h_{bw} A_b (T_b - T_w) + h_{ba} A_b (T_b - T_a) \quad (3.2.12)$$

where the term  $\alpha_b^A = \{(1 - R_g)(1 - \alpha_g)(1 - R_w)(1 - \alpha_w)\alpha_b\}$  refers (Appendix B) to the partial solar flux absorbed by the SDS basin composite liner. Whereas the term  $h_{ba}$  is the overall heat loss transfer coefficient from basin liner to the atmosphere through conductive, convective, and irradiative heat transfer portals (Tiwari, 2014).

$$T_b = \{\alpha_b^A \cdot I_s(t) + h_{bw} T_w + h_{ba} T_a\} / (h_{bw} + h_{ba}) \quad (3.2.12a)$$

By following Eqs. (3.2.9 – 3.2.10), one can get the expression for  $T_{gi}$  as expressed,

$$T_{gi} = (\alpha_g^A I_s(t) A_g + h_{t-wg} A_b T_w + U_c A_g T_a) / (h_{t-wg} A_b + U_c A_g) \quad (3.2.13)$$

Now, approaching the Eq. (3.2.11) and putting values of  $h_{bw}(T_b - T_w)$ ,  $\dot{Q}_{N-EAT}$ , and  $h_{t-wg}(T_w - T_{gi})$  into it, one can get,

$$m_w C_w \cdot \frac{dT_w}{dt} = \alpha_w^A \cdot I_s(t) \cdot A_b + \{ \alpha_{beff} I_s(t) A_b - U_{bwa} (T_w - T_a) A_b \} - \{ U_{ta} (T_w - T_a) A_b - h'_1 \cdot \alpha_g^A \cdot I_s(t) \cdot A_b \} + \{ F_1 (\alpha \tau)_{eff} I_b(t) (A_{rc} \cdot F_r) - (A_{rc} \cdot F_r) U_L (T_{fi} - T_a) - \dot{m}_f C_f \cdot T_{fi} (N - 1) \} \quad (3.2.14)$$

From the above equation, one can get the rearranged form of equation as follows,

$$\frac{dT_w}{dt} + a \cdot T_w = f(t) \quad (3.2.14a)$$

Now integrating Eq. (3.2.14) under the boundary conditions as at  $t = 0, T_w = T_{wo}$ , and further the equation results in the expression for  $T_w$  under  $\left\{ C = T_{wo} - \frac{f(t)}{a} \right\}$  as follows,

$$T_w = T_{wo} \cdot e^{-a} + \frac{\bar{f}(t)}{a} (1 - e^{-a}) \quad (3.2.15)$$

The different terms of the above equation are given in Appendix B.

### 3.1.5.3 Mass Flow Analysis of N-EATC-MCPC Parallel Array

The incident solar energy is utilized by the solar desalination chamber for the direct heat consumption, which is further heated by the water mass of the evacuated annulus tube through a natural circulation loop caused by thermo siphon working principle into it. The thermo siphon natural circulation loop actively replaces the lighter hot water stream with the heavier cold water stream entered concentrically into the EATC from the basin chamber of SDS. As the thermo siphon loop is generated profoundly into the EATC due to the circumferential utilization of solar energy (direct sunlight at the top of EATC + diffused sunlight from OCPC at lateral sides of EATC + diffused sunlight from CCPC at the underneath of EATC) and has not been reported by any researcher elsewhere. Further, the effectiveness of the overall thermo siphon and mass circulation rate into the EATC depends on the solar irradiative energy, circumferential heat distribution around EATC, and SDS basin water mass temperature that have been correlated and modeled accordingly under the effect of proposed novel combinations.

The heat gain per unit area ( $\dot{q}$ ) of flowing water mass from identical EATC can be obtained by following the aforementioned expressions and the corresponding relations as,

$$\dot{q} = \dot{Q}_{N-EAT} / (N \cdot A_{rc}) \quad (3.2.16)$$

Following *Budihardjo and Morrison (2009)*, the expression of Reynolds number ( $Re$ ) for the identical EATC under thermo siphon loop at the variable temperature conditions can also be represented as follows,

$$Re = 0.1914 \left\{ \frac{Nu.Gr}{Pr} \left( \frac{L_{EATC}}{2R_{i1}} \right)^{1.2} \cdot \cos\theta \right\}^{0.4084} \quad (3.2.16a)$$

$$\dot{m}_f = 1.52 \left[ \frac{[(A_{rc} \cdot F_r) \{ F_1(\alpha\tau)_{eff} I_b(t) - U_L(T_{fi} - T_a) \}] - \dot{m}_f C_f \cdot T_{fi}(N-1)}{N \cdot A_{rc}} \cdot \left( \frac{L_{EATC}}{d} \right)^{1.2} \cdot \frac{g \cdot \beta' \cdot \rho^2 \cdot R_{i1}^{6.45}}{C_f \cdot \mu^{0.55}} \cdot \cos\theta \right]^{0.41} \quad (3.2.17)$$

The different terms of the above equation are given in Appendix B and further, thermo-physical properties of water can be accessed by following Appendix A. The parameters expressed in the above equation are directly dependent on the water mass temperature inside the EATC that is a combined effect of direct solar irradiated energy over the top half of the EATC curved surface area and additionally diffused and concentrated solar thermal energy over either side (due to OCPC) and underneath half curved surface area (due to CCPC) of the identical EATC. Further, the resulting expression of mass flow rate ( $\dot{m}_f$ ) correlates the incident solar radiation, EATC orientation angle to vertical, and EATC aspect ratio under the instantaneous test conditions.

### 3.1.6 System Performance Parameters

#### 3.1.6.1 Yield Production

The expression for hourly distillate production can be written as,

$$\dot{m}_{ewg} = \frac{\dot{q}_{ewg}}{L} \times 3600 \quad (3.2.18)$$

where the term ( $\dot{q}_{ewg} = h_{e-wg} \cdot A_b(T_w - T_{gi})$ ) represents the net rate of change of useful heat transfer of evaporation in between basin water surface to the top cover inner glaze surface (condensing surface) and expressed as given,

#### 3.1.6.2 Energetic Observations

The equivalent energy produced by the proposed system can be obtained accordingly which is dependent on the amount of potable water production (hourly, daily, annually, or lifetime). So, the hourly energy gain ( $(E_e)_{hr}$ ) can be expressed as given,

$$(E_e)_{hr} = (\dot{m}_{ewg} \cdot L) / 3600 \quad (3.2.19)$$

Similarly, daily energy gain  $(E_e)_{daily}$  can also be expressed by summing up the hourly energy for the whole day as represented,

Now, to observe the energy efficiency of a particular instance  $(\eta_i)$  for the proposed system, one can express as given,

$$\eta_i = \frac{\dot{q}_{ewg}}{I_s(t) \cdot A_b + I_b(t) \cdot A_a} \times 100 \quad (3.2.20)$$

$$\eta_i = \left[ \frac{h_{e-wg} \cdot A_b}{I_s(t) \cdot A_b + I_b(t) \cdot A_a} \right] \cdot \left\{ T_{wo} \cdot e^{-a} + \frac{[I_s(t) \cdot A_b \cdot \alpha_{eff}^A + T_a \cdot U_{eff} + F_1 \cdot (\alpha \tau)_{eff} \cdot (A_{rc} F_r) I_b(t)] / (m_w C_w)}{[U_{eff} + \dot{m}_f C_f (N-1)] / (m_w C_w)} \cdot (1 - e^{-at}) \right\} - T_{gi} \quad (3.2.21)$$

This expression represents the generalized characteristic equation for the SS-SDS-N-EATC-MCPC. Further, the hourly energy efficiency  $(\eta_e)_{hr}$  of the proposed system (SS-SDS-EATC-MCPC) can be expressed similar to that of the above equations with the realistic addition of thermal energy gain from the parallel array of N-EATC-MCPC arrangement with SDS system and can be expressed as,

$$(\eta_e)_{hr} = \frac{(E_e)_{hr}}{\{I_s(t) \cdot A_b + \dot{Q}_{N-EATC}\}} \times 100 \quad (3.2.22)$$

Similarly, daily energy efficiency  $(\eta_e)_{daily}$  and annual energy efficiency  $(\eta_e)_{annual}$  of the system can be expressed by summing up the respective outputs for the whole day and the year, respectively.

### 3.1.6.3 Exergetic Observations

The system performance based on its qualitative perspective of the thermal behavior can be observed by applying the concept of entropy (2<sup>nd</sup> law of thermodynamics) and exergy concept over the system, as it is an important notion regarding the complementary work for energy observations in terms of exergy analysis. Further, under the steady state conditions, the exergy balance equation for the system can be expressed as,



$$(\dot{E}_x)_{in} - (\dot{E}_x)_{out} = (\dot{E}_x)_{des} \quad (3.2.23)$$

where the term  $(\dot{E}_x)_{des}$  refers to the destructed energy lost due to irreversibility. Further, expressing the hourly exergy gain as *Cengel and Boles (2013)*,

$$(\dot{E}_x)_{hr-ou} = h_{e-wg} \cdot A_b \left\{ (T_w - T_{gi}) - T_a \cdot \ln \left( \frac{T_w}{T_{gi}} \right) \right\} \quad (3.2.24)$$

Now, the net hourly exergy input  $(\dot{E}_x)_{hr-in}$  which is a combination of the exergy input  $(\dot{E}_{x_{sun}})_{hr-i}$  in addition with exergy input  $(\dot{E}_{x_{EATC}})_{hr-in}$  by the parallel array of N-EATC-MCPC, as followed (*Petela, 2003*),

$$(\dot{E}_x)_{hr-in} = (\dot{E}_{x_{sun}})_{hr-in} + (\dot{E}_{x_{EATC}})_{hr-in} \quad (3.2.25)$$

$$(\dot{E}_x)_{hr-in} = 0.933 \cdot I_s(t) \cdot A_b + \dot{m}_f C_f \left\{ (T_{N-fo} - T_{fi}) - T_a \cdot \ln \left( \frac{T_{N-fo}}{T_{fi}} \right) \right\} \quad (3.2.26)$$

As exergy refers to the qualitative part of the system performance, and hourly exergy efficiency is defined as,

$$(\eta_x)_{hr} = \frac{(\dot{E}_x)_{hr-out}}{[(\dot{E}_{x_{sun}})_{hr-in} + (\dot{E}_{x_{EATC}})_{hr-in}]} \times 100 \quad (3.2.27)$$

### 3.1.7 Energy-Exergy Matrices Observations

While evaluating the overall performance of the system, one must consider the energy matrices response for its feasible existence over a given period of time, and it should be achieved as early as possible. In this way, one can recognize the establishment of a renewable energy system with its full used and applied potential, which must be accomplished with due early period of time and the system referred to as better, as lesser its pay off time with better conversion efficiency. The analysis of energy matrices entirely involves the energy pay off time, factor, and system's conversion efficiency under the given life span considerations of the proposed system.

#### 3.1.7.1 Pay off Time

The pay off time of a system represents the reimbursed equivalent energy or exergy against the consumed embodied energy of the system and by the system. It should be as minimal as and

the system will be considered as better. The pay off time  $(EP)_T$  can be represented based on the energy pay off time  $(EP_e)_T$  and exergy pay off time  $(EP_x)_T$  as expressed,

$$(EP_e)_T = E_{in}/(E_e)_{yearly}; (EP_x)_T = E_{in}/(E_x)_{yearly-out} \quad (3.2.28)$$

where the term ' $E_{in}$ ' refers to the total embodied energy which is associated with the established system. The embodied energy covers all the energy from the beginning of the preparation of that individual component (Tiwari et al., 2016) which is being integrated with the proposed system and accumulatively with entire embodied energy will represent the net embodied energy ( $E_{in}$ ) of the SS-SDS-EATC-MCPC system.

### 3.1.7.2 Pay off Factor

The system's pay off factor represents the proportionate performance factor that is the reciprocal of energy or exergy pay off time of the system and can be represented as follows,

$$(EP_e)_F = 1/(EP_e)_T; (EP_x)_F = 1/(EP_x)_T \quad (3.2.29)$$

The pay off factor  $(EP)_F$  is expecting as high as possible for the better performing system considerations. Further, if  $(EP)_F \rightarrow 1$ , for  $(EP)_T = 1$ ; the system is considered a worthwhile one otherwise not so worthy as per energy or exergy point of view.

### 3.1.7.3 Efficiency for Life Cycle Conversion

The efficiency for the complete life cycle regarding the conversion  $(\eta)_{LCC}$  in net output against the total incident solar energy received over the proposed system as a whole (SS-SDS-N-EATC-MCPC) based on the energy and exergy perspective. So, following (Singh and Samsher, 2021a), the energy based efficiency for life cycle conversion  $(\eta_e)_{LCC}$  can be expressed as,

$$(\eta_e)_{LCC} = \frac{(E_e)_{yearly} \times n - E_{in}}{(E_e)_s}; (\eta_x)_{LCC} = \frac{(E_e)_{yearly} \times n - E_{in}}{(E_x)_s} \quad (3.2.30)$$

where the terms  $(E_e)_s$ , and  $(E_x)_s$  indicate the total incident solar energy-exergy for the lifetime span ( $n = 30$  years) and expressed as

$$(E_e)_s = n \times \sum_{i=1}^{i=275} \{I_s(t). A_b + I_b(t). A_a\} \quad (3.2.31)$$

$$(E_x)_s = 0.933 \times n \times \sum_{i=1}^{i=27} \{I_s(t).A_b + I_b(t).A_a\} \quad (3.2.32)$$

### 3.1.8 Economic Observations

The different probable economic considerations (the direct and indirect financial systems based on energy and exergy) have been analyzed in this segment to understand the system's feasible and sustainable existence of life throughout its service duration. Also, the impact of the proposed system on the environment has been analyzed for the verification of eco-friendly system design along with the monetary benefits to the nation in terms of carbon credits earned values.

#### 3.1.8.1 System Economics

The entire observation has been made for the 30years of the system's life of working. The whole procedure undertakes the various governing parameters as total annual cost (TAC), which is the resulting asset value under the effect of fixed annual cost (FAC), annually charged maintenance cost (AMC), and salvage cost on an annual basis (ASC).

##### a) Cost of distilled water

The cost of energy-exergy produced ( $C_e$ , and  $C_x$ ), and distillate water cost ( $C$ ) based on the present economic observations can be expressed as (Reddy *et al.*, 2018; Singh and Samsher, 2021a),

$$C = TAC / (M_{ewg})_a; TAC = FAC + AMC - ASC \quad (3.2.33)$$

$$C_e = \frac{TAC}{(E_e)_{yearly}}; C_x = \frac{TAC}{(E_x)_{yearly-ou}} \quad (3.2.34)$$

Based on the trending growth of the open market, the average interest rate ( $i$ ) for inflation has been taken as 10% for the complete study of economic observations. However, a minimal operating and maintenance cost as 5% of  $FAC$  have been taken for the study. And, the salvage value ( $S$ ) or appreciation value after the considered service life of the system has been taken as 20% of the primary capital cost ( $PCC$ ) or initial investment cost that holds individual component cost, and fabrication cost. Further, these can be represented as,

$$AMC = 0.05 \times FAC; S = 0.2 \times PCC \quad (3.2.35)$$

b) Productivity of the system

Productivity measurement for a system is a key parameter defining its sustainable and feasible existence during the service life. It establishes the relationship between the yields output to the responsible factors essentially required to achieve that output. Its prime aim is to get the maximum yield with the least investment of resources and defined in terms of the ratio of efficiency with effectiveness (*ILO, 1979; Ashcroft, 1950*). Further, the productivity (annual)  $(\eta_P)_{yearly}$  of the proposed system can be expressed as followed (*Cox, 1951; Benson, 1952*),

$$(\eta_P)_{yearly} = \frac{[(M_{ewg})_a \times C_s]}{TAC} \times 100 \quad (3.2.36)$$

### 3.1.8.2 Exergo-Economics

The exergy based economic observation that correlates the conventional economic analysis to the exergy analysis to identify the cost optimal parameter for a given structure of system design (*Tsatsaronis and Winhold, 1985; Tsatsaronis et al., 1993*). In this way, researchers can improve the performance of the establishment with more appropriated and cost effective manner (*Tsatsaronis and Park, 2002*).

Also, many researchers have applied this concept for evaluating exergo-economic analysis for a solar operated ground heat pump (*Ozgener and Hepbasli, 2005*), gas turbine (*Kwon et al., 2001*), a power plant with different fuels (*Rosen and Dincer, 2003*), hybrid PV module solar air collectors (*Agrawal and Tiwari, 2012*), etc. to analyses the design optimization, and overall performance improvements of the renewable energy conversion units.

Further, the exergy-economy factor  $(E_x)_{EF}$  defined as the ratio of annual exergy gain to the total annual cost as presented,

$$(E_x)_{EF} = (E_x)_{yearly-out} / TAC \quad (3.2.37)$$

### 3.1.8.3 Environ-Energy-Exergy-Economics

The environ-economic analysis is one of the most robust and effective techniques to encourage the researchers and users of renewable technology that reflects the hidden and appreciable revenue in terms of carbon credits without affecting any harm with toxic gases (CO<sub>2</sub>, SO<sub>2</sub>, NO, etc. emissions) to the environment.

#### a) Equivalent emission estimation of pollutants

This section refers to the environmental harmful gases emissions, especially CO<sub>2</sub>, SO<sub>2</sub>, and NO, which may be equivalently produced during the production of potable water for its lifetime service. As, it has been recognized that in the coal based power plants in India for electrical power production of 1kWh emit particularly CO<sub>2</sub>, SO<sub>2</sub>, and NO pollutants by an equivalent weight of 0.98kg, 0.008kg, and 0.003kg respectively. Further, the consideration of additional values in terms of transmission losses (~40%) and distribution losses (~20%), and then the effective value for the equivalent pollutant generations will be 1.58kg, 0.012kg, and 0.005kg of CO<sub>2</sub>, SO<sub>2</sub>, and NO respectively. So, the equivalent emissions for CO<sub>2</sub> ((*EEq*)<sub>CO<sub>2</sub></sub>), SO<sub>2</sub> ((*EEq*)<sub>SO<sub>2</sub></sub>), and NO ((*EEq*)<sub>NO</sub>) can be represented for the proposed system (SS-SDS-EATC-MCPC) as (Reddy *et al.*, 2018; Singh and Samsher, 2021a),

$$(EEq)_{CO_2} = E_{in} \times 1.58; (EEq)_{SO_2} = E_{in} \times 0.012; (EEq)_{NO} = E_{in} \times 0.005 \quad (3.2.38)$$

#### b) Energy-Exergy based mitigation of pollutants

Following Mittal *et al.* (2014), Singh and Samsher (2021a), the environment pollutant mitigates for the lifetime span from the proposed solar desalting system can be represented based on the environ-energy-economic considerations as,

$$(MEq_e)_{CO_2} = 1.58 \times \{(E_e)_{yearly} \times n - E_{in}\} \quad (3.2.39)$$

$$(MEq_e)_{SO_2} = 0.012 \times \{(E_e)_{yearly} \times n - E_{in}\} \quad (3.2.40)$$

$$(MEq_e)_{NO} = 0.005 \times \{(E_e)_{yearly} \times n - E_{in}\} \quad (3.2.41)$$

Similarly, the environ-exergy-economy based environment pollutant mitigates (CO<sub>2</sub>, SO<sub>2</sub>, and NO) can be represented in terms of (*MEq<sub>x</sub>*)<sub>CO<sub>2</sub></sub>, (*MEq<sub>x</sub>*)<sub>SO<sub>2</sub></sub>, and (*MEq<sub>x</sub>*)<sub>NO</sub> respectively.

## c) Energy-Exergy based carbon credit revenue

The mitigates of the pollutants from the system can be dematerialized and termed as carbon credits earned based on the pricing system available in the international market. As these rates are fluctuating time by time, however following *Roome (2019)*, *Singh and Samsher (2021)*, it has been accepted as \$9.99/ton of CO<sub>2</sub> and the earned monetary value is treated as the indirect revenue benefit in terms of carbon credit earned for the respective solar desalination system. So, the environmental cost ( $(E_{ce})_{CO_2}$ ) of carbon mitigates for the lifetime span from the proposed system can be expressed based on the environ-energy-economic considerations as,

$$(E_{ce})_{CO_2} = [1.58 \times \{(E_e)_{yearly} \times n - E_{in}\}] \times 9.99 \quad (3.2.42)$$

$$(E_{cx})_{CO_2} = [1.58 \times \{(E_x)_{yearly-ou} \times n - E_{in}\}] \times 9.99 \quad (3.2.43)$$

### 3.2 EVACUATED ANNULUS TUBE COLLECTOR ASSISTED DOUBLE SLOPE SOLAR DESALINATION SYSTEM

The available literatures are missing with the optimum utilization of EATC with the negligence of underneath, and either side areas usability for receiving uniform solar radiations all around its periphery. These may be resolved with the help of the proposed novel techno-eco-design combinations of DS-SDS-EATC-MCPC that performs a conical thermo siphon loop with better circulation rate and results well in terms of efficiency, economy, life cycle conversion, and potable water productivity in an ecological manner. With the research gap (large number of EATC, rectangular thermo siphon loop, imbalanced use of EATC's underneath and side segments), the present work rectifies it by the application of modified compound parabolic concentrators (MCPC, a set of novel arrangement of parabolic diffusers, i.e., oriented CPC (OCPC) in association with cusp CPC (CCPC) for EATC). It is observed that the basin type double slope solar desalination system incorporating modified compound parabolic concentrator and evacuated annulus tube collectors have not been analyzed by any researcher so far. The analysis is primed on the basis of performance evaluation of the proposed system (DS-SDS-EATC-MCPC) directly or indirectly that depends on the productivity of potable water, energy, exergy efficiencies, energy-exergy metrics, various economic analyses of the system, and also techno-eco impact to the environment.

### 3.2.1 System Depiction and Requisites (DS-SDS-EATC-MCPC)

A labeled diagram of a single slope solar desalination system with identical  $N$  numbers of parallel array EATC augmented with modified compound parabolic concentrator (DS-SDS-N-EATC-MCPC) is represented in Fig. 3.4. The specifications of the proposed system are given in Tables 3.4 – 3.5, and distinguishing features and parameters related to its components of the DS-SDS assisted with EATC have been represented. The SDS system is made up of fiber reinforced plastic (FRP) and attached with EATC-MCPC under passive working conditions. The still basin is oriented towards the East-West facing. The DS-SDS basin chamber is covered with window glass having  $0.78 \text{ W/m K}$  thermal conductivity and oriented at  $30^\circ$  (Tiwari and Tiwari, 2007; Tiwari, 2014), which is the best suited angle for such systems in Northern hemisphere to receive maximum radiation round the year. Further to improve the overall performance of the system, a significant solar thermal collector component is aligned in the parallel fashion of identical nature, i.e., evacuated annulus tube collector (EATC) integrated to the DS-SDS system. The OCPC and CCPC dimensions are so critically analyzed that it cannot offer any hindrances to receive diffused and concentrated solar radiation over the respective side halves of the EATCs.

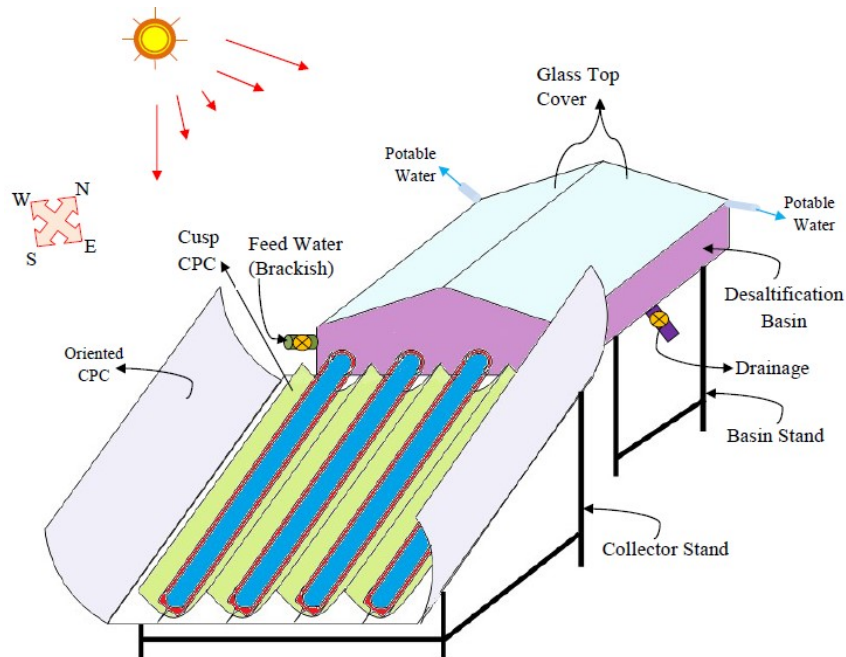


Fig. 3.4. Double slope solar desalination unit with evacuated annulus tube collector and modified compound parabolic concentrator (DS-SDU-EATC-MCPC)

Table 3.4 Specifications and computational design parameters of the proposed system (DS-SDS)

<b>Double Slope Solar Desalination System (DS-SDS)</b>			
<b>System Parameter</b>	<b>Specification</b>	<b>System Parameter</b>	<b>Specification</b>
Still length	1m	Framework material	Mild Steel
Still width	1m	Basin orientation	East-West
East-West wall height	0.260m	Depth of water	0.16m
Basin centre wall height	0.394m	Thickness (basin liner)	0.05m
Top glaze area	1.155m <sup>2</sup>	Thickness (insulation)	0.05m
Inclination (top glaze)	30°	$m_w$	160kg
Material of basin	FRP	$\alpha_g$	0.05
Insulating material	Glass wool	$\alpha_b$	0.97
Cover material	Glass	$\alpha_w$	0.34
Cover thickness	0.004m	$n_o$	1
$\sigma$	$5.6697 \times 10^{-8}$ W/m <sup>2</sup> K <sup>4</sup>	$n_g$	1.5
$\varepsilon_g$	0.9	$n_w$	1.3
$\varepsilon_w$	0.9	$K_g$	0.78 W/m K
C	0.54	$n$	0.25
$K_b$	0.33 W/m K	$K_{i(glass\ wool)}$	0.03 W/m K

Table 3.5 Specifications and computational design parameters of EATC-MCPC

<b>Evacuated Annulus Tube Collector (EATC)</b>		<b>MCPC: OCPC-CCPC</b>	
<b>System Parameter</b>	<b>Specification</b>	<b>System Parameter</b>	<b>Specification</b>
Tube length	1.8m	OCPC length	1.8m
CPC (Al-foil) density	2710 kg/m <sup>3</sup>	OCPC aperture (left-right)	0.935m
Inner tube ID	0.047m	OCPC overall aperture	2.87m
Inner tube OD	0.049m	OCPC-EATC effective concentration ratio	2.5
Outer tube ID	0.056m	CCPC length	1.8m



Outer tube OD	0.058m	CCPC aperture opening	0.314m
Concentric tube spacing (vacuum zone)	0.007m	CCPC-EATC effective concentration ratio	2
Thickness of glaze	0.002m	OCPC orientation to EATC	39.89°~ 40°
Selective absorber area	0.0034 m <sup>2</sup>	OCPC angle to horizontal	45°
EATC material	3.3 glass	CCPC orientation	45°
Center distance	0.314m	CPC (Al-foil) thickness	0.3mm
$F'$	0.968	Reflectivity	0.86
$R_{sc}$	0.05	CPC material	1060 Al alloy
$\alpha$	0.95	CPC color	Silver
$\tau$	0.95	CCPC-EATC gap	0.079m
$h_{saf}$	100 W/m <sup>2</sup> K	MCPC-EATC effective concentration ratio	2

### 3.2.2 Solar Irradiance: East-West Inclined Surface

The extensive utilization of EATC with its full potential has been maintained through the application of CCPC and OCPC. The geometrical diagram of identical EATC with CCPC in the influence of responsive solar insolation has been explored, as shown in Fig. 3.3. Further, the complete assembly of EATC-MCPC has been configured with the detailed exploration of OCPC and CCPC as demonstrated in Fig. 3.3a. The CCPC and OCPC have been efficiently parabolized to cover the entire peripheral area of EATC (approximately uniform) with respect to the incident solar radiation over it. The available solar irradiated energy on the horizontal surface is readily provided by the Indian Meteorological Department, Pune, India, which should be converted accordingly to get the respective solar insolation response over the inclined surface with the help of MATLAB computational tool. Following *Liu and Jordan (1960)* for computing the solar incidence response over the inclined surface, first of all, one can get the cosine component of inclination angle ( $\theta_i$  or East side inclination  $\theta_{iE}$ , and West side inclination  $\theta_{iW}$ ) of irradiated solar energy over the inclined surface as represented,

$$\begin{aligned} \cos\theta_i = & (\cos\phi \cdot \cos\beta + \sin\phi \cdot \sin\beta \cdot \cos\gamma) \cdot \cos\delta \cdot \cos\omega + \cos\delta \cdot \sin\omega \cdot \sin\beta \cdot \sin\gamma + \\ & \sin\delta \cdot (\sin\phi \cdot \cos\beta - \cos\phi \cdot \sin\beta \cdot \cos\gamma) \end{aligned} \quad (3.3a)$$

As the proposed system (DS-SDS-EATC-MCPC) is oriented towards the facing due East-West facing, so the azimuth angle ( $\gamma$ ) will be  $-90^\circ$ ,  $+90^\circ$  and inclined surface slope ( $\beta$ ) will be  $-30^\circ$ ,  $+30^\circ$  respectively. And, Zenith angle ( $\theta_z$ ) for that surface can be expressed as,

$$\text{Cos}\theta_z = \text{Cos}\phi \cdot \text{Cos}\delta \cdot \text{Cos}\omega + \text{Sin}\delta \cdot \text{Sin}\phi \quad (3.3b)$$

where the angles  $\phi$ ,  $\delta$ , and  $\omega$  are termed as latitude angle of the analytical regime, declination, and hour angle, respectively. Further, following the relation (Cooper, 1969) for computing declination as expressed,

$$\delta = 23.45 \cdot \text{Sin} \left[ \left( \frac{360}{365} \right) \cdot (284 + n) \right] \quad (3.3c)$$

where the terms  $\omega (= (ST - 12) \times 15^\circ)$ , and  $n$  represent the hour angle and  $n^{\text{th}}$  day of the year for which declination angle has to be depicted. Where  $ST$  refers to the local solar time and angle  $15^\circ$  is a multiplier factor representing the rotational angle of the Earth in its axis by  $15^\circ$  hourly. Further, the net amount of equivalent solar radiation over the inclined surface (East and West facing) at an arbitrary angle can be expressed as (Liu and Jordan, 1962),

$$I_s(t) = I_b(t) \cdot R_b + I_d(t) \cdot R_d + \rho' \cdot R_r \cdot \{I_b(t) + I_d(t)\} \quad (3.3d)$$

where the terms  $R_b (= \text{Cos} \theta_i / \text{Cos} \theta_z)$ ,  $R_d (= (1 + \text{Cos}\beta)/2)$ , and  $R_r (= (1 - \text{Cos}\beta)/2)$  refer the ratio of solar flux beam radiation over inclined (East and West facing) to the horizontal surface, ratio of solar flux diffused radiation for tilted to the horizontal surface, and reflected radiation multiplier factor from the ground, respectively.

### 3.2.3 Thermal Model: DS-SDS Unit

The development of the thermal model for the proposed system (DS-SDS-EATC-MCPC) is entirely dependent on the energy balance equations followed by the 1<sup>st</sup> law of thermodynamics (i.e. the conservation of energy law), and 2<sup>nd</sup> law of thermodynamics. Further, the developed thermal model and respective balanced energy equations for the different components of the system have been rearranged accordingly to get the generalized expressions of the unknown parameters in the form of known parameters for a particular instance of time. During the analytical observation, certain assumptions have been considered to simplify the complex mathematical analyses of the proposed thermal model (DS-SDS Unit) which are quite similar as

mentioned for the single slope solar desalination system. Also, the similar parametric observations are followed as expressed in respective equations (Eqs. 3.2.1 – 3.2.8) for the EATC-MCPC to analyze the net temperature out ( $T_{N-fo}$ ) and net heat output ( $\dot{Q}_{N-EAT}$ ) achieved by the parallel array of EATC-MCPC channels. Further, to observe the mass flow rate ( $\dot{m}_f$ ) through the parallel array of EATC, the similar expressions can be followed as mentioned in Eq. (3.2.17) because the additional mountings, i.e., EATC-MCPC parallel array is similar for both the proposed systems.

The thermal model analysis comprises the energy balance equations for East-West top glaze covers (inner-outer surfaces), basin water, and the underneath basin liner of DS-SDS unit in addition with the thermal energy supplied from N-EATC-MCPC (parallel array).

a) East-West ambient exposed, top cover glaze surface

The East faced solar radiation incident over the half top cover (east side) and after minimal absorption and reflection, the attenuated radiation enters into the basin. Now, the heat received at inner glaze surface gets conducted to outwards and further, convected to the atmosphere. The energy balance equation can be established accordingly as given,

$$\frac{K_g A_{gE}}{t_g} (T_{giE} - T_{goE}) = h_{t-gE} A_{gE} (T_{goE} - T_a) \quad (3.3.1)$$

Further, rearrangement of the above equation gives the outer surface temperature ( $T_{goE}$ ) of East side top glaze as,

$$T_{goE} = U_{cE} \cdot \frac{t_g}{K_g} \cdot [T_a - T_{giE}] + T_{giE} \quad (3.3.2)$$

Similarly, for the West side top glaze outer surface equations can be represented to find the outer surface temperature ( $T_{goW}$ ) as,

$$\frac{K_g A_{gW}}{t_g} (T_{giW} - T_{goW}) = h_{t-gW} A_{gW} (T_{goW} - T_a) \quad (3.3.3)$$

$$T_{goW} = U_{cW} \cdot \frac{t_g}{K_g} \cdot [T_a - T_{giW}] + T_{giW} \quad (3.3.4)$$

where the different terms of the above equation are given in Appendix C. The terms  $t_g$ ,  $h_{t-gE}$ , and  $h_{t-gW}$  refer top glaze cover thickness, and the net heat transfer coefficient from East and West inner glaze to the ambient, respectively.

b) East-West, top cover glaze condensing surface

The East side top cover condensing surface (inner) experiences heat gain by two sides, i.e., first from solar incident energy, and second from basin water surface through convection, evaporation, and radiation heat transfer modes. Also, a simultaneous heat loss appeared in two ways generally, first conductive heat loss from the East side inner glaze to ambient and secondly radiative heat loss from the East side inner glass to the West side inner glass into basin chamber. The entire energy transfer phenomenon can be represented accordingly in terms of an energy balance equation as written,

$$\alpha_g^A \cdot I_{SE}(t) \cdot A_{gE} + h_{t-gg} \cdot \frac{A_b}{2} \cdot (T_w - T_{giE}) = \frac{K_g \cdot A_{gE}}{t_g} (T_{giE} - T_{goE}) + h_{r-EW} \cdot A_{gE} \cdot (T_{giE} - T_{giW}) \quad (3.3.5)$$

Similarly, the West side top cover condensing surface (inner) energy balance equation can be expressed as follows,

$$\alpha_g^A \cdot I_{SW}(t) \cdot A_{gW} + h_{t-gg} \cdot \frac{A_b}{2} (T_w - T_{gi} ) = \frac{K_g \cdot A_{gW}}{t_g} (T_{giW} - T_{goW}) + h_{r-WE} \cdot A_{gW} (T_{giW} - T_{giE}) \quad (3.3.6)$$

where  $h_{r-EW} = h_{r-WE}$  and represents the radiative heat transfer coefficient for East-West side top glass surfaces. The terms  $h_{t-ggE}$ , and  $h_{t-ggW}$  refer net heat transfer coefficients East-West sides respectively (radiation, convection, and evaporation). The different terms of the above equation are given in Appendix C.

c) Energy equation: SDS basin water

The basin water receives thermal energy in many ways comprises solar irradiated energy (attenuated) from Sun through the East-West side of top glaze, thermal energy from basin liner through convective heat transfer, and a massive amount of heat energy received directly from the parallel array arrangement of EATC-MCPC through thermo siphon mass flow and can be represented in the form of energy balance equation as written,

$$\alpha_w^A \cdot \frac{A_g}{2} [I_{sE}(t) + I_{sW}(t)] + h_{bw} \cdot A_b \cdot (T_b - T_w) + \dot{Q}_{N-EATC} = h_{t-wgE} \cdot \frac{A_b}{2} \cdot (T_w - T_{giE}) + h_{t-w} \cdot \frac{A_b}{2} \cdot (T_w - T_{giW}) + m_w C_w \cdot \frac{dT_w}{dt} \quad (3.3.7)$$

d) Energy equation: SDS basin liner

The SDS basin liner is the final element where the rest part of the attenuated thermal energy gets absorbed with a simultaneous heat loss to the basin water (convection) and ambient (negligible) which can be expressed as follows according to energy balance equation,

$$\alpha_b^A \cdot \frac{A_b}{2} [I_{sE}(t) + I_{sW}(t)] = h_{bw} A_b (T_b - T_w) + h_{ba} A_b (T_b - T_a) \quad (3.3.8)$$

The resulting expression for the  $T_b$  can be obtained by rearranging Eq. (3.3.8) as follows,

$$T_b = \left[ \frac{1}{2} \cdot \alpha_b^A \{I_{sE}(t) + I_{sW}(t)\} + (h_{bw} \cdot T_w + h_{ba} \cdot T_a) \right] / (h_{bw} + h_{ba}) \quad (3.3.9)$$

Using above equations, one can get  $T_{giE}$  as written,

$$T_{giE} = \frac{\frac{A_b}{2} \cdot T_w \cdot h_{t-wgE} + A_{gE} \cdot [\alpha_g^A \cdot I_{sE}(t) + U_{cE} \cdot T_a + T_{giW} \cdot h_{r-EW}]}{\left[ \frac{A_b}{2} \cdot h_{t-wgE} + A_{gE} \cdot (U_{cE} + h_{r-EW}) \right]} \quad (3.3.10)$$

Similarly,  $T_{giW}$  can be rearranged to express as given,

$$T_{giW} = \frac{\frac{A_b}{2} \cdot T_w \cdot h_{t-wgW} + A_{gW} \cdot [\alpha_g^A \cdot I_{sW}(t) + U_{cW} \cdot T_a + T_{giE} \cdot h_{r-WE}]}{\left[ \frac{A_b}{2} \cdot h_{t-wgW} + A_{gW} \cdot (U_{cW} + h_{r-WE}) \right]} \quad (3.3.11)$$

The different terms of the above equation are given in Appendix C.

Further, Eqs. (3.3.10) – (3.3.11) can be rearranged into another form.

$$h_{t-wgE} \cdot (T_w - T_{giE}) = U_{taE} \cdot (T_w - T_a) + h'_{1E} \cdot h_{r-EW} \cdot (T_w - T_{giW}) - h'_{1E} \cdot \alpha_g^A \cdot I_{sE}(t) \quad (3.3.12)$$

$$h_{t-wgW} \cdot (T_w - T_{giW}) = U_{taW} \cdot (T_w - T_a) + h'_{1W} \cdot h_{r-WE} \cdot (T_w - T_{giE}) - h'_{1W} \cdot \alpha_g^A \cdot I_{sW}(t) \quad (3.3.13)$$

Now, after putting the values of  $h_{bw}(T_b - T_w)$ ,  $\dot{Q}_{N-EATC}$ ,  $h_{t-wgE} \cdot (T_w - T_{giE})$ ,  $h_{t-wgW} \cdot (T_w - T_{giW})$ , and  $T_{fi} = T_w$  in Eq. (3.3.7), one can find rearranged form of equation as written below,

$$\frac{dT_w}{dt} + \alpha_1 \cdot T_w = f(t) \quad (3.3.14)$$

Integrating Eq. (3.3.14) under the boundary conditions, at  $t = 0, T_w = T_{wo}$ ; with  $\left\{C = T_{wo} - \frac{f(t)}{a_1}\right\}$ , one can find basin water temperature ( $T_w$ ) as,

$$T_w = T_{wo} \cdot e^{-a_1 t} + \frac{\bar{f}_1(t)}{a_1} (1 - e^{-a_1 t}) \quad (3.3.15)$$

The different terms of the above equation are given in Appendix C.

### 3.2.4 Eco-Design Requisites and Performance Observations

#### a) Distillate Production

The production of distillate ( $\dot{m}_{ewg}$ ) directly depends on the temperature difference of basin water temperature to the top cover inner glaze surface temperatures and expressed as give below.

$$\dot{m}_{ewg} = \frac{\left\{h_{e-wgE} \cdot \frac{A_b}{2} \cdot (T_w - T_{giE})\right\} + \left\{h_{e-wgW} \cdot \frac{A_b}{2} \cdot (T_w - T_{giW})\right\}}{L} \times 3600 \quad (3.3.16)$$

Further, Eq. (3.3.16) can be expressed for the daily yield output ( $\dot{M}_{ewg}$ ) and annual yield output ( $M_{ewg}$ )<sub>a</sub> by summing up the hourly yield for 24 hours and for the whole year, respectively.

#### b) Energetic Analysis

The equivalent energy produced by the proposed system can be obtained that directly depends on the amount of potable water production. The hourly energy gain ( $E_e$ )<sub>hr</sub> can be observed by following Eq. (3.2.19)

Similarly, daily energy gain ( $E_e$ )<sub>daily</sub> and annual energy gain ( $E_e$ )<sub>annual</sub> can also be found by summing up the hourly energy for the whole day and for the whole year accordingly. Now, the energy efficiency for a particular instance ( $\eta_i$ ) of the proposed system can be expressed as

$$\eta_i = \frac{\left[\frac{A_b}{2} \cdot T_w (h_{e-wgE} + h_{e-wgW}) - (h_{e-wgE} \cdot T_{giE} + h_{e-wgW} \cdot T_{giW})\right]}{\frac{A_b}{2} \cdot \{I_{sE}(t) + I_{sW}(t)\} + I_b(t) \cdot A_a} \times 100 \quad (3.3.17)$$

Further, the hourly energy efficiency ( $\eta_e$ )<sub>hr</sub> of the proposed system (DS-SDS-EATC-MCPC) can be expressed similar to that of the above equations with the realistic addition of

thermal energy gain from the parallel array of N-EATC-MCPC arrangement with SDS system as given,

$$(\eta_e)_{hr} = \frac{(\dot{E}_e)_{hr}}{\frac{A_b}{2} \cdot \{I_{SE}(t) + I_{SW}(t)\} + \dot{Q}_{N-EATC}} \times 100 \quad (3.3.18)$$

Similarly, daily energy efficiency  $((\eta_e)_{daily})$ , and annual energy efficiency  $((\eta_e)_{annual})$  of the system can be expressed by summing up the values for the day and a year respectively.

### c) Exergetic Analysis

Under the steady state conditions, exergy balance equation for the system can be followed as given in the Eq. (3.2.23),

where the term  $(\dot{E}_x)_{des}$  refers to the destructed energy due to irreversibility or exergy destruction. Further, the hourly exergy  $(\dot{E}_x)_{hr-ou}$  and the daily exergy  $(\dot{E}_x)_{daily-ou}$  output or gain of the proposed system have been observed based on the laws of thermodynamics (energy and entropy) as followed by *Cengel and Boles (2013)* and expressing the hourly exergy gain as,

$$(\dot{E}_x)_{hr-ou} = h_{e-wgE} \cdot \frac{A_b}{2} \left\{ (T_w - T_{giE}) - T_a \cdot \ln \left( \frac{T_w}{T_{giE}} \right) \right\} + h_{e-wgW} \cdot \frac{A_b}{2} \left\{ (T_w - T_{giW}) - T_a \cdot \ln \left( \frac{T_w}{T_{giW}} \right) \right\} \quad (3.3.19)$$

Now, the net hourly exergy input  $(\dot{E}_x)_{hr-in}$  to the system which is a combination of the exergy input directly by the solar radiation  $(\dot{E}_{x_{sun}})_{hr-in}$  in addition with exergy input  $(\dot{E}_{x_{EATC}})_{hr-in}$  by N-EATC-MCPC can be represented as followed (*Petela, 2003*),

$$(\dot{E}_x)_{hr-in} = (\dot{E}_{x_{sun}})_{hr-in} + (\dot{E}_{x_{EATC}})_{hr-in} \quad (3.3.20)$$

$$(\dot{E}_x)_{hr-in} = 0.933 \cdot \frac{A_b}{2} \cdot \{I_{SE}(t) + I_{SW}(t)\} + \dot{m}_f C_f \left\{ (T_{N-fo} - T_{fi}) - T_a \cdot \ln \left( \frac{T_{N-fo}}{T_{fi}} \right) \right\} \quad (3.3.21)$$

Further, the daily exergy input  $(\dot{E}_x)_{daily-in}$  to the SDS basin chamber can be expressed as,

$$(\dot{E}_x)_{daily-in} = \sum_{t=1}^{t=10} \left[ 0.933 \cdot \frac{A_b}{2} \cdot \{I_{SE}(t) + I_{SW}(t)\} + (\dot{E}_{x_{EATC}})_{hr-in} \right] \quad (3.3.22)$$

As exergy refers to the qualitative part of the system performance, and hence exergy efficiency reflects the system's used performing efficiency out of the maximum available potential of performance. So, hourly exergy efficiency is expressed as,

$$(\eta_x)_{hr} = \frac{(\dot{E}_x)_{hr-o} + (\dot{E}_x)_{hr-out} W}{[(\dot{E}_x)_{sun} hr-in + (\dot{E}_x)_{EATC} hr-in]} \times 100 \quad (3.3.23)$$

Similarly, daily exergy efficiency is represented by the daily exergy output to the respective clear sunshine visibility hours (~10hrs).

### 3.2.5 Energy-Exergy Matrices Observations

The analysis of energy matrices involves the energy pay off time, factor, and system's conversion efficiency under the given life span considerations of the proposed system and can be calculated by following the similar expression as presented in Eqs. (3.2.28 – 3.2.30). One can recognize the establishment of a renewable energy system with its full used and applied potential, which must be accomplished with due early period of time and the system referred to as better, as lesser its pay off time with better conversion efficiency. Further, to observe the solar energy  $((E_e)_s)$  and exergy  $((E_x)_s)$  for the whole life of the system can be analyzed by following the expressions given below.

$$(E_e)_s = n \times \sum_{i=1}^{i=275} \left[ \frac{A_b}{2} \cdot \{I_{sE}(t) + I_{sW}(t)\} + I_b(t) \cdot A_a \right] \quad (3.3.24)$$

$$(E_x)_s = 0.933 \times n \times \sum_{i=1}^{i=275} \left[ \frac{A_b}{2} \cdot \{I_{sE}(t) + I_{sW}(t)\} + I_b(t) \cdot A_a \right] \quad (3.3.25)$$

### 3.2.6 Different Economic Observations

The entire observation has been made for 30 years of system's life of working. The whole procedure undertakes the various governing parameters as total annual cost (TAC), which is the resulting asset value under the effect of fixed annual cost (FAC); annually charged maintenance cost (AMC); and salvages cost on an annual basis (ASC), which are quite similar as depicted for single slope solar desalination system. This segment comprises the system economic analysis for analyzing distillate cost (Eqs. 3.2.33 – 3.2.35), productivity of the system (Eq. 3.2.36), exergo-economic factor (Eq. 3.2.37), equivalent emission estimation of pollutants (Eq. 3.2.38),



energy-exergy based mitigation of pollutants (Eqs. 3.2.39 – 3.2.41), and respective energy-exergy based carbon credit revenue (Eqs. 3.2.42 – 3.2.43).

*The next chapter contains the results and discussion for both the proposed systems (SS/DS-EATC-MCPC) that comprise the evaluation of glass cover temperatures, water (basin and EATC) temperature, effect of solar insolation for thermo siphon mass flow rate in EATC due to MCPC, yields, hourly energy-exergy and corresponding efficiencies of the system, energy-exergy matrices, various economic analyses (economic, exergo-economic, and environ-economic), and the evaluation of pollutants emission-mitigations, and environmental cost (i.e., carbon credit values in the international market) of the proposed systems. Further, a comparative study is being presented for both the proposed systems with each other as well as with the previous researches based on the similar parameters of different systems and selected accordingly the best performing solar desalting system under the respective parameters.*

## CHAPTER: 4

### *RESULTS AND DISCUSSION*

## CHAPTER: 4

### RESULTS AND DISCUSSION

---

#### 4.0 INTRODUCTION

The proposed systems (SS-SDS and DS-SDS) are being optimized to get the maximum possible basin water temperature (less than boiling point) for the larger water depth (0.16m) at the same orientation of SDS top cover and EATC (30°) under the influence of solar insolation with the corresponding thermo siphon circulation rate (maximum ~55 kg/hr) to produce better yield output. The SS/DS-SDS-EATC-MCPC systems observed for the daily overall energy-exergy efficiencies, daily yield and its production cost at a nominal selling price found good. The energy-exergy based pollutant emissions, mitigates and environmental earned revenue are also analyzed respectively and found appreciable results. The establishment cost of the system is quite low and the system's productivity is found as 940.8%, which is more than 100% that depicts the system as appreciably feasible.

The chapter also depicts the results analysis and discussion for the relative observations of the proposed systems in a comparative manner. The comparative observations are based on the yield production, energetic-exergetic gain and efficiencies, energy matrices, system economic analysis, and environ-economic analysis for both the studied systems. Finally, a comparative study is being presented for the both the proposed combinations of SDS systems with the previous researches based on the similar parameters. The evacuated annulus tube collector assisted double slope solar desalination system with modified parabolic concentrator (DS-SDS-EATC-MCPC) shows the best performance in overall observational perspectives than the SS-SDS-EATC-MCPC model and also for the other desalination systems taken into consideration for comparison. The DS-SDS-EATC-MCPC system has been optimized to get the maximum possible basin water temperature as 99.6°C for the larger water depth (0.16m) at the East-West) orientation of basin top cover (30°) and South oriented evacuated tube (30°). The maximum circulation rate (thermo siphon) is achieved ~55 kg/hr. The establishment cost of the DS-SDS system is lower by 6.6%, and both the system productivity is found more than 100%

that depicts, systems are appreciably feasible. The evident yield at little production cost, environmental returns, better mitigation and short EPT makes the DS-SDS-EATC-MCPC system better sustainable and viable for lesser collector areas and optimum EATC with MCPC as eco-design requisites for the projected scheme.

#### 4.1 EVACUATED ANNULUS TUBE COLLECTOR ASSISTED SINGLE SLOPE SOLAR DESALTIFICATION SYSTEM

The proposed model (SS-SDS-EATC-MCPC) is being analyzed for 0.16m water depth into basin besides the water filled EATCs (parallel array having 4 optimum numbered EATCs) with 30° orientation angle for both SDS as well as the EATC to face maximum irradiative solar energy throughout the sunshine hours of the archetypal clear day. Further, the average wind flow (4.11 m/s) and atmospheric temperature favor the desalting process better throughout the day. The average solar intensity is found as 401.8kW during the typical day of observation and the overall number of clear days in a year has been taken as 275 for the whole life of service of the system for analyzing different energetic-exergetic performances of the system.

Fig. 4.1 shows the hourly variations of different solar irradiative components (i.e., global, beam, and diffused solar radiations) on a horizontal surface (following Indian Meteorological Department, Pune, India source data of solar radiation) that is responsible for the respective solar radiations over the inclined surface (following *Liu and Jordan, 1960, 1962*) for the particular clear day.

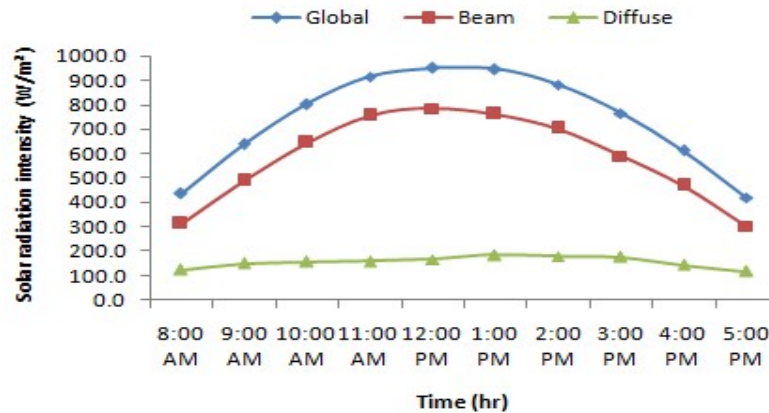


Fig. 4.1. Representation of hourly variations of different solar irradiative radiations on the horizontal surface round the sun shine hours

### 4.1.1 Thermal Model Validation With Comparative Improvement Observation

The results found in the observations are in good agreement appreciably where the impact of MCPC and water depth is negligible as shown in Fig. 4.2. The proposed model holds excellent results and shows 315% improved yield due to the respective increase in basin water mass (433%), basin water temperature (10.8%), and mass flow rate (28%). From the above validated observation of the results, the proposed system and thermal model justifies its correctness and can be utilized to evaluate the system performance under the proposed geometrical considerations of the model.

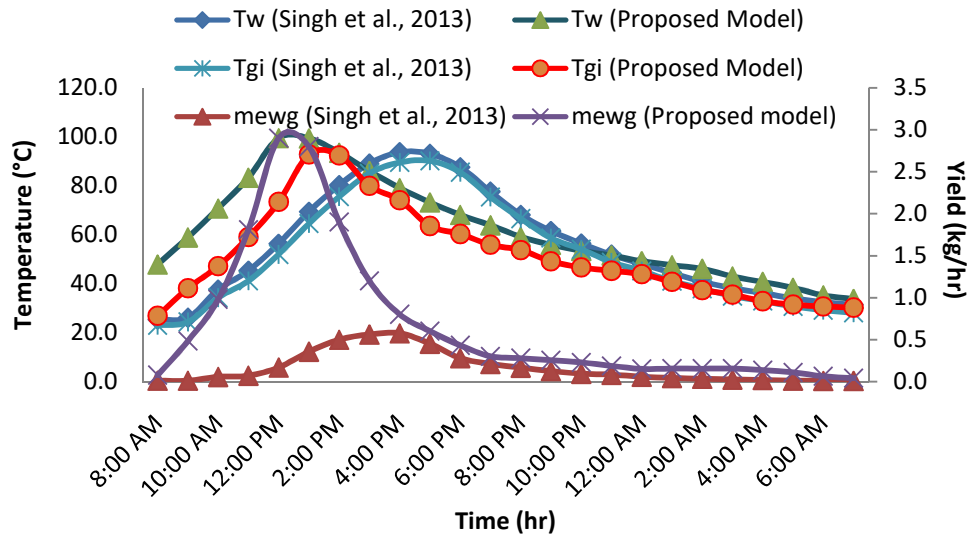


Fig. 4.2. Validation and comparative observation for the thermal models of the proposed system under the hourly variations of basin water, inner glass top cover temperature, and yield output

### 4.1.2 Optimization of the Proposed Model

The analysis has been done for a variable number of EATCs under the different basin water depth conditions for the fixed SDS basin design parameters and observed the 4 number of EATC with 0.16m water depth attains maximum 99.5°C temperature of basin water mass (Fig. 4.3).

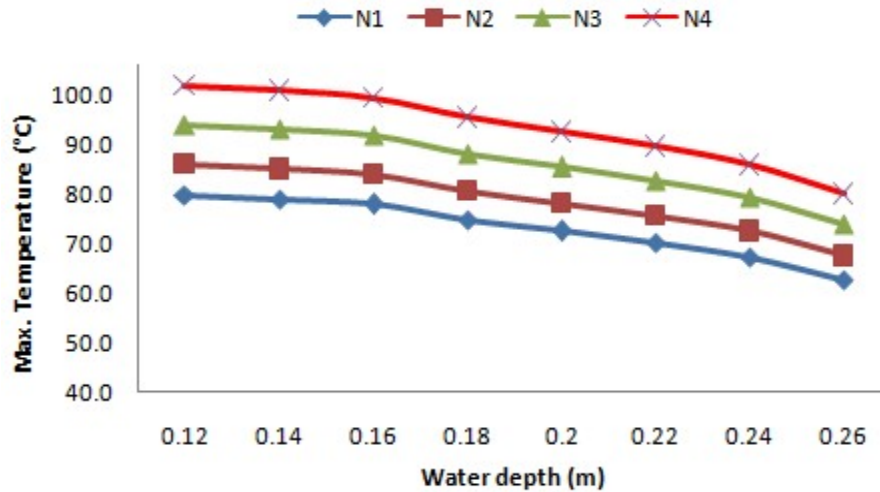


Fig. 4.3. Representation of basin water maximum temperatures against the variable water depth conditions and constant number of EATCs of the proposed system

#### 4.1.3 Performance Analysis: Energy-Exergy Considerations

Fig. 4.4 represents the temperature variations of different sections in the system for an archetypal clear day in the month of June. The water temperature of EATC effectively governs the basin water temperature and shows a rapid increase up to 1 pm with larger temperature differences that also cause a high mass flow rate. Also, a significant temperature difference i.e.  $T_w - T_{gi}$  appears up to 2 pm, and after that nominal temperature, differences are maintained even for late night also which provides diurnal and nocturnal yields respectively. Further, the respective variations in heat transfer coefficients in the basin chamber are represented in Fig. 4.5. It shows the evaporative heat transfer that plays a major role in transferring heat from water surface to top glass cover, whereas the radiative heat transfer affects least due to significantly lower water temperature ( $<100^{\circ}\text{C}$ ) and it works effectively at a higher temperature ( $>1000^{\circ}\text{C}$ ). The figure shows the most significant improvements at the mid of the day where the higher solar intensity appeared.

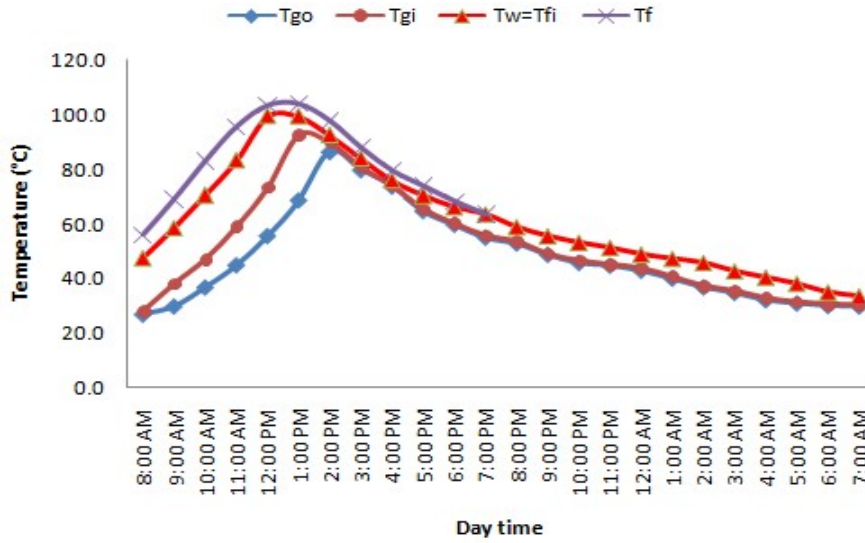


Fig. 4.4. Temperature variations at different sections in the system for an archetypal clear day in the month of June

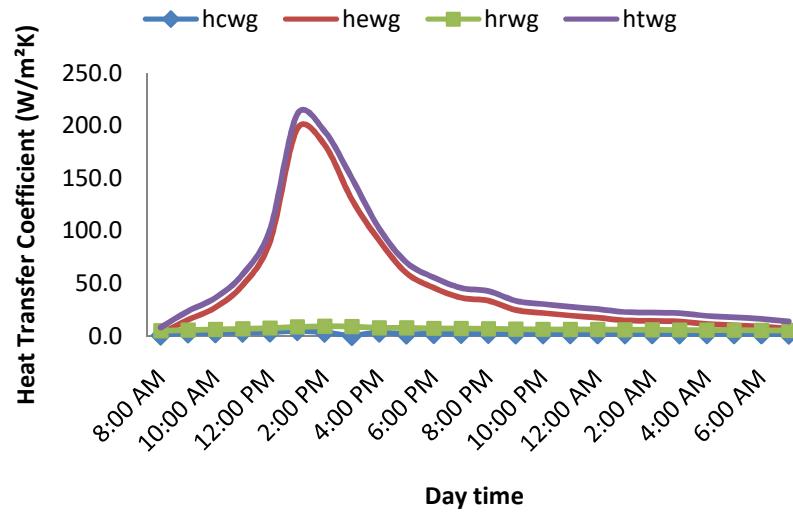


Fig. 4.5. Heat transfer coefficient variations at different segments in the system for an archetypal clear day in the month of June (N=4)

The production of yield with the corresponding thermo siphon at different temperature differences ( $T_w - T_{gi}$ ) throughout the day have been represented in Fig. 4.6. The yield production is following the  $\dot{m}_f$  and  $T_w - T_{gi}$ . But, the maximum yield (2.9kg) appeared at 1 pm due to the maximum  $T_w - T_{gi}$  (26.02°C), however, the mass flow rate is maximum (55.0 kg/hr)

at 2 pm because at that time maximum temperature difference ( $T_w - T_{gi}$ ) is reached, which rapidly increases basin water temperature, hence evaporation increased which is not effectively utilized due to excessive production of vapor under the increases vapor conditions, also re-evaporates the condensed vapor again and again at the condensing surface of top glass, which results in slightly less yield at that time.

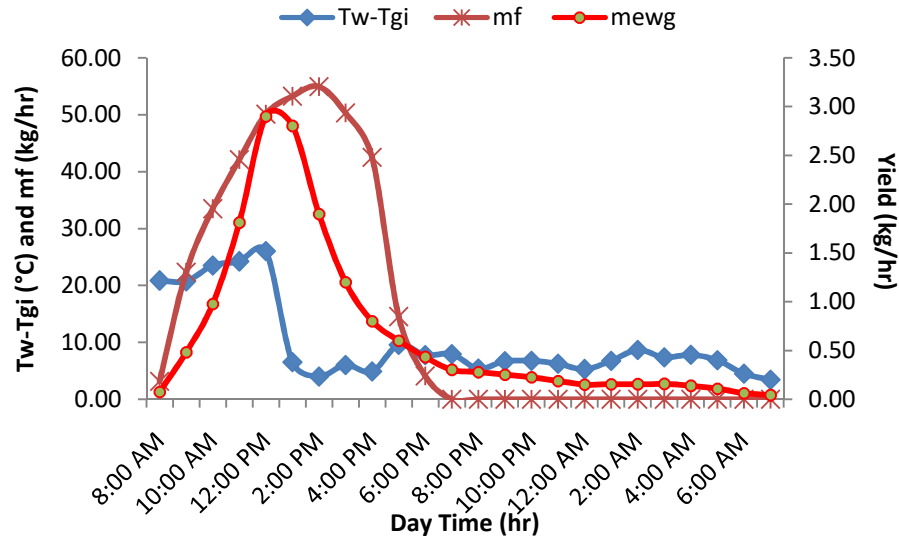


Fig. 4.6. Hourly variations of mass flow rate, yield output, and ( $T_w - T_{gi}$ ) in the month of June of an archetypal clear day

Fig. 4.7 represent the energy-exergy gain of the system under the respective clear day conditions and have the maximum gain of 2.33 kWh and 1.59 kWh, respectively that is found at the peak hours of solar intensities that have the least  $T_w - T_{gi}$ . Further, the energy and exergy efficiencies are sensitive parameters depends on both the important integral functionalities of SDS basin as well as EATC and the corresponding changes shown in Fig. 4.8. The energy efficiency depends on the temperature differences, i.e. ( $T_w - T_{gi}$ ), ( $T_{N-f} - T_w$ ), incident solar radiations, and energy transfer from EATC to SS-SDS. In this way, the energy efficiency is majorly governed by the temperature difference so, as the temperature difference goes higher; energy efficiency goes higher that is reflected up to noontime, after that, efficiencies are trending down because temperature differences and solar intensity, both go down all together. However, exergy efficiency follows energy efficiency adversely due to the involvement of exergetic



phenomenon and respective degradation into the different components of solar system where the temperature differences and energy efficiencies are much higher and vice versa.

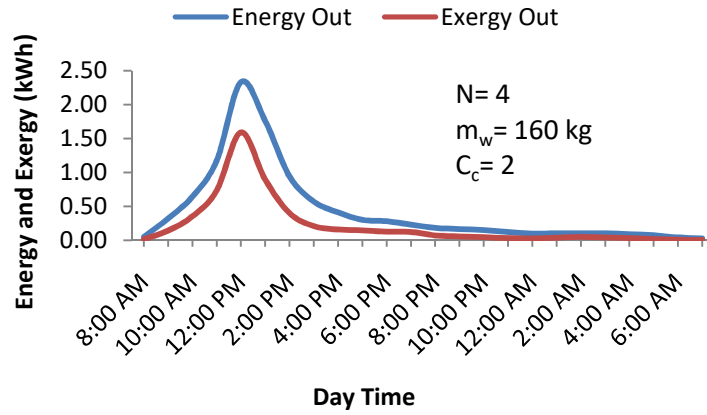


Fig. 4.7. Energy-Exergy gain of the system under the respective clear day conditions in the month of June

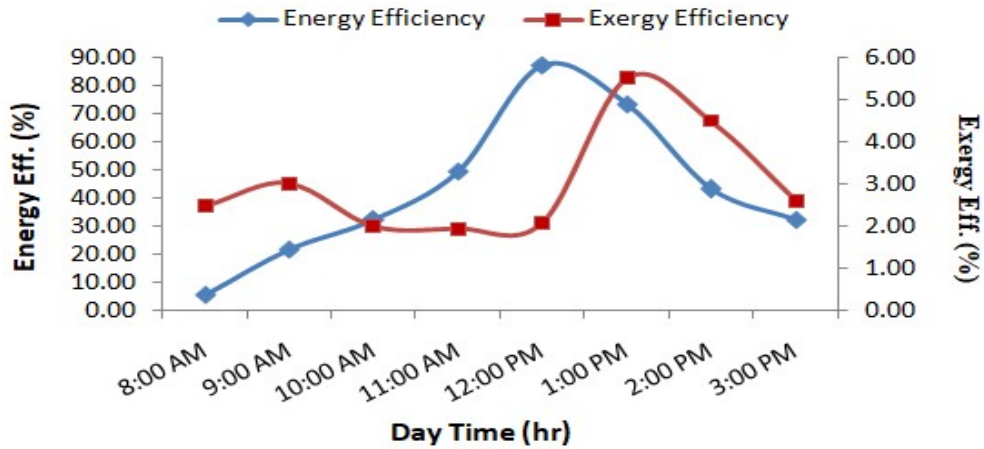


Fig. 4.8. Energy-Exergy efficiency variations of the system under the respective clear day conditions in the month of June ( $N=4$ )

#### 4.1.4 Energy Matrices Viabilities

Fig. 4.9 depicts the energy-exergy matrices observation of the proposed model for its 30 years of suggested life of working. The energy recovery time for the system is found quite well as 0.42 years whereas, little longer for the exergy pay off time (0.82 years). These results are mainly influenced by the embodied energy of the system and the respective annual yield

energy/exergy output from the system. It reflects the higher energy-exergy pay off time or factor for the higher yearly output, or lower embodied energy of the system. Fig. 4.10 represents the energy-exergy based life cycle conversion of the system, which is treated as better if the respective efficiencies are significantly higher (tending to 1) as appeared in the proposed system. It goes better with the increase in the system’s life, and the found 0.57 and 0.31 energy and exergy conversion efficiencies respectively for 30 years of the working life of the system.

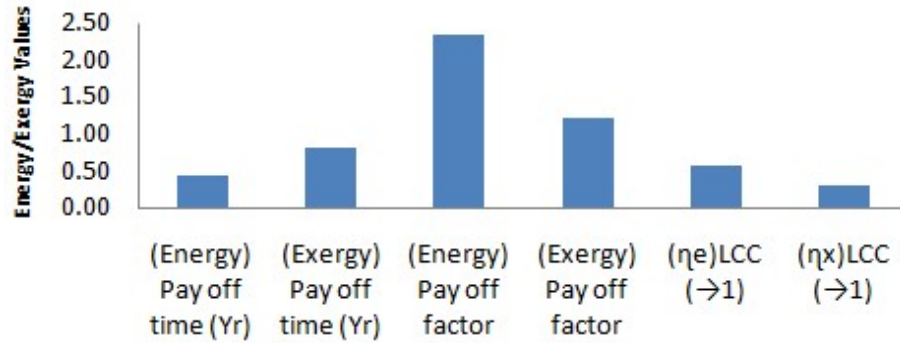


Fig. 4.9. Energy matrices distribution of the proposed model (n= 30yrs.).

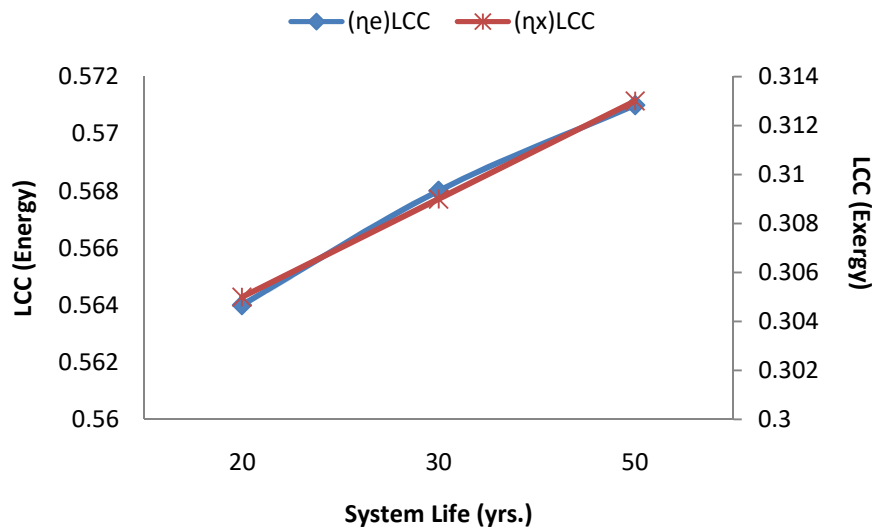
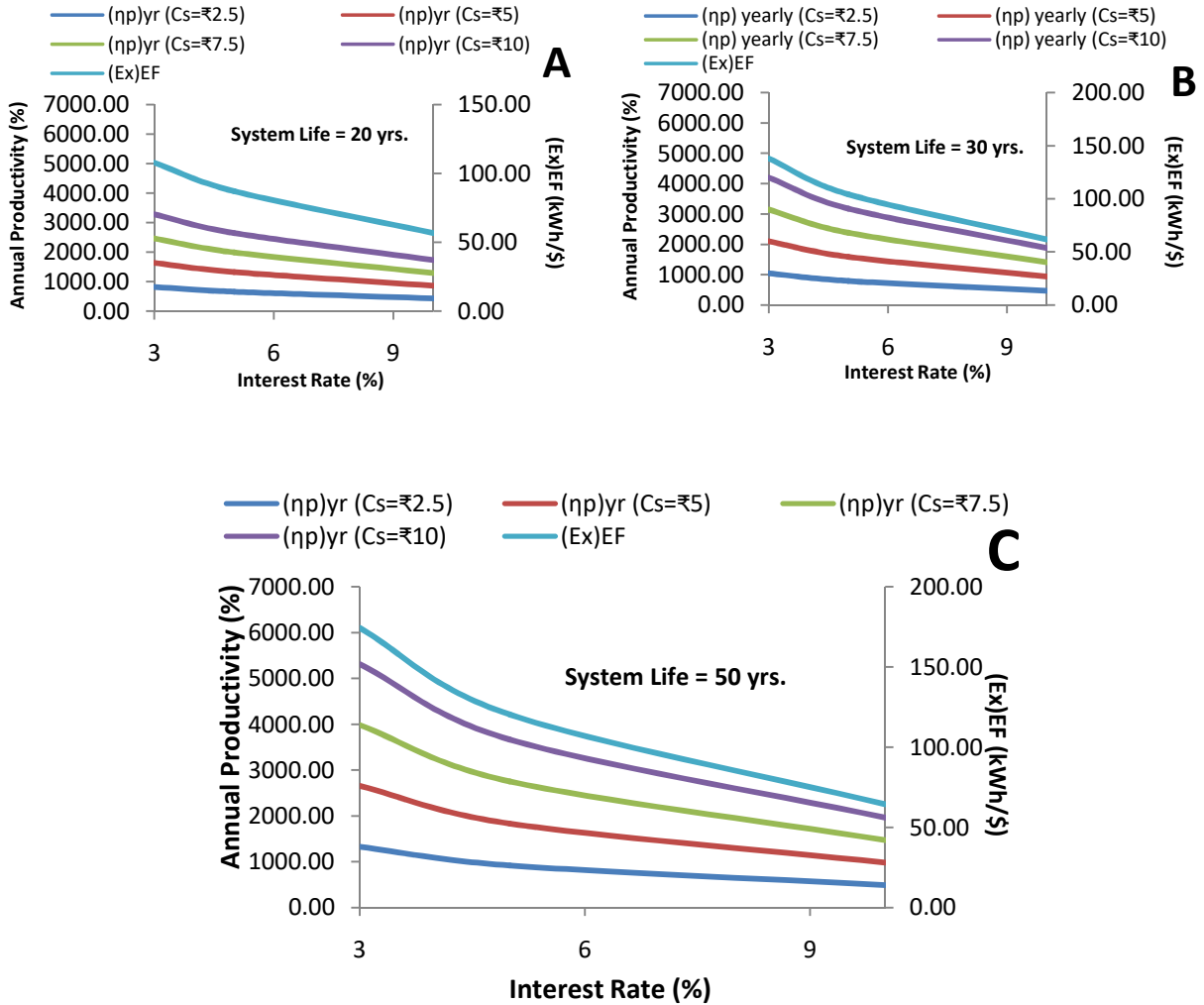


Fig. 4.10. Variations of life cycle conversion efficiency over a period of the system’s life

#### 4.1.5 Techno-Eco-Design Requisites: An Optimum-Environ-Economic Viability

Figs. 4.11 (A, B, C) represents the variations of annual productivity and exergo-economic factor under the influence of variable interest rates and yield selling prices of the proposed

system. Fig. 4.11 (B) represents the proposed system. The productivity and exergo-economic factor of the system keeps decreasing with the increase in interest rates, as higher interest rate increases the denominator value and the overall productivity and exergo-economic factor of the system correspondingly decreases. As the annual productivity for considered variables is more than 100%, hence the system is appreciably feasible for its continuous existence in the competitive market for the production of potable water.



Figs. 4.11 (A, B, C). Variation of annual productivity and exergo-economic factor under the influence of different interest rates of the proposed system

The results found for the productivity and exergo-economic factors as 940.8% and 61.8 respectively for 10% inflation interest rate and at 0.07\$/l selling price of the yield for the proposed system analysis. Further, the proposed system is good enough to mitigate the pollutants

(CO<sub>2</sub>, SO<sub>2</sub>, and NO) efficiently due to appreciable production of yield during its entire service life, and the corresponding energy-exergy mitigates are 131.97 tons and 64.44 tons for CO<sub>2</sub>, 1.00 tons, and 0.51 tons for SO<sub>2</sub>, 0.42 tons, and 0.21 tons for NO respectively. The environmental cost earned as carbon credit revenue (indirect cost) based on the energy-exergy observations is \$1318.4 and \$673.8 respectively of the proposed system.

## 4.2 Evacuated Annulus Tube Collector Assisted Double Slope Solar Desalination System

The proposed observation is being analyzed for 0.16m water depth into basin besides the water filled EATCs (parallel array having 4 optimum numbered EATCs) with 30° orientation angle for both SDS as well as the EATC to face maximum irradiative solar energy throughout the sunshine hours of the day. The entire observations have been analyzed by following meteorological data of New Delhi region, India, from IMD, Pune for an archetypal clear day in the month of June under the corresponding solar radiations over the inclined surface by following the *Liu and Jordan (1960)*.

### 4.2.1 Optimization of the Proposed Model

The analysis has been done for a variable number of EATCs under the different basin water depth conditions for the fixed SDS design parameters and observed the 4 number of EATC with 0.16m water depth attains 99.6°C temperature of basin water mass as represented in Fig. 4.12 and considered as the optimum design parameters. The optimum utilization of the components makes it possible to reach basin temperature up to 99.6°C and also a significantly large amount of water absorbs a higher amount of heat (sensible heat) and retains elevated temperature for a longer period that is helpful for nocturnal yield production also.

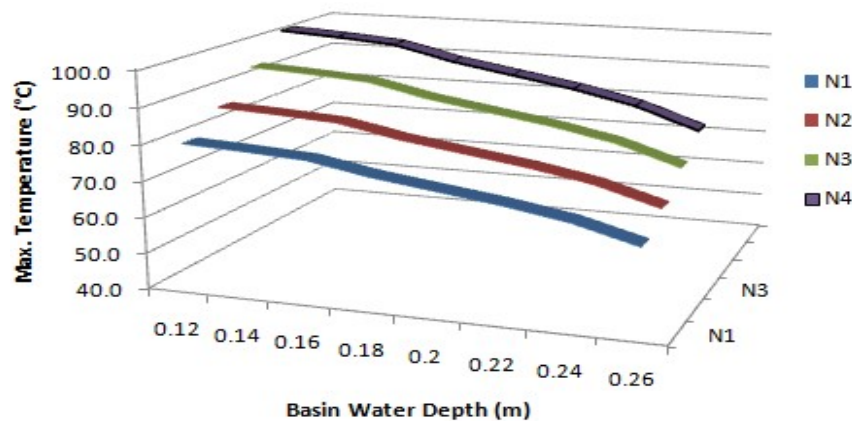


Fig. 4.12. Representation of basin water maximum temperatures against the variable water depth conditions and constant number of EATCs of the proposed system

#### 4.2.2 Performance Analysis: Energy-Exergy Considerations

Fig. 4.13 represents the temperature variations of different sections in the system for an archetypal clear day in the month of June. The water temperature of EATC effectively governs the basin water temperature and shows a rapid increase up to 1 pm with larger temperature differences that also cause a high mass flow rate. Also, a significant temperature difference i.e.  $T_w - T_{giE}$ ,  $T_w - T_{giW}$  appears up to 2 pm, and after that nominal temperature differences are maintained even for late night also, which provides diurnal and nocturnal yields respectively. Further, the respective variations in heat transfer coefficients in the basin chamber are represented in Fig. 4.14. It shows the East-West evaporative heat transfer plays major role in transferring heat from water surface to top glass cover, whereas the radiative heat transfer affects least due to significantly lower water temperature (i.e., lower than  $100^\circ\text{C}$ ) and it works effectively at higher temperatures more than  $1000^\circ\text{C}$ . The partial radiations transferred from East to West or West to East are quite similar for both the cases as shown in the Fig. 4.14.

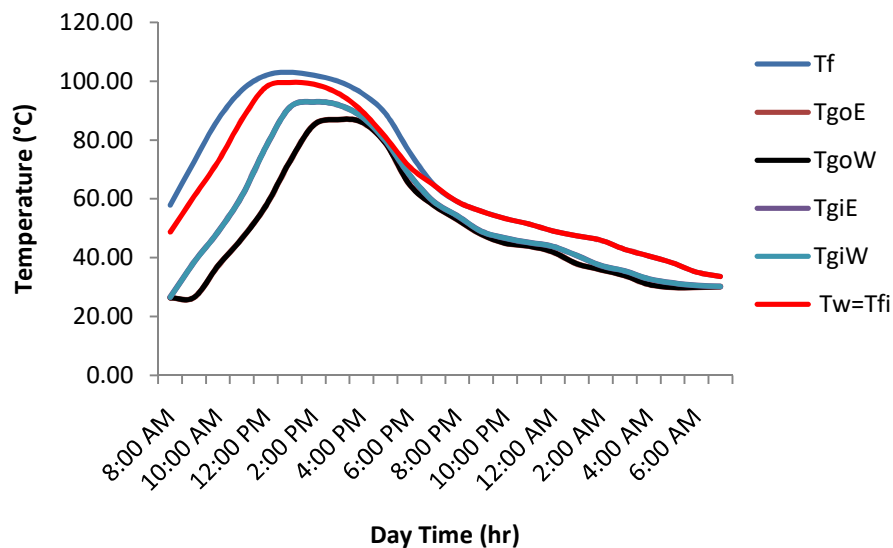


Fig. 4.13. Temperature variations at different sections in the system

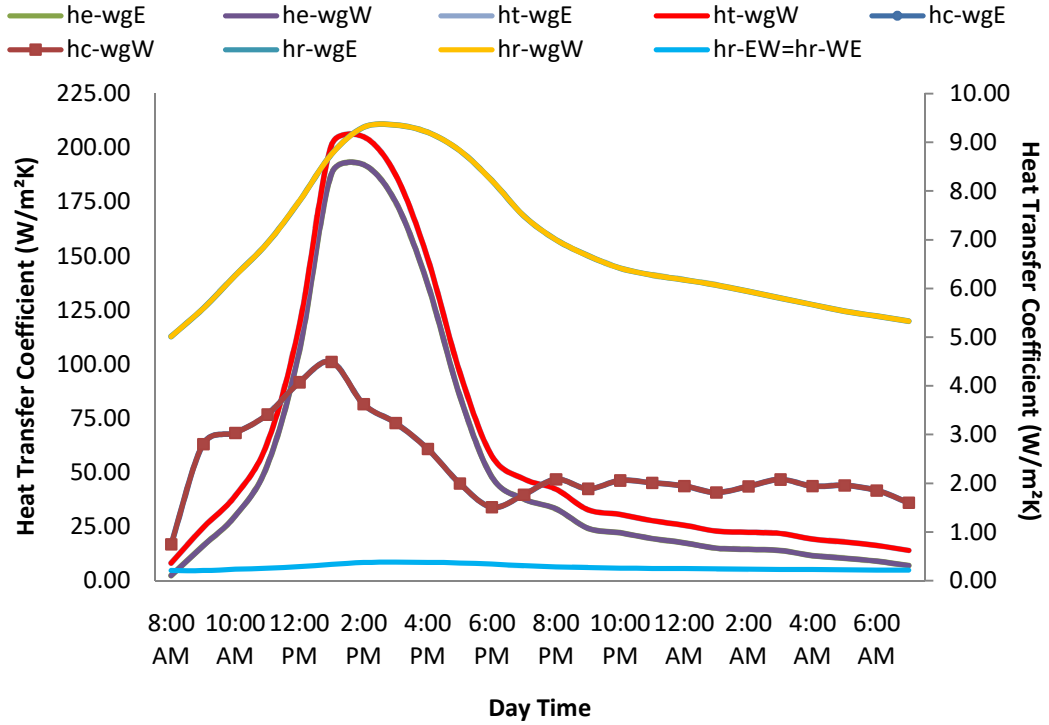


Fig. 4.14. Heat transfer coefficient variations at different segments in the system.

The production of yield with the corresponding thermo siphon at different basin water temperatures ( $T_w$ ) throughout the day have been represented in Fig. 4.15. The maximum yield (3kg) appeared at 1 pm due to the maximum  $T_w - T_{giE}$ ,  $T_w - T_{giW}$  (26°C), however the mass flow rate is maximum (55 kg/hr) at 2 pm because at that time maximum temperature difference is reached, which rapidly increases basin water temperature, hence evaporation increased which is not effectively utilized due to excessive production of vapor under the increases vapor conditions, also re-evaporates the condensed vapor again and again at the condensing surface of top glass, which results in slightly less yield at that time. The average yield of proposed system is significantly higher (0.71 kg/m<sup>2</sup>.hr).

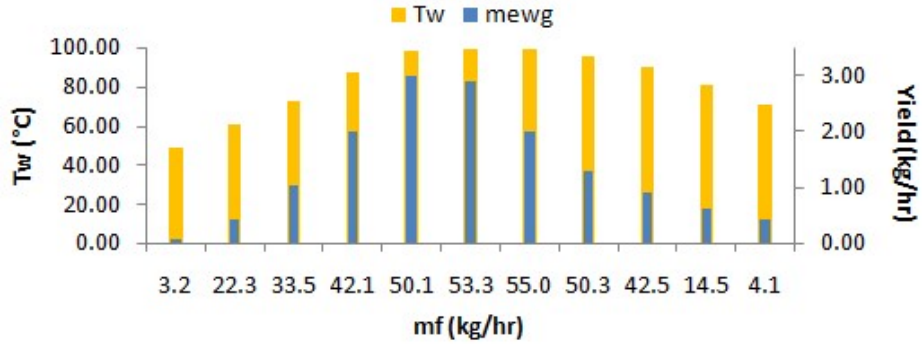


Fig. 4.15. Yield representation at different basin temperatures and corresponding mass flow rate

Fig. 4.16 represent the energy-exergy gain of the system under the respective clear day conditions and have the maximum gain of 1.91 kWh and 1.48 kWh respectively that is found at the peak hours of solar intensities that have least temperature differences ( $T_w - T_{giE}$ ,  $T_w - T_{giW}$ ). The energy efficiency goes higher at the higher temperature differences, so as the temperature difference goes higher; energy efficiency goes higher that is reflected up to noontime as shown in Fig. 4.17, and after that efficiencies are trending down because temperature differences and solar intensity, both go down all together. However, exergy efficiency follows energy efficiency adversely due to the involvement of exergetic phenomenon and respective degradation into the different components of solar system where the temperature differences and energy efficiencies are much higher and vice versa as depicted in Fig. 4.17 and found better exergy efficiency approximately at 2 pm. After that exergy efficiency keeps decreasing due slight increase in temperature differences and solar exergy.

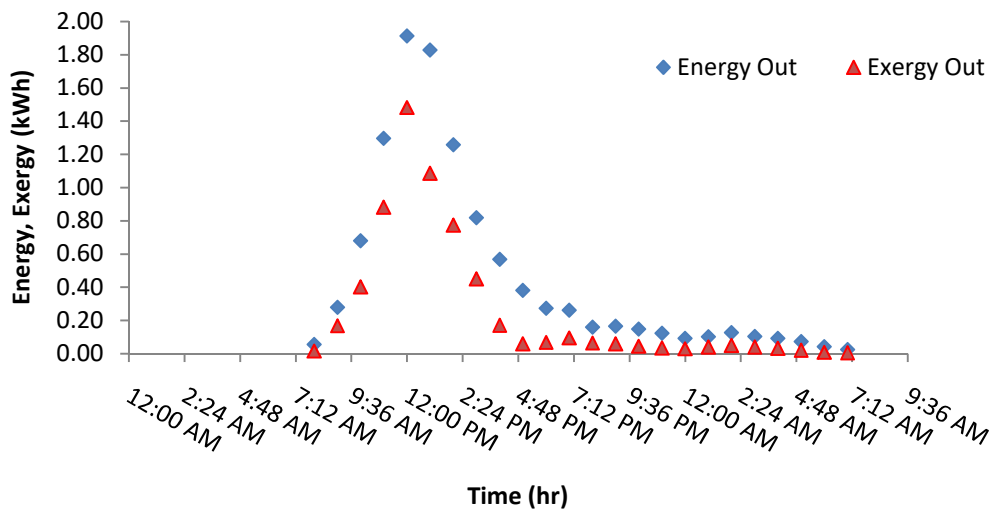


Fig. 4.16. Energy-Exergy gain of the system under the respective clear day conditions

The exergy efficiency decreases with the increase in solar exergy and temperature differences because of the involvement of more irreversible occurrences, particularly in solar peak moment in time (Fig. 4.17). Correspondingly, with the least temperature differences, higher exergy efficiency (14.6%) appeared and after that, exergy efficiency decreases due to the evaporation exergy transfer significantly decreased with the influence of irreversible exergy association of the respective components.

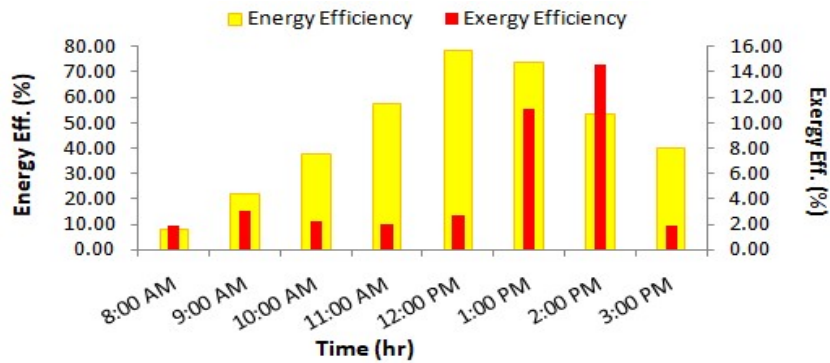


Fig. 4.17. Energy-Exergy efficiency variations of the system under the respective clear day conditions in the month of June (N= 4)

### 4.2.3 Energy Matrices Viabilities

Fig. 4.18 depicts the energy-exergy matrices observation of the proposed model for its 30 years of suggested life of working. The energy recovery time for the system is found quite well as 0.39 years whereas, for the exergy pay off time, it is a little longer, i.e., 0.69 years. The exergy pay off time is resulting in longer because of the higher amount of exergy destructions associated with it. Fig. 4.19 represents the energy-exergy based life cycle conversion of the system, which is treated as better if the respective efficiencies are significantly higher (tending to 1) as appeared in the proposed system. It goes better with the increase in system's life, and found 0.57 and 0.34 energy and exergy conversion efficiencies respectively for 30 years of the working life of the system.



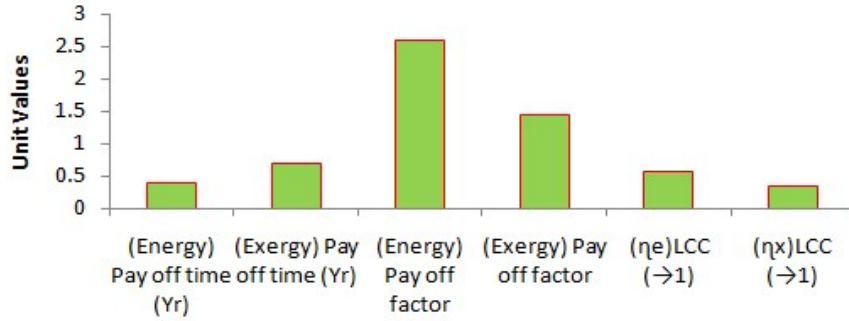


Fig. 4.18. Energy matrices distribution of the proposed model (n= 30yrs.).

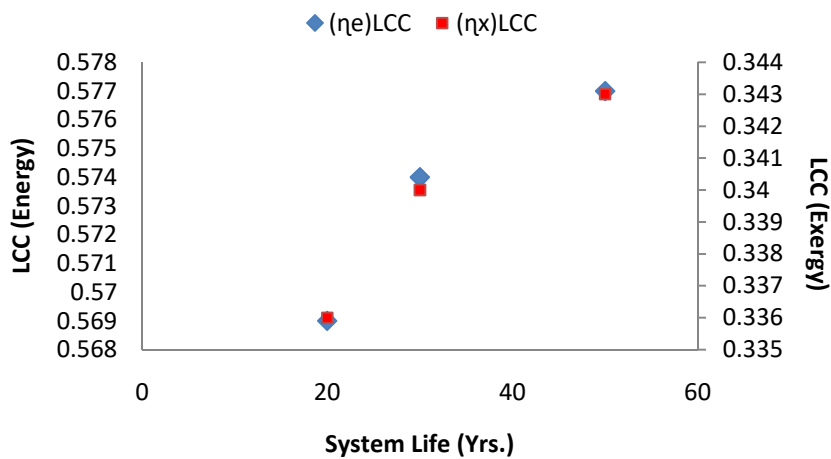


Fig. 4.19. Variations of life cycle conversion efficiency over a period of the system’s life

#### 4.2.4 Techno-Eco-Design Requisites: An Optimum-Environ-Economic Capability

The productivity and exergo-economic factor of the system keeps decreasing with the increase in interest rates, and the overall productivity and exergo-economic factor of the system correspondingly decreases (Fig. 4.20). As the annual productivity for considered variables is more than 100%, hence the system is appreciably feasible for its continuous existence in the competitive market for the production of potable water. The results found for the productivity and exergo-economic factors more than 100% and 75.46 respectively for 10% inflation interest rate and at 5₹/l or 0.07\$/l selling price of the yield for the proposed system analysis. Further, the proposed system is good enough to mitigate the pollutants (CO<sub>2</sub>, SO<sub>2</sub>, and NO) efficiently due to appreciable production of yield during its entire service life, and the corresponding energy-exergy mitigates are 139.74 tons and 77.30 tons for CO<sub>2</sub>, 1.16 tons, and 0.59 tons for SO<sub>2</sub>, 0.44

tons, and 0.24 tons for NO respectively. The environmental cost earned as carbon credit revenue (indirect cost) based on the energy-exergy observations is \$1396 and \$772.24 respectively of the proposed system for 30 years life.

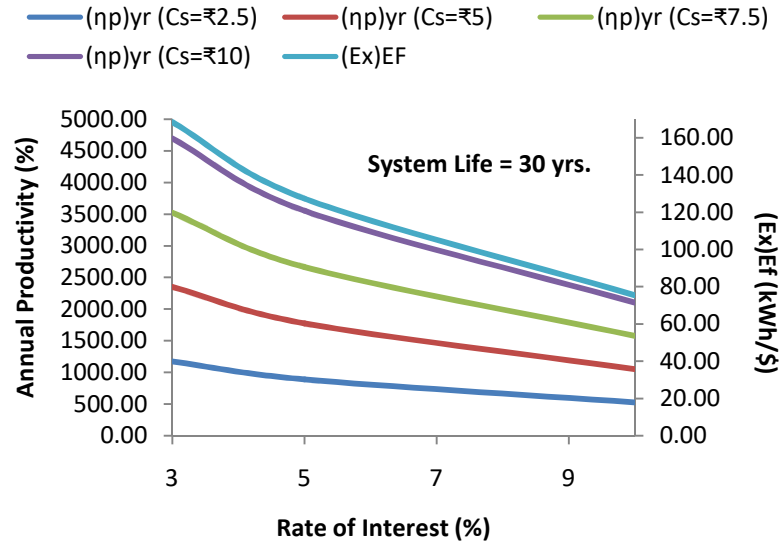


Fig. 4.20. Variation of annual productivity and exergo-economic factor under the influence of different interest rates of the proposed system

### 4.3 COMPARATIVE RESULT ANALYSIS

Both the designs of solar desalination systems have been analyzed comparatively based on the independent process parameters of the systems and this analysis also enumerates the individual performance observations of both the proposed systems (SS-SDS-EATC-MCPC, and DS-SDS-EATC-MCPC). The basic parameters for which the proposed systems are being compared, are taken as yield production, energy-exergy gain, energy-exergy efficiency, production cost, productivity, energy matrices, economic perspective, environ-exergo-economic observations (energy-exergy based), establishment, and environment costs, etc. as mentioned in the under given Table 4.1 that represents an overall glimpse of the results in a comparative manner and related observations with possible behavioral reasons.

Table 4.1 Overall glimpses of the results in a comparative manner and related observations with possible behavioral reasons

Parameters	SS Model	DS Model	Improvement Observations
Avg. hourly yield (kg/m <sup>2</sup> .h)	0.67	0.71	Improved hourly yield by 6% of DS model due to the significantly greater vapor generation and also have efficient condensing divided into two half at the top glaze surface throughout the day.
Energy gain (kWh)	10.27	10.86	Energy gain is directly dependent on the yield production, and the yield is better so improvement in energy gain appeared i.e. 5.7%.
Exergy gain (kWh)	5.32	6.07	The evaporative heat transfer coefficients and ( $T_w - T_{giE}$ , $T_w - T_{giW}$ ) are better than SS-SDS system, so 14.1% improvement is appeared in exergy gain.
Energetic Production cost (\$/kWh)	0.008	0.007	Due to large amount of yield production for fixed TAC that affects energetic production cost decreased (12.5%).
Exergetic Production cost (\$/kWh)	0.016	0.013	Due to large amount of yield production and fixed TAC which decreased exergetic production cost by 18.8%.
Productivity (%)	940.8	1052.98	Due to large yield production for fixed TAC, it affects productivity by significantly higher difference as 11.9%.
Establishment cost (\$)	214.92	200.79	Because of geometrical constraints, lower embodied energy is utilized to prepare DS model, so the overall establishment cost is also lower (6.6%) by SS model.
TAC (\$)	23.68	22.12	Because of the geometrical constraints, the lower embodied energy is utilized to prepare the DS-SDS model, so the overall TAC is also lower (6.6%).
$E_{in}$ (kWh)	1203.76	1152.87	Because of geometrical constraints, the lower embodied energy (4.2%) is utilized to prepare the DS-SDS model.
Exergo-economy (kWh/\$)	61.79	75.46	Due to large amount of yield production for fixed TAC, it affects exergo-economic factor as higher by 22.1%.

Energetic EPT (yrs.)	0.42	0.39	Due to higher yield production, the recovery time for the invested embodied energy is lower by 7.1%.
Exergetic EPT (yrs.)	0.82	0.69	Due to higher yield production, the exergetic recovery time for invested embodied energy is lower by 15.9%.
Energetic EPF (/yrs.)	2.36	2.59	As higher the energetic EPT, as lower the energetic EPF (9.8%) due to reciprocal in nature.
Exergetic EPF (/yrs.)	1.22	1.45	As higher the exergetic EPT, as lower the exergetic EPF (18.9%) due to reciprocal in nature.
LCCE	0.31	0.34	As both the responsible factors (yield, input energy) are higher in DS-SDS system, so an increase (9.7%) is appeared in exergetic LCCE because yield is proportionally higher than input energy.
CO <sub>2</sub> emission (kg)	1901.94	1821.53	Due to geometrical features, slightly lower embodied energy is consumed to construct DS model, hence related emissions of CO <sub>2</sub> also decreased (4.2%)
Energetic CO <sub>2</sub> mitigation (tons)	131.97	139.74	As the total yield production is higher for its entire life of DS-SDS model, so the related energetic mitigation of pollutant (CO <sub>2</sub> ) is also significantly higher (5.9%).
Exergetic CO <sub>2</sub> mitigation (tons)	67.44	77.30	As the total yield production is higher for the entire life of DS-SDS model, so the related exergetic mitigation of pollutant (CO <sub>2</sub> ) is also significantly higher (14.6%).
SO <sub>2</sub> emission (kg)	14.45	13.83	Due to geometrical features, slightly lower embodied energy is consumed to construct DS model, hence related emissions of SO <sub>2</sub> also decreased (4.3%)
Energetic SO <sub>2</sub> mitigation (tons)	1.0	1.06	The total yield is higher for the entire life of DS-SDS model, so the related energetic mitigation of pollutant (SO <sub>2</sub> ) is also significantly higher (6%).
Exergetic SO <sub>2</sub> mitigation (tons)	0.51	0.59	As the total yield is higher for the entire life of DS-SDS model, so the related exergetic mitigation of pollutant (SO <sub>2</sub> ) is also significantly higher (15.7%).
NO emission	6.02	5.76	Due to geometrical features, slightly lower embodied

(kg)			energy is consumed to construct DS model, hence related emissions of NO also decreased (4.3%)
Energetic NO mitigation (tons)	0.42	0.44	As the total yield is higher for the entire service life of DS-SDS model, so the related energetic mitigation of pollutant (NO) is also significantly higher (4.8%).
Exergetic NO mitigation (tons)	0.21	0.24	As the total yield is higher for the entire service life of DS-SDS model, so the related exergetic mitigation of pollutant (NO) is also significantly higher (14.3%).
Energetic environmental cost (\$)	1318.36	1395.99	Energetic environmental cost depends on yield, so higher yield mitigates more amounts of pollutants that benefit more (5.9%) in terms of environmental cost.
Exergetic environmental cost (\$)	673.77	772.24	This cost depends on yield, so higher yield offers more (14.6%) environmental cost from carbon credit revenue based on the pricing system in the International market.
Energy efficiency (%)	50.8	46.53	Energy gain is higher for DS model but due to better solar exposure, energy input is also higher, hence energy efficiency is diminished (8.4%) in DS-SDS system.
Exergy efficiency (%)	3.8	3.62	Besides the exergy gain is significantly higher but better solar exposure makes exergy input higher, hence exergy efficiency is diminished (4.7%) in DS-SDS system.

### 4.3.1 Energetic-exergetic Approach of Performance

The production of yield with the corresponding thermo siphon at different basin water temperatures ( $T_w$ ) and temperature differences throughout the day followed by mass flow rate and ( $T_w - T_{giE}$ ,  $T_w - T_{giW}$ ). The maximum yield appeared at 1 pm due to the maximum  $T_w - T_{giE}$ ,  $T_w - T_{giW}$  (26°C). The overall yield production appeared 4.6% better than the SS-SDS system. And, the average hourly yield of the proposed system is significantly higher, i.e., 0.71 kg/m<sup>2</sup> in comparison to other different models of solar desalination systems for similar areas of exposure, as represented in [Table 4.2](#).

Table 4.2 Comparative performance in terms of distillate output for various solar desalination systems in combination with solar thermal collectors

Study undertaken	SDS System	Solar Exposure (D+L/R+U)*	Avg. Yield (kg/m <sup>2</sup> .h)	Operating condition
Tiwari et al., 2003	Still basin	D	0.12	Conventional passive
Tiwari et al., 2003	Still basin and FPC	D	0.26	Active with fluid pump
Badran and Al-Tahaineh, 2015	Still basin and FPC	D	0.27	Active with fluid pump
Dev et al., 2012	SDS-EATC (24)	D	0.41	Passive thermo siphon
Sampathkumar et al., 2013	Still basin and heat pipe type EATC (15)	D	0.54	Active with fluid pump
Singh et al., 2013	Still basin and EATC (10)	D+Underneath mirror	0.56	Passive and thermo siphon
Mamouri et al., 2014	Still basin and heat pipe type EATC	D	0.32	Active with fluid pump
Kumar et al., 2014	Still basin and EATC (10)	D+Underneath mirror	0.58	Active with fluid pump
Yari et al., 2016	SDS basin and EATC (30)	D+Underneath mirror	0.48	Passive thermo siphon
Issa et al., 2017	Inclined SDS and EATC (5)	D	0.36	Active with fluid pump
Patel et al., 2019	Stepped SDS and EATC (5)	D	0.41	Passive thermo siphon
Xu et al., 2019	Tubular SDS-HP condenser and EATC (24)	D	0.57	Active with fluid pump
Dubey et al., 2021	SDS basin and EATC (10)	D+Underneath mirror	0.44	Active with fluid pump
<b>Proposed System (SS-SDS-EATC-MCPC)</b>	<b>Still basin, EATC-MCPC (4)</b>	<b>D+L/R+U</b>	<b>0.67</b>	<b>Passive and thermo siphon</b>
<b>Proposed System (DS-SDS-EATC-MCPC)</b>	<b>Still basin, EATC-MCPC (4)</b>	<b>D+L/R+U</b>	<b>0.71</b>	<b>Passive and thermo siphon</b>

\*D=direct solar exposure; L/R=left-right side solar exposure; U=underneath solar exposure around the EATC

The energy-exergy gain of the DS-SDS system under the respective clear day conditions have better gain with 5.7% and 14.1% improvements, respectively that is found at the peak hours of solar intensities that have least temperature differences as  $(T_w - T_{giE}, T_w - T_{giW})$ . Further, the energy and exergy efficiencies are sensitive parameters depends on both the important integral functionalities of the SDS basin as well as EATC and the corresponding energy efficiency depends on the temperature difference, incident solar radiations, heat transfer coefficients, and energy transfer from EATC to DS-SDS. The energy-exergy efficiency goes lower marginally by 8.4% and 4.7% at the higher temperature differences in comparison to SS-SDS-EATC-MCPC model. At the afternoon time, efficiencies are more significantly trending down because the temperature difference, as well as the solar intensity, goes marginally higher simultaneously. The exergy efficiency decreases with the increase in solar exergy and temperature differences due to more involvement of irreversible phenomenon, especially up to solar peak time. The exergy efficiency decreases due to the evaporation exergy transfer significantly decreased with the influence of irreversible exergy association of the respective components.

### 4.3.2 Energy Matrices Comparison

The findings of energy-exergy matrices of the proposed systems 275 average numbers of clear days for 30 years of working life considerations with the daily average solar intensity 401.8 kW found comparatively well by 7.1% and 15.9% improvement for energy pay-off time and factors respectively. The exergy pay off time is resulting in longer because of the higher amount of exergy destructions associated with it. These results are mainly influenced by the embodied energy of the system and the respective annual yield energy/exergy output from the system and reflected as the higher energy-exergy pay off time or factor for the higher yearly output, or lower embodied energy of the system. The energy-exergy based life cycle conversion of the system, which is treated as better if the respective efficiencies are significantly higher (tending to 1) as appeared in the proposed systems. The energy-exergy life cycle conversion efficiency trends are approximately similar under the variable system life working conditions. The DS-SDS system refers better with the increase in 9.7% increments in the exergy conversion efficiency in comparison to SS-SDS system.

### 4.3.3 System Economic Comparison

The study depicts, DS model is cheaper by 6.6% than the SS model due to its geometrical features. The productivity and exergo-economic factor for both the systems keeps decreasing with the increase in interest rates, as higher interest rate increases the denominator value in the resulting equations. As, annual productivity for considered variables is more than 100% for both the systems, hence systems are appreciably feasible for its continuous existence in competitive market for the production of potable water. The results found better for the productivity by 11.9% and exergo-economic factors by 22.1% than SS-SDS system under 10% inflation interest rate and at 5₹/l or 0.07\$/l selling price of the yield for both the proposed systems.

### 4.3.4 Environ-economic Comparison

The DS-SDS system is better enough to mitigate the pollutants (CO<sub>2</sub>, SO<sub>2</sub>, and NO) efficiently due to appreciable production of yield during its entire service life, and the corresponding energy-exergy mitigates are better by 5.9%, and 14.6% for CO<sub>2</sub>, 6%, and 15.7% for SO<sub>2</sub>, 4.8, and 14.3 for NO respectively. The environmental costs earned as carbon credit revenue (indirect cost) based on the energy-exergy observations are better by 5.9%, and 14.6%, respectively than the SS-SDS system for 30 years life.

Fig. 4.21 represents a generalized comparative observation of different enviro-economic parameters and yield of proposed systems with other solar desalination models. The observations reported by different researchers are rationalized accordingly for the similar system life (30 years), carbon mitigation (1.58 kg CO<sub>2</sub> per kWh mitigations or emissions), carbon credits earned revenue (9.99\$/ton of CO<sub>2</sub>) to compare the outputs on a similar platform of different systems. Based on the comparative observations, the DS-SDS system has more influence and is preferable in terms of different enviro-economic parameters and yield; hence the DS-SDS geometrical association is rather better in comparison to the SS-SDS system and also, other considered designs.



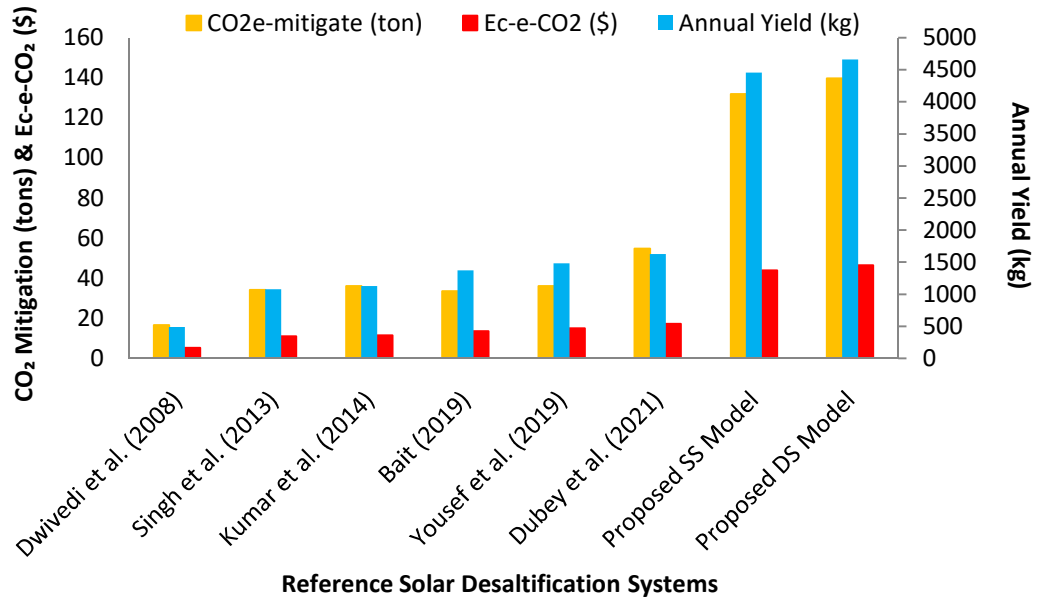


Fig. 4.21. Comparative observations of environ-economic perspectives under the influence of different solar desalination systems with respect to the proposed systems

*The chapter five represents the conclusion of the entire observations made for both the proposed systems in this Thesis. Further, the entire observations are concluded with recommendations for future work that may enlighten the researchers to move ahead for further possible developments in this field for the betterment to the environment, and the society.*

**CHAPTER: 5**

---

***CONCLUSIONS AND RECOMMENDATIONS FOR  
FUTURE WORK***

---

## CHAPTER: 5

### CONCLUSIONS AND RECOMMENDATIONS FOR FUTURE WORK

---

#### 5.0 INTRODUCTION

This chapter represents the conclusion of the entire observations made for both the proposed systems. The evacuated annulus tube collector assisted double slope solar desalination system with modified parabolic concentrator (DS-SDS-EATC-MCPC) shows the best performance in overall perspectives than the SS-SDS-EATC-MCPC model and also for other desalination systems taken into consideration for comparison. Further, the entire observations are concluded with future recommendations that may enlighten the researchers to move ahead for the additional possible developments in this field for the betterment to the society, environment, and the sustainable growth of human beings.

#### 5.1 CONCLUSION

The proposed model (SS-SDS-N-EATC-MCPC) under the novel design of MCPC considerations has been analyzed with a thermal model to predict the solar insolation responses over the performance, energy-exergy matrices, and various economic observations. Based on the present study, following conclusions at an optimal number of EATC associations are framed hereunder.

- i. The association of MCPC with 4 optimum numbers of EATCs integrated with SS-SDS performs well and reaches a maximum of 99.5°C basin water temperature at peak hours of the day under the highest solar irradiance.
- ii. The novel integration of MCPC-EATC provides approximately uniform peripheral solar radiation around the EATC with a concentration ratio 2 that improves the water temperature of higher water depth, and the well utilization of sensible heat makes the system much capable for nocturnal distillation also. The overall diurnal and nocturnal yield production is quite appreciable with a 16.2 kg daily yield.
- iii. The daily energy-exergy efficiencies are reported as 50.8% and 3.5%, respectively.

- iv. The interest rate, yield selling price, environmental revenue play an important role in the production cost, and consequently the energetic-exergetic yield production costs are quite appreciable of the proposed system for 30 years of life.
- v. The energy-exergy pay off time is reported as 0.42 years and 0.82 years, respectively. The energy-exergy conversion efficiency is reported as 0.57 and 0.31, respectively.
- vi. The energy-exergy mitigates of pollutants are 131.97 tons, and 64.44 tons for CO<sub>2</sub>, 1.00 tons, and 0.51 tons for SO<sub>2</sub>, 0.42 tons, and 0.21 tons for NO, respectively. The environmental revenue through carbon credit is good for energy-exergy as \$1318.4 and \$673.8, respectively. The exergy-economic factor results good as 61.79kWh/\$.

The proposed model (DS-SDS-N-EATC-MCPC) under the novel design of MCPC considerations is being developed with a thermal model to predict the solar insolation responses and eco-design requisites based on the optimum-environ-economic viabilities over the performance, energy-exergy matrices, and various economic observations.

- i. The association of MCPC with 4 optimum numbers of EATCs integrated with DS-SDS performs well and reaches a maximum of 99.6°C basin water temperature in peak hours of the day under the highest solar irradiance. The overall diurnal and nocturnal yield production is quite appreciable with a 16.94 kg daily yield.
- ii. The daily energy-exergy efficiencies are reported as 46.53% and 3.62%, respectively.
- iii. The interest rate, yield selling price, environmental revenue play an important role in the production cost, also the energetic-exergetic yield production costs are quite significant of the proposed system for 30 years of life. The energy-exergy pay off time is reported well enough with 0.39 years and 0.69 years, respectively. And, the energy-exergy conversion efficiency is reported as 0.57 and 0.34, respectively.
- iv. The energy-exergy mitigates of pollutants are 139.74 tons, and 77.30 tons for CO<sub>2</sub>, 1.06 tons, and 0.59 tons for SO<sub>2</sub>, 0.44 tons, and 0.24 tons for NO, respectively. The environmental revenue earned by the carbon credit is appreciable based on energy-exergy as \$1396 and \$772.24, respectively, and exergy-economic factor as 75.46kWh/\$.

The evacuated annulus tube collector assisted double slope solar desalination system with modified parabolic concentrator (DS-SDS-EATC-MCPC) shows the best performance in overall perspectives than the SS-SDS-EATC-MCPC model and also for other desalination systems

taken into consideration for comparison. The DS-SDS-EATC-MCPC system has been optimized to have with four numbers of EATCs and get the maximum possible basin water temperature as 99.6°C for the maximum circulation rate (thermo siphon) (~55 kg/hr), that accumulatively responses in terms of the highest yield (16.94 kg/m<sup>2</sup> day).

The daily overall energy-exergy efficiencies are showing a marginal decrement by 8.4%, and 4.7%, respectively than the SS-SDS system. The daily yield (improved by 4.6%) and its production cost at a nominal selling price found better than SS-SDS system.

The energy-exergy based CO<sub>2</sub> mitigates and environmental earned revenue are better by 5.9%, and 14.6%, respectively than the SS-SDS system. The establishment cost of DS-SDS system is appreciably lower by 6.6%, however both the system's productivity is found more than 100% that depicts the systems are appreciably feasible.

The evident yield at little production cost, environmental returns, elevated mitigation, and short pay-off time makes the DS-SDS-EATC-MCPC system better sustainable and viable for lesser collector areas and optimum EATC with MCPC as eco-design requisites for projected scheme.

## 5.2 RECOMMENDATIONS FOR FUTURE WORK

As the proposed models showing relatively lower yield at peak hours in an archetypal clear day with respect to the corresponding increase in mass flow rate. And this happens because the elevated temperature also creates a larger amount of vapor, and all those are not properly utilized to form relative yield. Therefore, an additional condensing chamber can be utilized to reconsider the left part of this excessive amount of vapors for getting the maximum amount of yields, especially in peak hours of the day.

Furthermore, MCPC study and experimental validation are recommended along with the CFD analysis for both the proposed models to check its validity, competency, and sustainability for the continuous existence in the competitive market for the production of potable water and also the corresponding responses under variable meteorological conditions.

## APPENDIX – A

SDS basin and EATC water mass thermo-physical properties influenced by temperature variations expressed in terms of the empirical relations (*Pissavi, 1982; IAPWS, 1996; IAPWS, 2008; Koffi, 2008*)

Parameter	Empirical Relation
Specific heat capacity (J/kg K)	$C_w = 4226 - 3.244T + 0.0575T^2 - 0.0002656T^3$
Water mass density (kg/m <sup>3</sup> )	$\rho = 1001 - 0.08832T - 0.003417T^2$
Thermal conductivity (W/m K)	$K_w = 0.557 + 0.002198T - 0.00000708T^2$
Factor of volumetric thermal expansion (K <sup>-1</sup> )	$\beta' = (0.3 + 0.116T - 0.0004T^2) \cdot 10^{-4}$
Kinematic viscosity (m <sup>2</sup> /s)	$\nu = [(0.5155 + 0.0192T)^{-1} - 0.12] \cdot 10^{-6}$
Dynamic viscosity (N.s/m <sup>2</sup> )	$\mu = 4.2844 \times 10^{-5} + \{0.517(T + 64.993)^2 - 91.296\}^{-1}$
Latent heat of vaporization (J/kg)	$L = 2.506 \times 10^6 - 2.369 \times 10^3T + 0.2678T^2 - 8.103 \times 10^{-3}T^3$

## APPENDIX – B

Relations utilized to solve Eq. (3.2.2) following (Duffie and Beckman, 2006; Singh and Samsher, 2020) as mentioned,

$$U_{saa} = \left( \frac{R_{i2} \ln\left(\frac{R_{i2}}{R_{i1}}\right)}{K_g} + \frac{1}{h_{r-v}} + \frac{R_{o2} \ln\left(\frac{R_{o2}}{R_{o1}}\right)}{K_g} + \frac{1}{h_o} \right)^{-1}$$

$$I_s(a) = I_b(t) \cdot (\alpha \tau)_{eff}$$

$$(\alpha \tau)_{eff} = R_{sc} \alpha \tau^2 (A_a / A_{rc})$$

$$h_o = h_{c-wg} + h_{r-wg} = 5.7 + 3.8V$$

$$h_{r-v} = \varepsilon_{eff} \cdot \sigma \left[ (T_f + 273.15)^2 + (T_{sa} + 273.15)^2 \right] \times [T_f + T_{sa} + 546.30]$$

$$\varepsilon_{eff} = (1/\varepsilon_g + 1/\varepsilon_w - 1)^{-1}$$

Expressions utilized to solve Eqs. (3.2.5), (3.2.7), and (3.2.9) as mentioned,

$$F_1 = \frac{F' \cdot h_{saf}}{(F' h_{saf} + U_{saa})}$$

$$U_L = \frac{F' \cdot h_{saf} \cdot U_{saa}}{(F' h_{saf} + U_{saa})}$$

$$F_2 = 1 - \frac{(A_{rc} \cdot F_r) U_L}{\dot{m}_f C_f}$$

$$F_r = \frac{\dot{m}_f C_f}{A_{rc} \cdot U_L} \left\{ 1 - \exp\left(-\frac{2\pi R_{i1} L_{EATC} \cdot U_L}{\dot{m}_f C_f}\right) \right\}$$

$$h_{t-g} = 5.7 + 3.8V$$

$$U_c = h_{t-g} / \left( 1 + \frac{h_{t-g}}{K_g / t_g} \right)$$

Relations utilized to solve Eq. (3.2.10) as mentioned (Dunkle, 1961; Cooper, 1973; Singh and Samsher, 2020; Singh and Samsher, 2021),

$$\alpha_g^A = (1 - R_g)\alpha_g$$

$$R_g = 1 - \frac{4n_o n_g}{(n_o + n_g^2)(1 + n_o)}$$

$$h_{t-w} = h_{r-wg} + h_{c-wg} + h_{e-wg}$$

$$h_{r-w} = \varepsilon_{eff} \cdot \sigma \left\{ (T_w + 273.15)^2 + (T_{gi} + 273.15)^2 \right\} \{T_w + T_{gi} + 546.30\}$$

$$h_{c-w} = 0.884 \left\{ (T_w - T_{gi}) + \frac{(P_w - P_{gi})(T_w + 273.15)}{268.9 \times 10^3 - P_w} \right\}^{1/3}$$

$$h_{e-wg} = 16.273 \times 10^{-3} h_{c-wg} \left\{ \frac{P_w - P_{gi}}{T_w - T_{gi}} \right\}$$

$$P_w = \exp \left( 25.317 - \frac{5144}{T_w + 273.15} \right)$$

$$P_{gi} = \exp \left( 25.317 - \frac{5144}{T_{gi} + 273.15} \right)$$

Equations utilized to solve Eq. (3.2.12) as mentioned,

$$\alpha_w^A = \{(1 - R_g)(1 - \alpha_g)(1 - R_w)\alpha_w\}$$

$$R_w = [1 - (4n_o n_w) / \{(n_o + n_w^2)(1 + n_o)\}]$$

$$R_a = \frac{g\beta' \rho^2 X^3 C_w \Delta T}{\mu K_w}$$

$$G_r = \frac{g\beta' \rho^2 X^3 \Delta T}{\mu^2}; P_r = \frac{\mu C_w}{K_w}$$

$$X = (L_o - B_o) / 2 \quad (\text{For rectangular horizontal surface})$$

$$X = \frac{\text{Area (A)}}{\text{Perimeter (P)}} \quad (\text{For other surfaces})$$

Expressions utilized to solve Eq. (3.2.12a) as mentioned (Tiwari, 2014),



$$h_{ba} = \{(t_b/K_b) + 0.357\}^{-1}$$

$$\alpha_{beff} = (\alpha_b^A \cdot h_{bw}) / (h_{bw} + h_{ba})$$

$$U_{bwa} = (h_{ba} \cdot h_{bw}) / (h_{bw} + h_{ba})$$

Relations utilized to solve Eqs. (3.2.14), (3.2.16) as mentioned,

$$U_{ta} = (h_{t-wg} \cdot U_c \cdot A_g) / (h_{t-wg} \cdot A_b + U_c \cdot A_g)$$

$$h'_1 = (h_{t-wg} \cdot A_g) / (h_{t-wg} \cdot A_b + U_c \cdot A_g)$$

$$a = \{U_{eff} + \dot{m}_f C_f (N - 1)\} / (m_w C_w)$$

$$U_{eff} = \{A_b (U_{bwa} + U_{ta}) + (A_{rc} F_r) U_L\}$$

$$\alpha_{eff}^A = (\alpha_w^A + \alpha_{beff} + h'_1 \cdot \alpha_g^A)$$

$$f(t) = \{I_s(t) A_b \cdot \alpha_{eff}^A + T_a \cdot U_{eff} + F_1 \cdot (\alpha \tau)_{eff} \cdot (A_{rc} F_r) I_b(t)\} / (m_w C_w)$$

$$(Nu \cdot Gr) / Pr = (g \cdot \beta' \cdot d^4 \cdot \dot{q}) / (v^2 \cdot \mu \cdot C_f)$$

$$Nu = \frac{h \cdot X}{K_w}; v = \mu / \rho$$

## APPENDIX – C

Expressions utilized to solve Eqs. (3.3.1), (3.3.2), and (3.3.4) (Duffie and Beckman, 2006; Singh and Samsher, 2020) as mentioned,

$$F_1 = \frac{F' \cdot h_{saf}}{(F' h_{saf} + U_{saa})}; F_2 = 1 - \frac{(A_{rc} \cdot F_r) U_L}{\dot{m}_f C_f}; U_L = \frac{F' \cdot h_{saf} \cdot U_{saa}}{(F' h_{saf} + U_{saa})}$$

$$F_r = \frac{\dot{m}_f C_f}{A_{rc} \cdot U_L} \left\{ 1 - \exp\left(-\frac{2\pi R_{i1} L_{EATC} \cdot U_L}{\dot{m}_f C_f}\right) \right\}$$

$$h_{t-gE} = h_{t-gW} = 5.7 + 3.8V$$

$$U_{cE} = h_{t-gE} / \left(1 + \frac{h_{t-gE}}{K_g/t_g}\right); U_{cW} = h_{t-gW} / \left(1 + \frac{h_{t-gW}}{K_g/t_g}\right)$$

Relations utilized to solve Eqs. (3.3.5 – 3.3.6) as mentioned (Dunkle, 1961; Cooper, 1973; Singh and Samsher, 2020; Singh and Samsher, 2021),

$$\alpha_g^A = (1 - R_g) \alpha_g; R_g = 1 - \frac{4n_o n_g}{(n_o + n_g^2)(1 + n_o)}$$

$$h_{t-wgE} = h_{r-wgE} + h_{c-wgE} + h_{e-wgE}$$

$$h_{t-wgW} = h_{r-wgW} + h_{c-wgW} + h_{e-wgW}$$

$$h_{r-wgE} = \varepsilon_{eff} \cdot \sigma \left\{ (T_w + 273.15)^2 + (T_{giE} + 273.15)^2 \right\} \{ T_w + T_{giE} + 546.30 \}$$

$$h_{r-wgW} = \varepsilon_{eff} \cdot \sigma \left\{ (T_w + 273.15)^2 + (T_{giW} + 273.15)^2 \right\} \{ T_w + T_{giW} + 546.30 \}$$

$$h_{c-wgW} = 0.884 \left\{ (T_w - T_{giW}) + \frac{(P_w - P_{giW})(T_w + 273.15)}{268.9 \times 10^3 - P_w} \right\}^{1/3}$$

$$h_{c-wgE} = 0.884 \left\{ (T_w - T_{giE}) + \frac{(P_w - P_{giE})(T_w + 273.15)}{268.9 \times 10^3 - P_w} \right\}^{1/3}$$

$$h_{e-wgE} = 16.273 \times 10^{-3} h_{c-wgE} \left\{ \frac{P_w - P_{giE}}{T_w - T_{giE}} \right\}$$

$$h_{e-wgW} = 16.273 \times 10^{-3} h_{c-wgW} \left\{ \frac{P_w - P_{giW}}{T_w - T_{giW}} \right\}$$

$$h_{r-EW} = h_{r-WE} = 0.034 \times \sigma \left\{ (T_{giE} + 273.15)^2 + (T_{giW} + 273.15)^2 \right\} \{T_{giE} + T_{giW} + 546.3\}$$

$$P_w = \exp \left( 25.317 - \frac{5144}{T_w + 273.15} \right)$$

$$P_{giE} = \exp \left( 25.317 - \frac{5144}{T_{giE} + 273.15} \right)$$

$$P_{giW} = \exp \left( 25.317 - \frac{5144}{T_{giW} + 273.15} \right)$$

Equations utilized to solve Eq. (3.3.7) as mentioned (Tiwari, 2014; Singh and Samsher, 2021),

$$h_{bw} = (K_w/t_b) \{C(R_a)^{1/n}\}$$

$$\alpha_w^A = \{(1 - R_g)(1 - \alpha_g)(1 - R_w)\alpha_w\}$$

$$R_w = [1 - (4n_o n_w) / \{(n_o + n_w^2)(1 + n_o)\}]$$

$$R_a = \frac{g\beta' \rho^2 X^3 c_w \Delta T}{\mu K_w}; G_r = \frac{g\beta' \rho^2 X^3 \Delta T}{\mu^2}; P_r = \frac{\mu c_w}{K_w}$$

$$X = (L_o - B_o)/2 \quad (\text{For rectangular horizontal surface})$$

$$X = \frac{\text{Area (A)}}{\text{Perimeter (P)}} \quad (\text{For other surfaces})$$

Expressions utilized to solve Eq. (3.3.9) as mentioned (Tiwari, 2014),

$$h_{ba} = \{(t_b/K_b) + 0.357\}^{-1}$$

$$\alpha_{beff} = (\alpha_b^A \cdot h_{bw}) / (h_{bw} + h_{ba})$$

$$U_{bwa} = (h_{ba} \cdot h_{bw}) / (h_{bw} + h_{ba})$$

Relations utilized to solve Eqs. (3.3.10 – 3.3.15), and (3.3.17) as mentioned,

$$U_{taE} = (h_{t-wgE} \cdot U_{cE} \cdot A_{gE}) / \left[ \frac{A_b}{2} \cdot h_{t-wgE} + A_{gE} \cdot (U_{cE} + h_{r-EW}) \right]$$

$$U_{taW} = (h_{t-wgW} \cdot U_{cW} \cdot A_{gW}) / \left[ \frac{A_b}{2} \cdot h_{t-wgW} + A_{gW} \cdot (U_{cW} + h_{r-WE}) \right]$$

$$h'_{1E} = (h_{t-wgE} \cdot A_{gE}) / \left[ \frac{A_b}{2} \cdot h_{t-wgE} + A_{gE} \cdot (U_{cE} + h_{r-E}) \right]$$

$$h'_{1W} = (h_{t-wgW} \cdot A_{gW}) / \left[ \frac{A_b}{2} \cdot h_{t-wgW} + A_{gW} \cdot (U_{cW} + h_{r-WE}) \right]$$

$$h'_{2E} = \left( \frac{A_b}{2} \cdot h_{t-wgE} \right) / \left[ \frac{A_b}{2} \cdot h_{t-wgE} + A_{gE} \cdot (U_{cE} + h_{r-EW}) \right]$$

$$h'_{2W} = \left( \frac{A_b}{2} \cdot h_{t-wgW} \right) / \left[ \frac{A_b}{2} \cdot h_{t-wgW} + A_{gW} \cdot (U_{cW} + h_{r-WE}) \right]$$

$$a = \left[ U_{eff}^{DS} + \frac{A_b}{2} \cdot h_{r-EW} \cdot (h'_{1E} + h'_{1W}) + \dot{m}_f C_f \cdot (N - 1) \right] / (m_w C_w)$$

$$U_{eff}^{DS} = A_b \left( U_{bwa} + \frac{U_{taE}}{2} + \frac{U_{taW}}{2} \right) + (A_{rc} \cdot F_r) \cdot U_L$$

$$f(t) = \left[ T_a \cdot U_{eff}^{DS} + \{I_{sE}(t) + I_{sW}(t)\} \times \left( \alpha_w^A \cdot \frac{A_g}{2} + \alpha_{beff} \cdot \frac{A_b}{2} \right) + (A_{rc} \cdot F_r) \cdot F_1 \cdot (\alpha \tau)_{eff} \cdot I_b(t) + \frac{A_b}{2} \{T_{giW} \cdot h_{r-EW} (h'_{1E} + h'_{1W}) + \alpha_g^A (h'_{1E} \cdot I_{sE}(t) + h'_{1W} \cdot I_{sW}(t))\} \right] / (m_w C_w)$$

$$(Nu \cdot Gr) / Pr = (g \cdot \beta' \cdot d^4 \cdot \dot{q}) / (v^2 \cdot \mu \cdot C_f)$$

$$Nu = \frac{h \cdot X}{K_w}; v = \mu / \rho$$

## REFERENCES

---

- Abbaspour, M. J., Faegh, M., Shafii, M. B., 2019. Experimental examination of a natural vacuum desalination system integrated with evacuated tube collectors. *Desalination* 467, 79–85.
- Agrawal, S., Tiwari, G.N., 2012. Exergoeconomic analysis of glazed hybrid photovoltaic thermal module air collector. *Sol. Energy* 86 (9), 2826–2838.
- Ashcroft, H., 1950. The productivity of several machines under the care of one operator. *J. Roy. Stat. Soc. (Lond.) Ser. B XII*, 145–151.
- Badran, O., Al-Tahaineh, H., 2005. The effect of coupling a flat-plate collector on the solar still productivity. *Desalination* 183, 137–142.
- Bait, O., 2019. Exergy, environeeconomic and economic analyses of a tubular solar water heater assisted solar still. *J Cleaner Production*, 212, 630 – 46.
- Behnam, P., Shafii, M. B., 2016. Examination of a solar desalination system equipped with an air bubble column humidifier, evacuated tube collectors and thermosyphon heat pipes. *Desalination* 397, 30–37.
- Benson, F., 1952. Further notes on the productivity of machines requiring attention at random intervals. *J. Roy. Stat. Soc. B XIV*, 200–210.
- Budihardjo, I., Morrison, G.L., 2009. Performance of water-in-glass evacuated tube solar water heaters. *Solar Energy*, 83, 49–56.
- Budihardjo, I., Morrison, G.L., Behnia, M., 2007. Natural circulation flow through water-in- lass evacuated tube solar collectors. *Solar Energy*, 81, 1460–1472.
- Camacho, L.M., et al., 2013. Advances in membrane distillation for water desalination and purification applications. *Water* 5, 94e196.
- Cengel, X.A., Boles, M.A., 2013. *Thermodynamics, an engineering approach*, McGraw-Hill Education Pvt. Ltd., New York.

- Cooper, P. I., 1973. The maximum efficiency of single-effect solar stills, *Solar Energy* 15: 205 – 217.
- Cooper, P.I., 1969. The absorption of solar energy radiation in solar stills, *Solar Energy* 12:133.
- Cornelissen, R.L., Hirs, G.G., 2002. The value of the exergetic life cycle assessment besides the LCA, *Energy Conversion and Management* 43: 1417–24.
- Cox, D.R., 1951. The productivity of machines requiring attention at random intervals. *J. Roy. Stat. Soc. B XIII*, 65–82.
- Dev, R., Singh, H. N., Tiwari, G. N., 2011. Characteristic equation of double passive solar still. *Desalination* 267, 261 – 266.
- Dev, R., Tiwari, G. N., 2009. Characteristic equation of passive solar still. *Desalination* 245, 246 – 265.
- Dev, R., Tiwari, G. N., 2012. Annual performance of evacuated tubular collector integrated solar still. *Desalination Water Treatment* 41, 204–223.
- Dubey A, Kumar S, Arora A, 2021. Enviro-Energy-Exergo-Economic Analysis of ETC Augmented Double Slope Solar Still with ‘N’ Parallel Tubes under Forced mode: Environmental and Economic Feasibility. *Journal of Cleaner Production*, DOI: <https://doi.org/10.1016/j.jclepro.2020.123859>
- Duffie, J.A., Beckman, W.A., 2006. *Solar engineering of thermal processes*. New Jersey: Hoboken- Wiley.
- Dunkle, R. V., 1961. Solar water distillation: the roof type solar still and a multiple effect diffusion still, *International Developments in Heat Transfer ASME* 895 – 902.
- Dwivedi, V.K., Tiwari, G.N., 2010. Thermal modeling and carbon credit earned of a double slope passive solar still. *Desalination and Water Treatment*, 13(1/3), 400 – 410.
- El-Sebaii, A. A., El-Bialy, E., 2015. Advanced designs of solar desalination systems: A review. *Renewable and Sustainable Energy Reviews* 49, 1198 – 1212.

EPA, 1988. Risk Assessment Forum. Special Report on Ingested Inorganic Arsenic. Skin Cancer; Nutritional Essentiality. DC US Environmental Protection Agency, Washington (EPA-625/3-87/013).

EPA, 2007. European Communities (Drinking Water) (No. 2) Regulations (2007) S.I. 278.

Feilizadeh, M., Estahbanati, M. R. K., Khorram, M., Rahimpour, M. R., 2019. Experimental investigation of an active thermosyphon solar still with enhanced condenser. *Renewable Energy* 143, 328 – 334.

Gadgil, A., 1998. Drinking water in developing countries. *Annu. Rev. Energy Environ.* 23, 253e286.

Garg, H.P., Mann, H.S., 1976. Effect of climatic, operational and design parameters on the year round performance of single sloped and doubled sloped solar still under Indian arid zone conditions. *Sol. Energy* 18, 159e163.

Goh, P.S., Matsuura, T., Ismail, A.F., Hilal, N., 2016. Recent trends in membranes and membrane processes for desalination. *Desalination* 391, 43e60.

Hanson, A., Zachritz, W., Stevens, K., Mimbela, L., Polka, R., Cisneros, L., 2004. Distillate water quality of a single-basin solar still: laboratory and field studies. *Sol. Energy* 76, 635e645.

Hedayati-Mehdiabad, E., Sarhadd, F., Sobhnamayan, F., 2020. Exergy performance evaluation of a basin-type double-slope solar still equipped with phase-change material and PV/T collector. *Renewable Energy*, 145, 2409 – 2425.

Hussain, M.I., Lee, G.H., 2015. Parametric performance analysis of a concentrated photovoltaic co-generation system equipped with a thermal storage tank. *Energy Convers. Manag.* 92, 215e222.

IAPWS, 1996. International association for the properties of water and steam, for the thermodynamic properties of ordinary water substance for general and scientific use, 1996.

IAPWS, 2008. International association for the properties of water and steam, the viscosity of ordinary water substance, 2008.

- ILO, 1979. Introduction to Work Study. International Labor Organization, Geneva, ISBN 81-204-0602-8.
- Imad, A., Badran, O., 2004. The effect of using different designs of solar stills on water desalination. *Desalination* 169, 121e127.
- IRENA, 2015. Renewable Desalination: Technology Options for Islands.
- Issa, R. J., Chang, B., 2017. Performance study on evacuated tubular collector coupled solar still in west texas climate. *International Journal of Green Energy*, DOI: 10.1080/15435075.2017.1328422.
- Kalogirou, S., 2003. The potential of solar industrial process heat applications. *Appl Energy* 76, 337–61.
- Koffi, P.M.E., Andoh, H.Y., Gbaha, P., Toure, S., Ado, G., 2008. Theoretical and experimental study of solar water heater with internal exchanger using thermosiphon system. *Energy Conversion and Management*, 49, 2279 – 2290.
- Kumar, S., Dubey, A., Tiwari, G., 2014. A solar still augmented with an evacuated tube collector in forced mode. *Desalination* 347, 15–24.
- Kumar, S., Tiwari, G.N., 2011. Analytical expression for instantaneous exergy efficiency of a shallow basin passive solar still. *International Journal of Thermal Sciences*, 50, 2543– 2549.
- Kwon, Y.H., Kwak, H.Y., Oh, S.D., 2001. Exergoeconomic analysis of gas turbine cogeneration systems. *Exergy* 1, 31–40.
- Lawrence, S. A., Tiwari, G. N., 1990. Theoretical evaluation of solar distillation under natural circulation with heat exchanger. *Energy Conversion Management* 30, 205–213.
- Liu, B.Y.H., Jordan, R.C., 1960. The interrelationship and characteristic distribution of direct, diffuse and total solar radiation, *Solar Energy* 4(3).
- Liu, B.Y.H., Jordan, R.C., 1962. Daily insolation on surfaces tilted towards equator, *ASHRAE Journal* 3(10): 53.



- Lu, F.J., 1990. Blackfoot disease: Arsenic or humic acid? *Lancet* 336 (8707), 115e116.
- Malaeb, L., Ayoub, G.M., 2011. Reverse osmosis technology for water treatment: state of the art review. *Desalination* 267, 1e8.
- Malik, M. A. S., Tiwari, G. N., Kumar, A., Sodha, M. S., 1982. Solar distillation—a practical study of a wide range of stills and their optimum design, construction and performance. Pergamon Press, Oxford, U. K.
- Mamouri, S. J., Derami, H. G., Ghiasi, M., Shafii, M., Shiee, Z., 2014. Experimental investigation of the effect of using thermosyphon heat pipes and vacuum glass on the performance of solar still. *Energy* 75, 501–507.
- Mittal, M.L., Sharma, C., Singh, R., 2014. Decadal emission estimates of carbon dioxide, sulphur dioxide and nitric oxide emissions from coal burning in electric power generation plants in India. *Environ Monit Assess*, 186, 6857–66.
- Morrison, G., Tran, N., McKenzie, D., Onley, I., Harding, G., Collins, R., 1984. Long term performance of evacuated tubular solar water heaters in Sydney, Australia. *Solar Energy* 32, 785–91.
- Morrison, G.L., Budihardjo, I., Behnia, M., 2005. Measurement and simulation of flow rate in a water-in-glass evacuated tube solar water heater. *Solar Energy*, 78, 257–267.
- Mosleh, H. J., Mamouri, S. J., Shafii, M., Sima, A.H., 2015. A new desalination system using a combination of heat pipe, evacuated tube and parabolic trough collector. *Energy Convers. Manag.* 99, 141–150.
- Nebbia, G., Menozzi, G. N., 1966. Historical aspects of dissalzione. *Acqua Ind.* 41–42, 3–20.
- Omara, Z.M., Kabeel, A.E., Abdullah, A.S., 2017. A review of solar still performance with reflectors. *Renewable and Sustainable Energy Review*, 68, 638–649.
- Ozgener, O., Hepbasli, A., 2005. Exergoeconomic analysis of a solar assisted ground source heat pump greenhouse heating system. *Appl. Therm. Eng.* 25, 1459–1471.

- Patel, J., Markam, B. K., Maiti, S., 2019. Potable water by solar thermal distillation in solar salt works and performance enhancement by integrating with evacuated tubes. *Solar Energy* 188, 561–572.
- Petela, R., 2003. Exergy of undiluted thermal radiation. *Solar Energy* 74, 469–88.
- Pissavi, P., 1982. Modelling of the dynamic behavior of a tank for solar storage with internal exchanger. *Re'v Ge'n Thermique* 246–247:521–35.
- Pugsley, A., Zacharopoulos, A., Mondol, J.D., Smyth, M., 2016. Global applicability of solar desalination. *Renewal Energy*, 88, 200–219.
- Rai, S. N., Tiwari, G. N., 1983. Single basin solar still coupled with flat plate collector. *Energy Conversion Management* 23, 145–149.
- Ranjan, K.R., Kaushik, S.C., Panwar, N.L., 2016. Energy and exergy analysis of passive solar distillation systems. *Low–Carbon Technology*, 11(2), 211–221.
- Rashidi, S., Karimi, N., Mahian, O., Esfahani, J.A., 2018. A concise review on the role of nanoparticles upon the productivity of solar desalination systems. *J. Therm. Anal. Calorim.*, 135, 1145–1159.
- Reddy, K.S., Sharon H., 2017. Energy–environment–economic investigations on evacuated active multiple stage series flow solar distillation unit for potable water production. *Energy Conversion and Management*, 151, 259–285.
- Reddy, K.S., Sharon, H., Krithika, D., Philip, L., 2018. Performance, water quality and environmental economic investigations on solar distillation treatment of reverse osmosis reject and sewage water, *Sol. Energy* 173: 160–172.
- Roome, J., 2019. *State and Trends of Carbon Pricing (2019)*. World Bank Group, Washington DC.
- Sampathkumar, K., Arjunan, T., Senthilkumar, P., 2013. The experimental investigation of a solar still coupled with an evacuated tube collector. *Energy Sources, Part A* 35, 261–270.

- Sato, A.I., Scalon, V.L., Padilha, A., 2012. Numerical analysis of a modified evacuated tubes solar collector. International Conference on Renewable Energies and Power Quality (ICREPPQ'12).
- Shafii, M., Mamouri, B. S. J., Lotfi, M. M., Mosleh, H. J., 2016. A modified solar desalination system using evacuated tube collector. *Desalination* 396, 30–38.
- Singh, A. K., Singh, D. B., Mallick, A., Harender, Sharma, S. K., Kumar, N., Dwivedi, V.K., 2019. Performance analysis of specially designed single basin passive solar distillers incorporated with novel solar desalting stills: A review. *Solar Energy* 185, 146–164.
- Singh, A. K., Singh, D. B., Mallick, A., Kumar, N., 2018. Energy matrices and efficiency analyses of solar distiller units: A review. *Solar Energy* 173, 53–75.
- Singh, A.K., 2020. An inclusive study on new conceptual designs of passive solar desalting systems, *Heliyon* 7, e05793.
- Singh, A.K., Samsher, 2020. Analytical study of evacuated annulus tube collector assisted solar desalting system: A review, *Solar Energy* 207: 1404–1426.
- Singh, A.K., Samsher, 2021. A Review Study of Solar Desalting Units with Evacuated Tube Collectors. *Journal of Cleaner Production* 279: 123542.
- Singh, A.K., Samsher, 2021a. Material conscious energy matrix and enviro-economic analysis of passive ETC solar still. *Materials Today: Proceedings*, 38, 1–5.
- Singh, A.K., Samsher, 2021b. Tech-en-econ-energy-exergy-matrix (T4EM) observations of evacuated solar tube collector augmented solar desalting unit: A modified design loom. *Materials Today: Proceedings*, <https://doi.org/10.1016/j.matpr.2021.09.088>
- Singh, A.K., Samsher, 2022. Techno-enviro-economic-energy-exergy-matrices performance analysis of evacuated annulus tube with modified parabolic concentrator assisted single slope solar desalination system. *Journal of Cleaner Production*, 332:129996.

- Singh, A.K., Samsheer, 2022a. Optimum Techno-Eco Performance Requisites for Vacuum Annulus Tube Collector–Assisted Double-Slope Solar Desalination Unit Integrated Modified Parabolic Concentrator. *Environmental Science and Pollution Research*, 29, 34379–34405.
- Singh, A.K., Samsheer, 2022b. Eco-Design Requisites for Solar Desalination Still Augmented Evacuated Annular Tube Collectors with Parabolic Concentrator: An Optimum-Environmental Economic Viability. *Environment Development and Sustainability*. DOI: <https://doi.org/10.1007/s10668-022-02518-w>
- Singh, A.K., Yadav, R.K., Mishra, D., Prasad, R., Gupta, L.K., Kumar, P., 2020. Active solar distillation technology: A wide overview, *Desalination* 493, 114652.
- Singh, D. B., Dwivedi, V. K., Tiwari, G. N., Kumar, N., 2017. Analytical characteristic equation of N identical evacuated tubular collectors integrated single slope solar still. *Desalination and Water Treatment* 88, 41–51.
- Singh, R. V., Kumar, S., Hasan, M., Khan, M. E., Tiwari, G., 2013. Performance of a solar still integrated with evacuated tube collector in natural mode. *Desalination* 318, 25–33.
- Sodha, M. S., Kumar, A., Tiwari, G. N., Tyagi, R. C., 1981. Simple multiple wick solar still: analysis and performance. *Solar Energy* 26, 127–131.
- Soliman, H. S., 1976. Solar still coupled with solar water. Mosul University, Mosul, Iraq, p. 43.
- Sow, O., Siroux, M., Desmet, B., 2005. Energetic and exergetic analysis of a triple effect distiller driven by solar energy. *Desalination*, 174, 277–286.
- Tang, R., Li, Z., Zhong, H., Lan, Q., 2006. Assessment of uncertainty in mean heat loss coefficient of all glass evacuated solar collector tube testing. *Energy Convers Manag* 47, 60–7.
- Tayeb, A.M., 1992. Performance studies of some designs of solar stills. *Energy Convers. Manag.* 33, 889e898.
- Tiwari, A.K., Tiwari, G.N., 2007. Annual performance analysis and thermal modelling of passive solar still for different inclination of condensing cover. *Energy Res.*, 31 (4), 1358–1382.

Tiwari, G. N., Sharma, S. B., Sodha, M. S., 1984. Performance of double condensing cover multi wick solar still. *Energy Conversion Management* 24, 155–159.

Tiwari, G. N., Garg, H. P., 1985. Studies on various designs of solar distillation systems. *Solar & Wind Technology* 1, 161–165.

Tiwari, G. N., Yadav, Y. P., 1987. Comparative designs and long term performance of various designs of solar distillery. *Energy Conversion Management* 27, 327–333.

Tiwari, G., Shukla, S., Singh, I., 2003. Computer modeling of passive/active solar stills by using inner glass temperature, *Desalination* 154, 171e185.

Tiwari, G.N., 2014, *Solar Energy: Fundamentals, Design, Modelling and Applications*. Narosa Publishing House, New Delhi.

Tiwari, G.N., Raj, K., Maheshwari, K.P., Sawhney, R.L., 1992. Recent advances in solar distillation. In: *International Journal of Solar Energy and Energy Conversion*. Wiley Eastern, New Delhi, pp. 32e149 (Chapter 2).

Tiwari, G.N., Yadav, J.K., Singh, D.B., Al-Helal, I.M., Abdel-Ghany, A.M., 2015. Exergoeconomic and enviroeconomic analyses of partially covered photovoltaic flat plate collector active solar distillation system. *Desalination*, 367, 186–196.

Torchia-Nunez, J.C., Porta-Gandara, M.A., Cervantes-de Gortari, J.A., 2008. Exergy analysis of a passive solar still. *Renewable Energy*, 33, 608–616.

Tripathi, R., Tiwari, G. N., 2005. Effect of water depth on internal heat and mass transfer for active solar distillation. *Desalination* 173, 187–200.

Tsatsaronis, G., Lin, L., Pisa, J., 1993. Exergy costing in exergoeconomics. *J. Energy Resour. – ASME* 115, 9–16.

Tsatsaronis, G., Winhold, M., 1985. Exergoeconomic analysis and evaluation of energy conversion plants – a new general methodology. *Energy* 10, 69–94.

Tseng, W.P., 1977. Effects of dose-response relationship of skin cancer and black foot disease with arsenic. *Environ. Health Perspect.* 19, 109e119.

- Tsilingiris, P. T., 2010. Modelling heat and mass transport phenomena at higher temperatures in solar distillation systems- The Chilton-Colburn analogy. *Solar Energy* 84, 308–317.
- WHO, 2011. Safe drinking-water from desalination. [http://who.int/water\\_sanitation\\_health/publications/2011/desalination\\_guidance/en/](http://who.int/water_sanitation_health/publications/2011/desalination_guidance/en/).
- Xiao, C., Luo, H., Tang, R., Zhong, H., 2004. Solar thermal utilization in China. *Renew Energy* 29, 1549–56.
- Xu, L., Liu, Z., Li, S., Shao, Z., Xia, N., 2019. Performance of solar mid-temperature evacuated tube collector for steam generation. *Solar Energy* 183, 162–172.
- Yari, M., Mazareh, A. E., Mehr, A. S., 2016. A novel cogeneration system for sustainable water and power production by integration of a solar still and PV module. *Desalination* 398, 1–11.
- Yousef, M.S., Hassan, H., Sekiguchi, H., 2019. Energy, exergy, economic and enviro economic (4E) analyses of solar distillation system using different absorbing materials. *Applied Thermal Engineering*, 150, 30 – 41.
- Yousef, Md.S., Hassan, H., 2019. Assessment of different passive solar stills via exergoeconomic, exergoenvironmental, and exergoenvironoeconomic approaches: a comparative study. *Sol. Energy*, 182, 316–331.
- Zarasvand, R.A., Suja, F., Hafidz, M.R., Nurul'ain, A.J., 2013. The application of a solar still in domestic and industrial waste water treatment. *Sol. Energy* 93, 63e71.
- Zhou, L., Tan, Y., Wang, J., Xu, W., Yuan, Y., Cai, W., Zhu, S., Zhu, J., 2016. 3D selfassembly of aluminium nanoparticles for plasmon-enhanced solar desalination. *Nat. Photon.* 10, 393e399.

## LIST OF PUBLICATIONS

---

### INTERNATIONAL JOURNAL PUBLICATIONS

1. **Singh, A.K., Samsher, 2020.** Analytical study of evacuated annulus tube collector assisted solar desalination system: A review, *Solar Energy* 207: 1404–1426. <https://doi.org/10.1016/j.solener.2020.07.097> (SCI Indexed, Impact Factor- **7.188**)
2. **Singh, A.K., Samsher, 2021.** A Review Study of Solar Desalting Units with Evacuated Tube Collectors. *Journal of Cleaner Production* 279: 123542. <https://doi.org/10.1016/j.jclepro.2020.123542> (SCI Indexed, Impact Factor- **11.072**)
3. **Singh, A.K., Samsher, 2022.** Techno-Environ-Economic-Energy-Exergy-Matrices Performance Analysis of Evacuated Annulus Tube with Modified Parabolic Concentrator Assisted Single Slope Solar Desalination System: A Novel Design Perspective. *Journal of Cleaner Production* 332:129996. <https://doi.org/10.1016/j.jclepro.2021.129996> (SCI Indexed, Impact Factor- **11.072**)
4. **Singh, A.K., Samsher, 2022.** Optimum Techno-Eco Performance Requisites for Vacuum Annulus Tube Collector Assisted Double Slope Solar Desalination Unit Integrated Modified Parabolic Concentrator. *Environmental Science and Pollution Research* 29:34379–34405. <https://doi.org/10.1007/s11356-021-18426-x> (SCI Indexed, Impact Factor- **5.190**)
5. **Singh, A.K., Samsher, 2022.** Eco-Design Requisites for Solar Desalination Still Augmented Evacuated Annular Tube Collectors with Parabolic Concentrator: An Optimum-Environ-Economic Viability. *Environment Development and Sustainability*. <https://doi.org/10.1007/s10668-022-02518-w> (SCI Indexed, Impact Factor- **4.080**)
6. **Singh, A.K., Samsher, 2022.** Parametric Analysis of Evacuated Annular Parabolic Solar Receiver Integrated Solar Stills: A Relative Optimization Approach. *Environment Development and Sustainability* (SCI Indexed, Impact Factor-**4.080**) (**Under Review**)

## **INTERNATIONAL CONFERENCE PUBLICATIONS**

- 1. Singh, A.K., Samsher, 2021.** Material conscious energy matrix and enviro-economic analysis of passive ETC solar still. *Materials Today: Proceedings* 38: 1 – 5. **Presented** in 2<sup>nd</sup> International Conference ‘Future Learning Aspects of Mechanical Engineering 2020’, <https://doi.org/10.1016/j.matpr.2020.05.117> (SCOPUS Indexed, Cite Score- **2.3**)
- 2. Singh, A.K., Samsher, 2021.** Tech-en-econ-energy-exergy-matrix (T4EM) observations of evacuated solar tube collector augmented solar desaltification unit: A modified design loom. *Materials Today: Proceedings* 61 (2) 258 – 263. **Presented** in F-EIR International Conference 2021 ‘Environment Concerns and its Remediation: Materials Science’. <https://doi.org/10.1016/j.matpr.2021.09.088> (SCOPUS Indexed, Cite Score- **2.3**)





## **Curriculum Vitae**

***Ashok Kumar Singh***

*agashok26@gmail.com*

*ashokkumar\_phd2k18@dtu.ac.in*

*Mr. Ashok Kumar Singh* was born in 01<sup>st</sup> February, 1983 in Lucknow, Uttar Pradesh, India. He is a Research Scholar and pursuing his Ph.D. at Mechanical Engineering Department with specialization in Thermal Engineering from Delhi Technological University, Delhi. He has received his B.Tech. degree from Uttar Pradesh Technical University, Lucknow (presently AKTU, Lucknow) in Mechanical Engineering in 2007 and M.Tech. from Maharshi Dayanand University, Rohtak, Haryana in Manufacturing Technology and Automation in 2010.

*Mr. Ashok Kumar Singh* has teaching experience about 15 years and published more than 10 SCI indexed papers in reputed International Journals, and more than 23 Scopus indexed papers in International Conferences and Journals. He has received “Commendable Research Award – 2020 & 2021” in 2021 and 2022, respectively from Delhi Technological University, Delhi and also, featured in the list of “World Ranking of Top 2% Scientists” in the 2022 database (Published: 6<sup>th</sup> October 2022) created by the experts at Stanford University, United States of America. His research areas of interests are solar thermal and solar desalination systems.